RICE UNIVERSITY

Bioactive Scaffolds for Optimizing Engineered Tissue Formation

by

Solitaire A. DeLong

A THESIS SUBMITTED
IN PARTIAL FULFILLMENT OF THE
REQUIREMENTS FOR THE DEGREE

Doctor of Philosophy

APPROVED, THESIS COMMITTEE:

Jennifer West, Isabel C. Cameron
Professor Bioengineering

Michael Gustin, Associate
Professor Biochemistry and Cell
Biology

K. Jane Grande-Allen, Assistant
Professor Bioengineering

HOUSTON, TEXAS
NOVEMBER 2004

UMI Number: 3168079

INFORMATION TO USERS

The quality of this reproduction is dependent upon the quality of the copy submitted. Broken or indistinct print, colored or poor quality illustrations and photographs, print bleed-through, substandard margins, and improper alignment can adversely affect reproduction.

In the unlikely event that the author did not send a complete manuscript and there are missing pages, these will be noted. Also, if unauthorized copyright material had to be removed, a note will indicate the deletion.

UMI®

ABSTRACT

Bioactive scaffolds for optimizing engineered tissue formation

by

Solitaire A. DeLong

Tissue-engineering scaffolds were designed to mimic several features of the extracellular matrix using a combination of the synthetic polymer, PEG diacrylate, and bioactive factors. Scaffolds were formed by exposing aqueous solutions of PEG diacrylate and bioactive factors modified with PEG monoacrylate to ultraviolet or visible light in the presence of a suitable photoinitiator. Light exposure generated free radicals that targeted acrylate groups in the monomer and in PEG conjugated bioactive factors resulting in crosslinked hydrogel scaffolds with bioactive factors covalently incorporated. This study extended the capability for directing cell behavior using PEG-based hydrogels to include control over the spatial distribution of bioactive factors and the presentation of the growth factor, bFGF. Additionally, PEG hydrogels were modified with a degradable peptide sequence to enable cells to remodel the scaffold by secreting matrix metalloproteinases (MMPs).

A continuous linear gradient was formed by simultaneously using a gradient maker to combine hydrogel precursor solutions with photopolymerization, which locks the gradient in place. Coomassie blue staining confirmed the formation of protein gradients. Fibroblast cells responded to covalently immobilized gradients of the adhesive peptide, RGD, by changing their morphology to align in the direction of increasing RGD concentration and by migrating differentially on RGD-gradient hydrogels compared to

control hydrogels. Next, bFGF was covalently immobilized to hydrogels with retention of its mitogenic and chemotactic effects on smooth muscle cells (SMCs). A covalently immobilized bFGF gradient was also formed using the gradient maker and shown to increase linearly along the hydrogel's length by silver staining. SMCs responded to these bFGF-gradient hydrogels by aligning in the direction of increasing bFGF concentration and by migrating differentially, up the concentration gradient, compared to migration on control hydrogels. Finally, the MMP-sensitive peptide sequence, GPQGILGQ, was inserted into the main polymer chain's backbone to allow targeted degradation by cell-secreted proteases. Cells were observed to change their morphology and migrate when seeded within these degradable hydrogel scaffolds, but not in scaffolds lacking this degradable peptide sequence. This hydrogel system is expected to be useful for studying tissue formation leading eventually to an improved understanding of the factors needed to form engineered tissues.

ACKNOWLEDGEMENTS

A special thanks to my advisor, Jennifer West, for providing a very interesting and challenging project and seemingly unlimited financial support. I am also grateful to all members of the West lab for many useful discussions and opportunities to learn a variety of techniques and I am especially grateful to Andi and Andre Gobin for their initial work using the gradient maker to form gradient hydrogel scaffolds. A special thanks also goes out to my labmates and fellow graduate students at Rice University in various departments for their friendship and support.

I am also deeply grateful for the love and support provided by my family and especially by my boyfriend, Grant Lindsay, who has been extraordinarily patient throughout this graduate school experience. Finally, I thank God for love, forgiveness, for making all things possible.

TABLE OF CONTENTS

CHAPTER 1: BACKGROUND

This research extends the opportunities to mimic the cellular environment's role in guiding tissue development and directing tissue repair by using PEG-based hydrogel scaffolds to form engineered tissues. In 1986, Weinberg and Bell were the first to develop an engineered tissue that grossly resembled a blood vessel by using collagen scaffolds seeded with bovine vascular cells. Since then, our understanding of the extracellular matrix (ECM) and the development of biomaterials have combined to provide methods to specifically direct cell proliferation and differentiation within scaffolds, while allowing scaffold remodeling by localized proteolytic activity and ECM protein deposition. Thus, the use of PEG-based bioactive hydrogel scaffolds that mimic the biological signals provided by the body's natural scaffolding and the ability for cells to remodel the ECM can result in the formation of engineered tissues that better resemble the structural and functional characteristics of natural tissues.

EXRACELLULAR MATRIX COMPONENTS

The ECM is the cellular environment that surrounds every cell found in every tissue of the body (Scott-Burden, 1994). It consists of a wide variety of molecules including collagen, elastin, glycosaminoglycans, and glycoproteins that are presented in different amounts and spatial arrangements depending on the tissue type (Rosso *et al.*, 2004). Blood vessels, for example, have a multilayered structure consisting of three main cell types and their associated matrix. The three layers include an inner—intimal layer,

an intermediate—medial layer, and an outer—adventitial layer. The medial layer confers the majority of the blood vessel's mechanical properties, which is contributed in large part by collagen and elastin fibers. Cartilage, in comparison, is mostly dominated by the proteoglycan—aggrecan and a form of collagen not found in any other tissue of the body—type II collagen (van der Kraan *et al.*, 2002; Rosso *et al.*, 2004). The ECM components found in these tissues and others are secreted by cells and distributed to form the appropriate cellular environment required to provide support and mechanical strength and to maintain tissue homeostasis. In addition, the different types of ECM components contribute differentially towards the mechanical and biological properties present in the ECM.

Several collagen types can form fibrils that provide support and mechanical strength. These molecules include collagen types I, II, III, and V, which are synthesized in the rough endoplasmic reticulum as individual α-chains and then braided together in the cisternal space of the endoplasmic reticulum to form a triple helical structure (Scott-Burden, 1994; Rosso *et al.*, 2004). Individual tropocollagen molecules can then be glycosylated and secreted into the extracellular space (Fessler and Fessler, 1978; Scott-Burden, 1994). Linear associations are formed by these molecules and then these are covalently crosslinked. This crosslinking occurs via the action of lysyl oxidase, which stabilizes collagen fibers and provides tensile strength (Csiszar, 2001). Lysyl oxidase also forms crosslinks in elastin that provide elasticity (Vrhovski and Weiss, 1998; Myllyharju and Kivirikko, 2001). Inactivating the lysyl oxidase gene, *Lox*, severely affects arterial wall structure and cardiovascular function. *Lox* $^{-/-}$ mice develop aortic aneurysms, fragmented elastic lamellae, and thickened aortic walls and small aortic

lumens, which culminates in perinatal death (Mäki *et al.,* 2002). Thus, crosslinks play an essential role in maintaining arterial wall structure and normal cardiovascular function.

Elastic fibers are formed by the combination of elastin, fiber-forming glycopeptides, and lysyl oxidase crosslinking. As noted above, these fibers provide structural support in blood vessels as well as other tissues including heart valves, skin, and lungs (Rosso *et al.,* 2004). In blood vessels and heart valves, elastic fibers have a bearing on tissue mechanics at low strains, while stiffer collagen fibers are engaged at higher strains (Bank *et al.,* 1996). These fibers also confer elasticity by stretching in response to load and then as the load is released recoiling to return to their original configuration (Ross and Bornstein, 1971). Mice that are hemizygous for the elastin gene (*Eln* $^{+/-}$) produce 50% less elastin mRNA and protein, which is accompanied by a 35% increase in the number of elastic lamellae (Li *et al.,* 1998). In spite of these variations, arterial extensibility and diameter are nearly normal at physiologic pressures. The increased number of elastic lamellae, therefore, can compensate for reduced elastin content in the arterial wall. Although these structural changes minimized potential functional effects of reduced elastin content, they also point out the important structural role contributed by elastic fibers.

The other major components of the ECM are glycoproteins and glycosaminoglycans, which contribute to the overall organization of the ECM, without playing a major structural role (Scott-Burden, 1994; Rosso *et al.,* 2004). Glycoproteins are ECM molecules that contain several binding domains. These molecules can bind other ECM molecules like collagen and proteoglycans as well as cell surface receptors. Some examples include fibronectin, laminin, and vitronectin, which facilitate cell

attachment and spreading in the ECM (Scott-Burden, 1994; Rosso *et al.,* 2004). Glycosaminoglycans (GAGs) are linear polysaccharides that include chondroitins, keratins, dermatins, heparans, and hyaluranan. Except for hyaluranan, the GAG carbohydrate chains can attach to a core protein to form a proteoglycan (Rosso *et al.,* 2004). These proteoglycans can play a variety of roles that include acting as receptors on cell surfaces and binding growth factors such as basic fibroblast growth factor (bFGF) to protect it from proteolytic degradation (Moscatelli, 1998).

CELLS INTERACT WITH ECM COMPONENTS VIA SURFACE RECEPTORS

Cells can interact with ECM components via nonintegrin and integrin receptors, which are present on the cell surface. Nonintegrin receptors include the proteoglycan, syndecan, and the glycoprotein, CD44 (Rosso *et al.,* 2004). Syndecan spans the cell membrane and consists of cytoplasmic and extracellular domains and a hydrophobic membrane region. Syndecans can bind a variety of ECM components including collagen, fibronectin, and bFGF. CD44 is a glycoprotein with GAG side chains and attached sugars that can bind types I and IV collagen and hyaluranan (Rosso *et al.,* 2004). Integrin receptors are a family of glycoproteins that are heterodimeric. That is, integrin receptors consist of α and β subunits that associate non-covalently to bind specific ECM components (Figure 1). Different combinations of α and β subunits can give rise to receptors that bind a diverse array of ECM molecules. The $\beta1$-subunit, for example, can associate with multiple α subunits (e.g. $\alpha1$, $\alpha2$, $\alpha10$, and $\alpha11$) to bind collagen (Hynes, 2002; van der Flier and Sonnenberg, 2001). Alternatively, the $\beta1$-subunit can associate with $\alpha1$, $\alpha2$, $\alpha3$, $\alpha6$, and $\alpha7$ integrins to form a receptor that can bind laminin (Hynes,

2002; van der Flier and Sonnenberg, 2001). These cell-ECM interactions for both non-integrin and integrin receptors change the receptor's cytoplasmic domain, which then associates with the cytoskeleton at focal adhesion sites (Rosso *et al.*, 2004). Downstream events can include receptor clustering, protein kinase activation, cytoskeletal protein phosphorylation, and signal transmission to the nucleus (Schlaepfer *et al.*, 1994). Ultimately, receptor binding to an ECM molecule provides a signal that can lead to dramatic changes in cell behavior—altered cell morphology, proliferation, differentiation, migration, and/or extracellular matrix production (Kim *et al.*, 1999; Mann *et al.*, 1999; Nikolovski and Mooney, 2000; Long and Tranquillo, 2003; Rosso *et al.*, 2004).
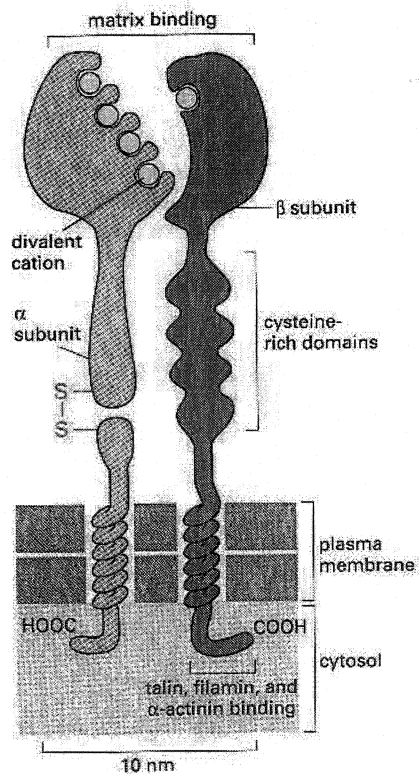

Figure 1. This cartoon depicts the subunit structure of integrin cell-surface receptors, which consist of α and β subunits that interact non-covalently. A wide variety of ECM molecules can bind integrin receptors and trigger cell signaling events that alter cell behavior (image obtained from Alberts *et al.*, 2002).

CELL-ECM INTERACTIONS INFLUENCE CELL BEHAVIOR

Several studies have demonstrated the importance of ECM composition on cell differentiation. For example, monkey blastocyst stem cells differentiate *in vivo* into cartilage if grown in the presence of cartilage matrix prior to injection (Kleinman *et al.,* 2003). Mammary epithelial cells express differential levels of mRNA for laminin, type IV collagen, and fibronectin when grown on tissue culture dishes and floating gels of type I collagen (Streuli and Bissell, 1990). Although these cells produce lower levels of ECM proteins when grown on collagen gels compared to plastic dishes, these cells are able to organize the proteins into a basement membrane. The appearance of this membrane then supports enhanced expression of proteins associated with lactational differentiation. Thus, the ECM can influence the developmental lineage of stem cells and the differentiated morphology of epithelial cells.

Individual components in the ECM can also shift cellular behavior. Fibronectin promotes a change in vascular smooth muscle cell phenotype *in vitro* from one that is contractile to one that is synthetic (Hedin and Thyberg, 1987; Hedin *et al.,* 1988). This process enables the smooth muscle cells to proliferate and secrete ECM proteins. In contrast, vascular smooth muscle cells maintain their contractile phenotype for an extended duration when cultured on laminin or type IV collagen substrates. The addition of soluble fibronectin was also shown to stimulate the growth of fibronectin-null cells, which were adhered to collagen substrates (Sottile *et al.,* 1998). Laminin, on the other hand, promotes a more differentiated phenotype in endothelial cells (Pauly *et al.,* 1992). These cells rapidly stop proliferating and begin to form tube-like structures when grown on laminin or Matrigel (reconstituted basement membrane) substrates. In contrast,

endothelial cells dedifferentiate on tissue culture plastic and are able to migrate and proliferate.

GROWTH FACTORS INTERACT WITH ECM

In addition to the interactive effects of ECM molecules on cell behavior, the ECM binds growth factors. Transforming growth factor-β (TGF-β), for example, is most often secreted from cells in a latent, inactive form non-covalently complexed to its prodomain, TGF-β latency-associated protein (LAP). This prodomain can associate with additional proteins like the latent TGF-β binding proteins (LTBP), which bind the ECM. Immunohistochemistry has indicated that LTBP-1 is localized in fibronectin-rich pericellular fibers and in elastin-associated microfibrils (Taipale *et al.,* 1996). Active TGF-β can also bind to several ECM proteins: thrombspondin, decorin, fibronectin, and collagen type IV (Ruoslahti *et al.,* 1992; Schultz-Cherry; 1993; reviewed in Taipale and Keski-oja, 1997). Basic fibroblast growth factor (bFGF), in contrast, is secreted by cells in an active form that readily associates with heparan sulfate proteoglycans in the ECM and on the cell surface. This growth factor can also associate with extracellular forms of FGF receptors (Hanneken *et al.,* 1995). Although TGF-beta and bFGF are sequestered from cell interaction by their association with ECM proteins, these growth factors can be released by proteolytic enzymes and/or activated to enable growth factor activity. In this respect, the ECM acts like a storage depot for growth factors—making the growth factors readily available without the need for additional protein synthesis (Taipale and Keski-oja, 1997). Further, this binding allows the ECM to control local growth factor

concentrations by preventing diffusion out of the local environment (Rosso *et al.,* 2004; Hubbell, 2003).

ECM-growth factor interactions also help to control the growth factors' biological activity by preventing degradation. For example, bFGF binding to heparan sulfate proteoglycan stabilizes bFGF in the presence of proteolytic enzymes (Moscatelli, 1988; Sakesela *et al.,* 1988; Gospodarowicz and Cheng, 1986). This protection can then prolong bFGF's effect on cell proliferation (Moscatelli, 1988).

CELL REMODELING OF THE EXTRACELLULAR MATRIX BY MATRIX METALLOPROTEINASES

As noted above, cell-ECM interactions can lead to dramatic changes in cell behavior. Likewise, cells can alter ECM composition by degrading ECM components and/or secreting ECM proteins. Thus, cell-ECM interactions are bi-directional and dynamic. To remodel the ECM's composition, cells can secrete a variety of enzymes including serine proteases and matrix metalloproteinases (MMPs) that can potentially target every ECM molecule.

Plasmin is a prominent member of the serine protease family, which is derived from plasminogen and plays a key role in enabling cells to migrate in physiological and pathological processes. Following injury to the vascular wall, for example, by balloon angioplasty, vascular smooth muscle cells migrate from the media to form a neointima. Neointimal formation is reduced in knockout mice lacking either plasminogen or the plasminogen activator, urokinase plasminogen activator (uPA; reviewed in Carmeliet and Collen, 1998). In wound healing, kerotinocytes express uPA at their leading edge, while

migrating through fibrin-rich matrix (Figure 2; reviewed in Johnsen *et al.,* 1998). Mice

homozygous for the plasminogen gene (*Plg* $^{-/-}$) suffer from delayed wound healing

compared to wild-type mice because the kerotinocytes cannot degrade the fibrin-matrix

and then interact with fibroblasts to repair the wound (Farrell *et al.,* 1992; reviewed in

Werb, 1997). As these studies show, proteolysis is critical for cells to migrate and

participate in tissue remodeling activities (Werb, 1997).
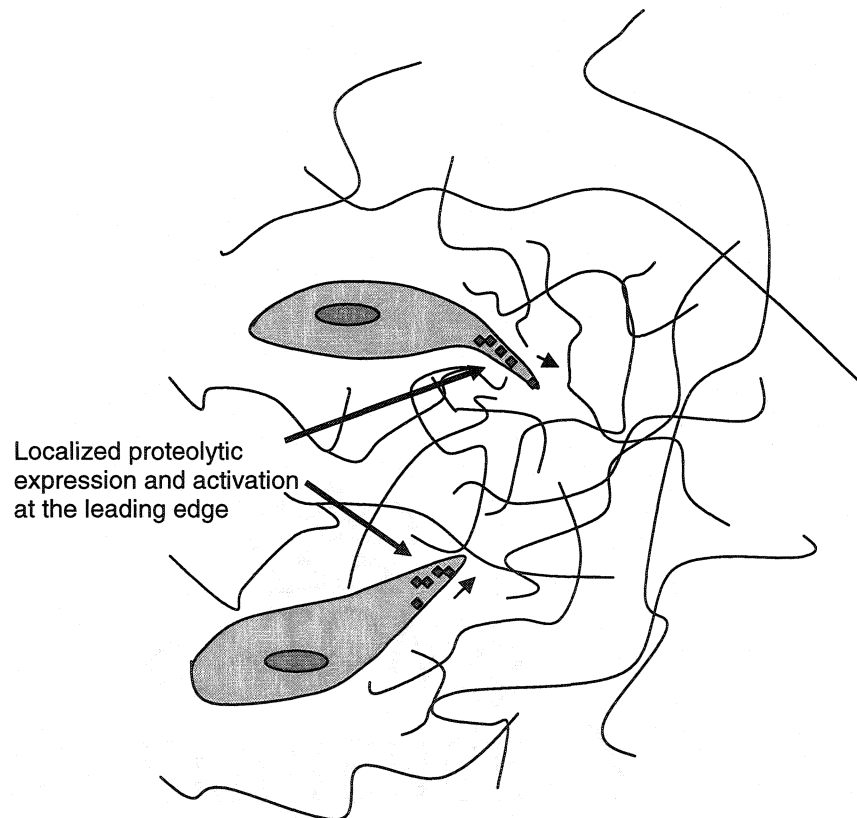
Figure 2. This cartoon depicts the infiltration of a fibrin-rich matrix by keratinocytes. Proteolytic activity is localized at the cell's leading edge and enables keratinocyte migration into this provisional matrix.

The MMPs also enable cells to remodel the ECM in a variety of processes

including tissue development, angiogenesis, and cancer invasion. Gene targeting studies

have revealed that mice lacking the membrane-bound MMP, MT1-MMP, develop severe

connective tissue growth and remodeling disorders (Holmbeck *et al.,* 1999). MT1-MMP-deficiency results in dwarfism, osteopenia, arthritis, and connective tissue disease. Bone formation is impaired to the extent that dome-shaped skulls and shortened limbs (65% of the length of controls) are evident by day 5 and day 45, respectively. In angiogenesis, MT1-MMP is required for endothelial cells to form neovessels (Hiraoka *et al.,* 1998). Several MMPs including MMP-1, MMP-2, MMP-3, MMP-11, and MMP-14 promote cancer cell invasion (reviewed in Johnsen *et al.,* 1998). These studies and others provide further evidence of the importance of proteolytic enzymes for cell migration and tissue repair and growth.

As noted above, proteolytic enzymes have profound effects on biological processes as these enzymes enable cells to migrate and participate in tissue remodeling. Proteolytic activity is also tightly controlled. Plasmin is formed by the action of plasminogen activators on the inactive zymogen—plasminogen (Johnsen *et al.,* 1998). Further, plasminogen activators like urokinase plasminogen activator (uPA) can localize to cell surfaces by binding cell surface receptors (Johnsen *et al.,* 1998; Murphy and Gavrilovic, 1999). In the absence of inhibitory factors, the uPA/plasminogen system can then degrade ECM in the immediate pericellular environment. Most MMPs are secreted by cells as inactive zymogens, which contain a propeptide domain that maintains the secreted MMP in an inactive state (Figure 3). This domain consists of a cysteine residue that interacts with zinc, covering the active site. Disrupting this interaction activates the MMP. This activation mostly occurs by the action of tissue or plasma proteinases *in vivo*. Pro-MMP-2, however, is primarily activated on the cell surface (reviewed in Nagase and Woessner, 1999). This process requires both MT1-MMP and a complex of

TIMP-2 and MT1-MMP (Strongin *et al.,* 1995; Butler *et al.,* 1998; Kinoshita, *et al.,* 1998). Alternatively, pro-MMP-2 can be activated by the uPA/plasmin system

$$\text{plasminogen} \xrightarrow{\text{uPA}} \text{plasmin}$$

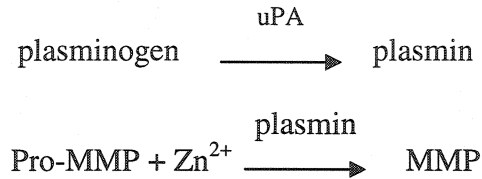$$\text{Pro-MMP} + Zn^{2+} \xrightarrow{\text{plasmin}} \text{MMP}$$

Figure 3. Proteolytic activity by serine proteases and matrix metalloproteinases is precisely controlled. Plasmin, for example, is formed by the activation of plasminogen by plasminogen activators such as urokinase plasminogen activator (uPA). Matrix metalloproteinases are generally secreted in a latent form that binds Zn^{2+}. Destabilizing the interaction between Zn^{2+} and the propeptide domain activates the MMP. Several proteases can activate secreted pro-MMPs including plasmin, chymase, and tryptase.

when associated with the cell surface (Mazzieri *et al.,* 1997). MMP activity is further regulated by tissue inhibitors of metalloproteinases (TIMPs; Ward, 1991). These proteinase inhibitors bind active MMPs in a 1:1 stoichiometric ratio. TIMP-1 and TIMP-2 can also bind pro-MMP-2 and pro-MMP-9.

In their active form, proteolytic enzymes can hydrolyze a variety of ECM molecules. Most MMPs, for example, can cleave fibronectin, laminin, and gelatins, while plasmin substrates include fibronectin, laminin, and proteoglycans (Birkedal-Hansen, 1993; Werb, 1997). Table 1 describes the various substrates cleaved by MMPs and plasmin (adapted from Werb, 1997). Notably, MMPs 1, 2, 3, MT1-MMP (or MMP-14), and MT2-MMP (MMP-15) can cleave fibrillar collagens (types I, II, and III).

Table 1. ECM and Cell Surface Substrates of Pericellular Proteinases (adapted from Werb, 1997)

Enzymes	Other Names	Substrates[a]
MMP-1	collagenase-1	Col I, II, III, VII, X, GL, EN, LP, AG, TN,
MMP-8	collagenase-2	L-selectin, IGF-BP, Pro-MMP-2, -9, α2M,
MMP-13	collagenase-3	α1PI
MMP-2	gelatinase-A	GL, ColI, IV, V, VII, X, XI, EL, FN, LN,
MMP-9	gelatinase-B	LP, AG, galectin-3, IGF-BP, VN, FGF
		receptor-1, Pro-MMP-2, -9, -13
MMP-3	stromelysin-1	PG, LN, FN, GL, Col III, IV, V, IX, X, XI,
MMP-10	stromelysin-2	LP, FB, EN, TN, VN, Pro-MMP-1, -8, -9, -
MMP-7	Matrilysin	13, α2M, α1PI, L-selectin
MMP-12	metalloprotease	EL, FB, FN, LN, PG, MBP, PL, α1PI
MMP-14	MT1-MMP	Col I, II, III, GL, FN, LN, VN, PG, Pro-
MMP-15	MT2-MMP	MMP-2, -13, α2M, α1PI
MMP-11	stromelysin-3	LN, FN, AG, α2M, α1PI
Plasmin		FB, FN, TN, LN, AG, latent TGFβ BP, PG,
		Pro-MMP-1, -3, -9, -14, C1, C3, C5
uPA		PL, FN, HGF

Abbreviations: aggrecan, AG; α1-proteinase-inhibitor, α1PI; α2-macroglobulin, α2M; binding protein, BP; collagen type, Col; complement, C; elastin, EL; entactin, EN; fibrin/fibrinogen, FB; fibronectin, FN; gelatins, GL; hepatocyte growth factor, HGF; laminin, LN; link protein, LP; myelin basic protein, MBP; plasminogen, PL; proteoglycans, PG; tenascin, TN; vitronectin, VN

[a]Substrates are grouped for similar enzymes, but not all of the proteins in each group are cleaved by all the enzymes in the group.

In addition to degrading ECM components, MMPs can cleave ECM proteins at specific sites. This change affects the presentation of ECM proteins resulting in differential effects on cell behavior. MMP-2 and MT1-MMP shift the biological effect of laminin 5 from supporting cell adhesion to promoting cell migration (Giannelli *et al.,*

1997; reviewed in Streuli, 1999; Koshikawa *et al.,* 2000; reviewed in Blobel, 2000). MMP cleavage likely reveals a cryptic site that potentially binds to an alternative cell surface receptor, which provides a signal that triggers cell migration. Proteolytic activity can also release growth factors from the ECM. Serine proteases degrade latent TGF-β and insulin-like growth factor (IGF) binding proteins, which associate with their respective growth factors to sequester them in the ECM (Parker *et al.,* 1995; Imai *et al.,* 1997). Proteolytic release then enables cells to interact with these growth factors, which can alter cellular phenotype.

As described above, the interactions between the ECM and cells are both bi-directional and dynamic. The ECM provides support and biological signals that regulate cell behavior, while cells are capable of remodeling the ECM's composition. Cells receive signals within tissue from ECM proteins and growth factors. These signals are transmitted into the cell via cell surface receptors. These signals individually or in combination can increase or decrease SMC proliferation, migration, and/or ECM synthesis. Meanwhile, cells can remodel the ECM by secreting ECM proteins and proteolytic enzymes that degrade ECM components. Proteolytic degradation provides room for cells to migrate, proliferate, and deposit ECM proteins. Thus, the interaction between cells and the ECM are essential determinants of a tissue's structural and functional properties.

In order to provide a source of replacement tissues, several research groups have developed scaffolds and *in vitro* cell culture conditions that promote tissue formation. These efforts rely on the use of scaffolds that mimic several important aspects of the ECM including its role in providing structural support and biological signal presentation.

Some labs have even taken advantage of the cell's role in remodeling the ECM through proteolytic degradation of ECM components. Continued efforts may result in engineered tissues with the appropriate structural and functional characteristics needed to serve as tissue replacements.

TISSUE ENGINEERING SCAFFOLD MATERIALS

Collagen-based tissue-engineering scaffolds

As noted above, collagen is an important ECM molecule that can provide structural support. Collagen also interacts with cells via cell surface receptors to influence differentiated cell morphology. These characteristics and the ability to isolate collagen from animal and human tissues and reconstitute it into gels, has focused the attention of many research groups on the use of collagen-based tissue-engineering scaffolds. Weinberg and Bell (1986) were the first to develop an engineered tissue with the blood vessel's trilayered composition using collagen scaffolds seeded with bovine vascular cells and cultured under static conditions. This blood vessel grossly resembled an artery as it contained a nearly confluent layer of endothelial cells and some evidence that the smooth muscle cells were still differentiated. However, there were important differences from native arteries: smooth muscle cells were longitudinally oriented, there was little or no elastin in the matrix, smooth muscle cell densities were one-eighth to one-fourth those in normal blood vessels, and the vessels lacked the necessary mechanical strength for implantation into an animal model.

Several investigators have continued the work of Weinberg and Bell using collagen scaffolds to produce vascular grafts with somewhat improved properties.

L'Heureux *et al.* (1993) and Hirai and Matsuda (1995) engineered blood vessels with circumferentially oriented smooth muscle cells by mechanically constraining smooth muscle cell compaction of the collagen gel. This was achieved by simply placing a mandrel in the lumen during the compaction period. Tranquillo *et al.* (1996) also aligned smooth muscle cells circumferentially, but used a different method, magnetic prealignment, which involved the application of a strong magnetic field during collagen fibrillogenesis. These vascular grafts better mimicked the organization of smooth muscle cells in native arteries and as a result had increased burst pressures. However, there was little or no elastin synthesis and the mechanical properties were still too weak to withstand the forces generated by pulsatile flow in the vascular system.

Fibrin-based scaffolds

Alternatively, engineered tissues can be developed using fibrin-based scaffolds. Fibrin is the major structural protein of a blood clot and is formed when thrombin cleaves specific sites within the monomeric form of fibrin, which is fibrinogen. The fibrinogen monomers then associate to form linear fibrils. These blood clotting components can be readily purified from animal and human plasma sources to form fibrin scaffolds. Embedded smooth muscle cells can then be aligned as described above for collagen scaffolds through compaction of the fibrin network. Neonatal smooth muscle cells are differentially affected by fibrin scaffolds compared to collagen scaffolds. These smooth muscle cells produce up to 5 times more collagen and 4 times more elastin when seeded in fibrin scaffolds (Grassl *et al.,* 2002; Long and Tranquillo, 2003). This enhanced ECM protein production can then result in engineered tissues with improved mechanical

properties (Mann *et al.,* 2001a). The differential effects of scaffold type on ECM protein production are likely due to differences in cell interaction with the scaffold. For example, smooth muscle cell interaction with fibrin is mediated by the $\alpha_v\beta_3$ integrin and with collagen via the $\alpha_2\beta_1$ integrin (Feng *et al.,* 1999; Moiseeva, 2001; Nikolovski and Mooney, 2001). When these integrins are engaged by ECM proteins, differential signaling cascades can be promoted that affect cell behavior to potentially improve engineered tissue formation (Hynes, 1992; Luscinskas and Lawler, 1994; Schwartz and Ingber, 1994).

Thus, scaffolds based on such natural materials as fibrin and collagen, can direct embedded cells to remodel the matrix by secreting ECM proteins and by reorganizing their alignment. However, major disadvantages of using these materials exist and include the possibility of transmitting diseases and of problems with immunogenicity. In contrast, scaffolds based on synthetic biodegradable polymers do not present biosafety issues and the scaffold degrades leaving only natural tissue with no permanent foreign material (Kim and Mooney, 1998a).

Synthetic biodegradable polymer scaffolds

Synthetic scaffolds based on polyglycolic acid (PGA) and/or polylactic acid (PLA) are frequently used as tissue engineering scaffolds (reviewed in Agrawal and Ray, 2001). These polymers are synthesized by ring-opening polymerization of the cyclic diesters of glycolide and lactide (Gilding and Reed, 1979; Eling *et al.,* 1982; Agrawal and Ray, 2001). Engineered blood vessels fabricated using PGA fibers have been shown to contain detectable amounts of elastin and higher cell densities even under static culture

conditions than that shown using type I collagen scaffolds (Weinberg and Bell, 1986; Ziegler and Nerem, 1994, Kim and Mooney, 1998a; Kim et al., 1998b). These same scaffolds have also been shown to lack detectable amounts of elastin after tissue formation (Niklason et al., 1999). The mechanisms underlying these differences in elastin production within PGA scaffolds are unclear. However, the PGA scaffold that produced vessels with no elastin was processed so as to increase the hydrophilicity of the polymer surface by converting ester bonds to hydroxyl and carboxylic acid groups. This may have altered both the types and concentrations of adhesion proteins adsorbed to the scaffold from the cell culture medium. Differences in the type of adsorbed adhesion proteins have been shown to vary depending on the scaffold chemistry and result in differential cell behavior including modified ECM production (Kim et al., 1999; Nikolovski and Mooney, 2000). In addition, the conformation of adsorbed proteins may have played a role in altering cell behavior by enabling or preventing adhesion to different regions of the adsorbed protein by a variety of integrin receptors (Kim et al., 1999).

These synthetic biodegradable scaffolds can be designed to degrade at varying rates to make room for cell proliferation and extracellular matrix production. The degradation rate is determined by the ratio of PLA and PGA present in the polymeric scaffold where the primary mechanism for degradation is by hydrolysis of the ester linkages (Miller et al., 1977; Lewis, 1990). For tissue-engineering applications, the scaffold composition must be designed to degrade on a time-scale that matches the rate of tissue formation. Initially, this degradation rate allows the scaffold to provide support and structure. As the cells proliferate and secrete ECM proteins, the scaffold then

degrades until there is only natural material consisting of cells and ECM proteins. Three-dimensional constructs are also designed to be porous because this allows cells to initially infiltrate the scaffold (reviewed in Agrawal and Ray, 2001). Several fabrication methods exist which rely upon one or more of the following: solvents, heat, pressure, and additives that form pores (reviewed in Agrawal and Ray, 2001). These pores are essential for cell attachment throughout the three-dimensional construct and also allow for cells to migrate, while providing room for ECM protein synthesis.

To enhance engineered tissue formation, growth factors can be incorporated within synthetic biodegradable scaffolds. For example, Richardson *et al.* stimulated new blood vessel formation in PLG scaffolds containing both vascular endothelial growth factor (VEGF) and platelet derived growth factor (PDGF-BB). VEGF was mixed with polymer particles prior to scaffold fabrication, while PDGF-BB was first encapsulated within polymer microspheres. The different methods enabled VEGF to be released more rapidly at first within the first few days followed by a slower release over the next few weeks. PDGF-BB was released at a steadier pace and depended on the degradation rate of the polymer. The dual delivery of growth factors significantly promoted new blood vessel formation within scaffolds implanted in a hindlimb ischemia model (non-obese diabetic mouse) compared to the delivery of either growth factor alone. Thus, these scaffolds demonstrate the positive effect of growth factors on vascular network formation in three-dimensional scaffolds. This technique can potentially be applied to alternative growth factors to influence several other aspects of engineered tissue formation—cellularity, differentiation, and ECM protein production. However, care must be taken in choosing a fabrication technique because the chosen method may irreversibly denature

the protein. It may also be difficult to sustain a growth factor's release profile in the presence of mechanical forces such as those encountered *in vivo* and in fluid flow systems.

PROMOTION OF CELLULAR RESPONSE BY TISSUE ENGINEERING SCAFFOLDS

Scaffolds based on such natural materials as fibrin and type I collagen and such synthetic materials as polyesters of PGA and/or PLA provide limited opportunities to control cell behavior. The natural scaffolds contain intrinsic adhesion sites that allow cells to attach to the scaffold in addition to adsorbed ECM proteins. The synthetic scaffolds do not inherently have natural cell binding sites, but interact with cells via the adsorption of ECM proteins. For example, adhesion to collagen scaffolds was shown to be mediated by the collagen itself and the proteins, vitronectin and fibronectin, which adsorbed to collagen scaffolds from the cell culture medium (Kim *et al.,* 1999; Nikolovski and Mooney, 2000). Adhesion to PGA and poly(lactic-co-glycolic acid) (PLGA) was mostly mediated by adsorbed vitronectin (Kim *et al.,* 1999; Nikolovski and Mooney, 2000). The differences in adsorbed proteins were correlated with modulated cell behavior including higher cell densities and enhanced rates of elastin production on PGA and PLGA scaffolds compared to collagen scaffolds. Changing the scaffold formulation made it possible to alter protein adsorption and thus, modulate SMC growth and biosynthetic properties. However, none of these scaffolds provided the opportunity to control the identity *and* concentration of incorporated bioactive signals. These signals may shift SMCs to a more or less proliferative, differentiated, or synthetic state

depending on their identity, concentration, and combined presentation with other bioactive and mechanical signals. To engineer functional tissue, it is critical that scaffolds be developed that specifically provide the appropriate bioactive signals for tissue formation. PEG-based hydrogel scaffolds may provide a solution because these scaffolds are inherently resistant to protein adsorption, yet provide the opportunity to add bioactive factors by chemical incorporation. The combination of relatively non-adhesive scaffolds and bioactive factors enable these scaffolds to simultaneously promote specific cellular interactions, while discouraging other unwanted cellular interactions.

PEG DIACRYLATE HYDROGELS AS SCAFFOLDS FOR ENGINEERED TISSUES

Polyethylene glycol (PEG) diacrylate hydrogels are currently being investigated for use as scaffolds for tissue-engineered vascular grafts. As depicted in Figure 4, these hydrogel scaffolds are based on a macromer consisting of a PEG chain with an acrylate moiety coupled to each end. The PEG chain is biocompatible and hydrophilic, while the
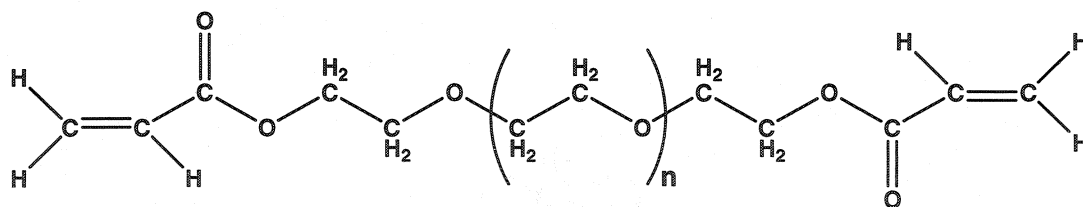

Figure 4. This figure depicts the chemical structure of PEG diacrylate. The acrylate groups at either end of the PEG chain form micelle-like structures in water and can undergo rapid photopolymerization to form three-dimensional covalently crosslinked gels.

acrylate moieties are hydrophobic causing the macromers to form micelle-like structures in water, and able to undergo rapid free-radical polymerization (Sawhney *et al.,* 1993). Exposure to low levels of ultraviolet or visible light converts aqueous solutions containing PEG diacrylate in the presence of a suitable photoinitiator into three-dimensional, covalently crosslinked gels. These hydrogels possess several biologically useful features that may be useful for engineering tissues (Hubbell, 1999). These hydrogels have a mesh size that permits the diffusion of small molecules like oxygen and low molecular weight nutrients (Hubbell, 1999). They are also mechanically flexible and are highly swollen with water (Hubbell, 1999).

PEG diacrylate hydrogels are polymerized in conditions that are compatible with cells. Cells are simply suspended in an aqueous solution containing the gel precursor, PEG diacrylate, and a photoinitiator solution. Exposure to ultraviolet light (365 nm, 10mW/cm^2) converts the aqueous solution into a crosslinked hydrogel comprised of oligoacrylate nodes connected by linear chains of PEG. Gel conversion occurs in water under physiological conditions (pH 7.4, 37°C) and in the presence of oxygen (Sawhney *et al.,* 1993). Gelation also occurs within physiologically acceptable temperatures since the number of vinyl bonds per unit mass is very small leading to diminished amounts of heat produced as a result of polymerization (Sawhney *et al.,* 1993).

PEG diacrylates form micellar structures in water that enhances the polymerization rate of the acrylate groups. The macromer gets oriented in water so that there is an increase in the effective concentration of double bonds within the micelle (Sawhney *et al.,* 1993). This causes the rate of the propagation reaction to increase in a free-radical polymerization. Further, the radical termination reaction, which is diffusion

controlled, slows as the medium viscosity increases (Sawhney *et al.,* 1993). Thus, the increase in propagation rate and the decrease in termination rate result in a high polymerization rate and fast gelation time (Sawhney *et al.,* 1993).

Cell Adhesion to PEG Diacrylate Substrates

PEG diacrylate hydrogels are highly resistant to protein adsorption and subsequent cell adhesion. This property has been taken advantage of in several applications. For example, thin conformal coatings have been formed on tissue surfaces by interfacial photopolymerization. This approach nearly eliminated thrombosis following injury by balloon angioplasty in the rat and rabbit carotid arteries (Hill-West *et al.,* 1994). Thrombus formation was blocked because of the hydrogel's cell non-adhesive material properties. Moreover, this resistance to protein adsorption depends on the hydrogel's hydrophilic and nonionic character (Andrade and Hlady, 1986).

An engineered adhesive character can be added to intrinsically cell non-adhesive hydrogel substrates through the chemical incorporation of synthetic adhesion peptides. Short peptide sequences responsible for binding to cell surface receptors have been shown to be sufficient for cell adhesion and spreading when incorporated into biomaterial surfaces in sufficient numbers (Massia and Hubbell, 1991). Although, short adhesion peptides lack the total activity present within the complete protein, their size permits incorporation at much higher concentrations and renders them easier to chemically modify (Hern and Hubbell, 1997). The combination of relatively non-adhesive hydrogels and adhesion peptides provide the opportunity to promote specific cellular interactions while discouraging other unwanted cellular interactions. This property can allow one to

create cell-selective materials by utilizing adhesion ligands that interact with receptors found on limited cell types. For example, the peptide REDV has been used to create an endothelial cell-selective material (Massia and Hubbell, 1992).

Several peptides have been functionalized through the reaction of the N-terminal primary amine with an N-hydroxysuccinimidyl ester of PEG monoacrylate (Hern and Hubbell, 1997; Mann and West, 2002; Mann *et al.,* 2001a and 2001b). This chemically modified peptide could then be incorporated throughout the bulk of the hydrogel during rapid photopolymerization of the acrylate endgroups. RGD-containing peptides immobilized with a MW 3400 spacer arm specifically promoted spreading of human foreskin fibroblasts on PEG diacrylate hydrogels, while the control peptide YR<u>DG</u>S did not promote any significant spreading (Hern and Hubbell, 1997). Thus, PEG diacrylate hydrogels did not support nonspecific spreading and the RGD-containing peptide was available and recognized by cell surface receptors to mediate adhesion to the substrate.

Cell adhesion peptides also exert effects on other aspects of vascular smooth muscle cell behavior. ECM production was decreased when smooth muscle cells were seeded on glass surfaces modified with either RGDS, VAPG, or KQAGDV compared to control surfaces with no adhesive ligand (Mann *et al.,* 1999). Migration and proliferation were also lowered as the surface concentration increased for surfaces modified with each peptide (RGDS, VAPG, and KQAGDV) (Mann and West, 2002). Thus, it may be necessary to optimize smooth muscle cell adhesion to scaffolds simultaneously with migration, proliferation, and ECM production. PEG diacrylate hydrogels are advantageous because this scaffold material provides the opportunity to control the identities and concentrations of adhesive peptides presented to cells. This enables one to

study the effects of cell interactions with adhesive peptides on cell behavior and matrix synthesis. This information can then be used to specifically guide tissue formation within engineered constructs.

Growth Factor Incorporation in Hydrogel Scaffolds

In addition to cell adhesion, hydrogel scaffolds should support robust ECM production in order to maintain the mechanical integrity of the engineered tissue as the scaffold material degrades. Mann *et al.* (1999) showed that increased cell adhesion to glass surfaces modified with adhesive peptides could result in decreased ECM protein production. Matrix production by vascular smooth muscle cells, however, was increased in the presence of transforming growth factor-$\beta 1$ (TGF-$\beta 1$) on glass surfaces modified with the adhesion peptides, RGDS and KQAGDV (Mann *et al.*, 1999). Thus, the decrease in ECM synthesis caused by immobilized cell adhesion ligands was counteracted by TGF-$\beta 1$. In addition, TGF-$\beta 1$ was covalently attached to a polymer chain retaining its ability to increase ECM production (Mann *et al.,* 2001a). Acryloyl-PEG-TGF-$\beta 1$ was then tethered to a hydrogel scaffold and stimulated increased collagen production by vascular SMCs that exceeded the amount produced by cells exposed to unmodified TGF-$\beta 1$ (Mann *et al.,* 2001a). The unmodified TGF-$\beta 1$ probably diffused out of the hydrogel scaffold and into the culture medium or was internalized by cells, while the tethered TGF-$\beta 1$ remained within the hydrogel scaffold since it is covalently bound. Thus, TGF-$\beta 1$ can be tethered to hydrogel scaffolds with retention of activity and result in improved collagen production.
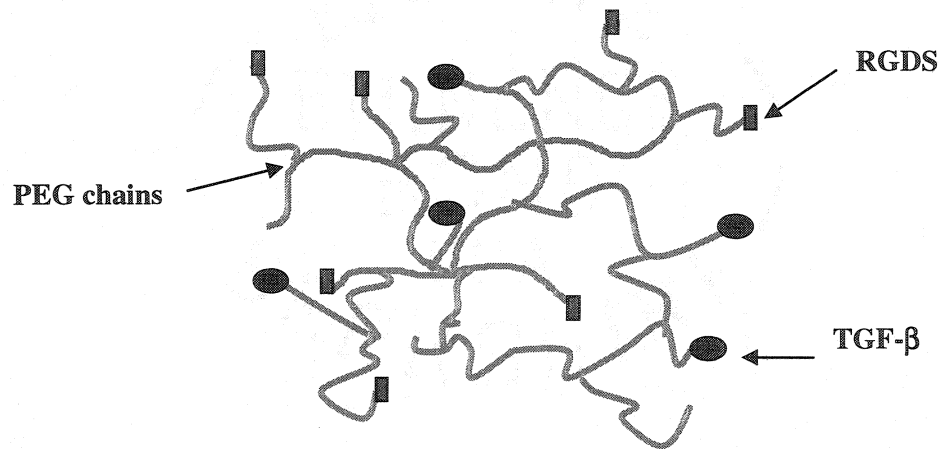
Figure 5. This schematic depicts the covalent immobilization of bioactive factors within hydrogel scaffolds. The bioactive factors can include adhesion peptides such as RGDS and growth factors like TGF-β, which enable cells to interact with the scaffold. Meanwhile, the PEG chains form a crosslinked network that is resistant to protein adsorption.

Proteolytically Controlled Degradation of Hydrogel Scaffolds

Scaffolds should initially provide support for tissue formation, but degrade to make room for new tissue synthesized by the cells. Sequences can be incorporated into PEG diacrylate gels that cells degrade by releasing proteolytic enzymes, typically as they migrate (West and Hubbell, 1999). As the scaffold degrades, the cells can synthesize ECM proteins to replace scaffold material. Thus, scaffold degradation makes room for new tissue formation eventually leaving only natural tissue.

Since proteases specifically degrade components of the ECM, degradable hydrogel scaffolds can be formed by incorporating these components. Polyalanine (AAA) could be incorporated as it has been shown to be highly specific for elastase (Feinstein *et al.,* 1973). NRV and LGPA are additional sequences specifically degraded by plasmin or collagenase (West and Hubbell, 1999). As depicted in Figure 6, these

sequences can be incorporated into the backbone of the polymer and subsequently

degraded if the specific protease is present. Thus, we can tune the degradation of the

polymeric scaffold to tissue formation and potentially create materials that are

preferentially degraded by specific cell types. In contrast, type I collagen scaffolds allow

cells to migrate independently of proteolytic enzymes due to the collagen networks'

larger mesh size (Hubbell, 2003). PGA and/or PLA scaffolds have a pore size on the

order of microns and as a result enable cells to migrate regardless of proteolytic enzyme
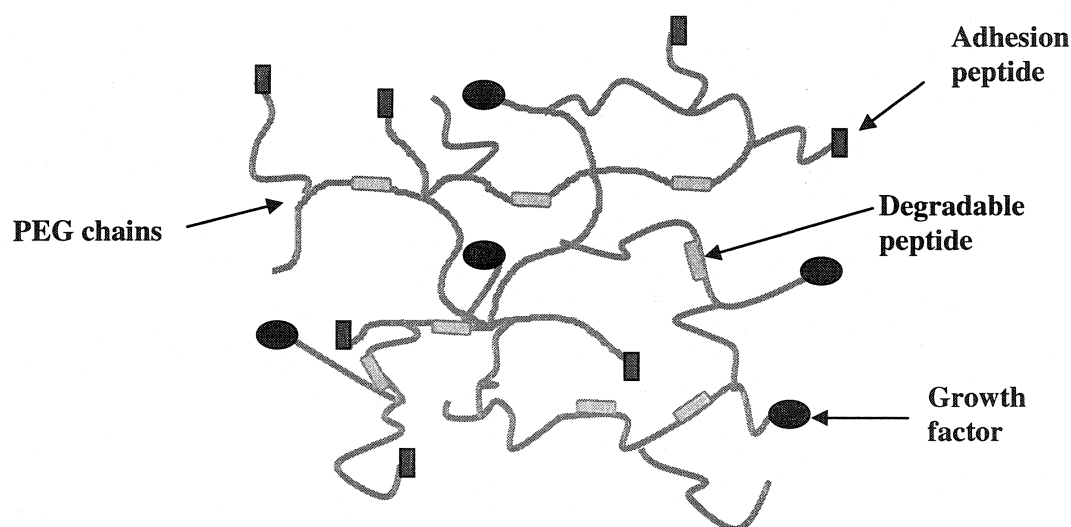
activity.

Figure 6. This schematic depicts the bioactive scaffold, which contains covalently immobilized adhesion peptides and growth factors and peptide sequences that are susceptible to degradation by proteolytic enzymes.

CONCLUSIONS

Signals present within the ECM have profound effects on cell behavior. These

include dramatic effects on cell proliferation, differentiation, and matrix production by

cell adhesion molecules and growth factors. It is critical that the interactions between

cells and these environmental signals be understood and appropriately controlled in order

to guide tissue formation within scaffolds. PEG diacrylate hydrogel scaffolds are inherently cell non-adhesive, but can be modified to specifically interact with cells through the covalent incorporation of bioactive factors. These bioactive factors may include combinations of cell adhesion peptides and growth factors. Thus, we can control the identity and concentration of bioactive molecules that cells are exposed to within hydrogel scaffolds. Additionally, PEG-based hydrogels can be modified to degrade in response to proteolytic enzymes secreted by entrapped cells. This characteristic better mimics the natural ECM and when combined with the optimum bioactive factors can potentially result in engineered tissues with the appropriate structural and functional features. This will enable us to better understand tissue formation within bioactive scaffolds and use this information to specifically and reproducibly guide tissue formation. This research extends the opportunities available to control cell interactions with PEG-based hydrogel scaffolds to include control over the spatial distribution of bioactive factors and the use of covalently immobilized bFGF to influence cell proliferation, migration, and alignment. Hydrogels have also been designed to allow cells to specifically remodel the scaffold by secreting MMPs.

These modifications have the potential to improve the formation of a variety of engineered tissues. However, there are opportunities that readily come to mind for the application of these bioactive scaffolds towards the development of tissue-engineered vascular grafts. These tissue-engineered blood vessels should mimic the structure and function of native vessels in order to result in similar long-term patency. Normal arteries have a multilayered structure consisting of three main cell types and their associated matrix. The three layers are depicted in Figure 7 and include: an inner layer called the

intima, an intermediate layer called the media, and an outer layer called the adventitia.

Cells in each layer play an important role in the blood vessel's function including a

monolayer of endothelial cells in the intimal layer, which prevents thrombosis and

releases molecules like nitric oxide that help regulate vascular smooth muscle cell

behavior. In contrast, the smooth muscle cells in combination with alternating layers of

ECM proteins confer the majority of the artery's mechanical properties. In addition, this

medial-smooth muscle cell layer is responsible for the contractile and dilatory responses

of the artery to external stimuli. PEG hydrogel scaffolds provide the opportunity to direct

the formation of tissue-engineered vascular grafts. These bioactive scaffolds have the
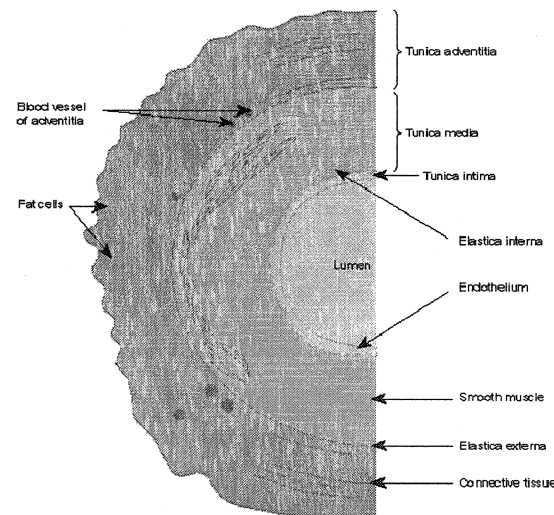

Figure 7. Normal arteries contain three main layers: an intima, media, and adventitia. The intima is a monolayer of endothelial cells that helps prevent thrombosis. The media consists of alternating layers of SMCs and ECM proteins that confer the majority of the artery's mechanical properties. The adventitia contains mostly fibroblasts along with the artery's nerve and blood supply (http://fellows.emma.cam.ac.uk/barnes/THE_STRUCTURE_AND_FUNCTION_OF BLOOD_VESSELS.HTM, 3 DEC 2001).

potential to direct the migration of vascular cell types to specific regions of the tissue-engineering scaffold using a combination of cell-type specific adhesive peptide sequences and gradient presentation. In addition, gradient presentation can potentially result in improved endothelial coverage of the blood-contacting layer of the engineered tissue by directing cell migration onto the tissue-engineering scaffold. Mitogens like basic fibroblast growth factor can also be used to stimulate vascular endothelial and smooth muscle cell proliferation in order to achieve cell densities comparable to those found in native blood vessels. These applications should result in engineered tissues that better mimic the cell density and overall organization of native blood vessels.

CHAPTER 2: COVALENTLY IMMOBILIZED GRADIENTS OF RGD FOR DIRECTED CELL MIGRATION

INTRODUCTION

The spatial distribution of proteins can play an important role in the organization

of tissues. Protein gradients, for example, can provide necessary biochemical cues that

direct the organized formation of tissue (Swartz, 2003). This role impacts

embryogenesis, capillary sprouting, and wound healing. In wound healing, for example,

chemotactic factors released by platelets and macrophages can recruit fibroblasts into the

wound where the fibroblasts in part repopulate the wound and deposit connective tissue

(Clark, 1988). Protein gradients may also be useful for optimizing engineered tissue

formation by enhancing migration and the recruitment of cells into scaffolds.

Researchers have developed a number of techniques that enable one to control the spatial

distribution of proteins. However, these methods are limited to two-dimensional

applications or are very short term in their protein gradient presentation.

Photolithography techniques, for example, have made it possible to restrict cell

adhesion to specific areas of a biomaterial surface. Singhvi *et al.* imprinted nonadhesive

gold surfaces with patterns of self-assembled monolayers (SAMs) using an elastomeric

stamp with defined features (1994). The stamp exposed the gold surface to

hexadecanethiol, while the remaining regions were exposed to a solution of polyethylene

glycol-terminated alkanethiol to form SAMs resistant to protein adsorption. This

produced protein adsorptive regions with lateral dimensions ranging from 2 to 80 μm.

This surface was subsequently exposed to the extracellular matrix protein, laminin, which

resulted in cell-adhesive regions of defined geometry. These regions matched the pattern provided by the elastomeric stamp, which formed SAMs of hexadecanethiol. Cell adhesion was then mostly restricted to the protein-covered regions. In addition, many cells mimicked the square and rectangular shape of the laminin-adsorbed areas. Since cell shape influences cell proliferation and function, hepatocyte proliferation, in turn, was affected by the extent that the cells could spread out on adhesive islands of varying area. DNA synthesis was highest (60%) when hepatocytes could spread out on unpatterned surfaces. In contrast, DNA synthesis was reduced to 3% on the smallest adhesive regions where the surface area was less than 1600 μm^2. Thus, photolithographic methods can provide opportunities to control cell behavior by defining the geometry and distribution of regions that can adsorb proteins. Although this technique is relatively simple to apply and flexible in providing a range of shapes and sizes that can be dictated, it is difficult to apply this method to three-dimensional constructs. The selected protein—laminin can also be easily displaced by the adsorption of alternative serum proteins that can alter cell behavior in undesirable ways.

In addition to providing patterns of cell-adhesive and cell non-adhesive regions, photolithographic techniques can also enable the formation of immobilized protein gradients. Immobilized gradients of EGF and heparin were prepared by using a photomask with a gradient micropattern (Chen and Ito, 2001; Ito *et al.*, 2001). Chinese hamster ovary cell growth on EGF-immobilized gradients depended on cell position. After 48 hours, a higher density of cells was observed in regions of high EGF density. NIH-3T3 cells were also affected by heparin immobilized gradients. In regions of high heparin density, cell growth was reduced. The addition of basic fibroblast growth factor

(bFGF) reversed the effect of high heparin density alone—increasing cell growth in regions of high heparin density because heparin activates bFGF's stimulatory effect on cell proliferation. Thus, stable gradients of immobilized protein can be patterned onto surfaces using photolithographic techniques and retain their effect on cell growth. Since the effect on cell growth also depended on protein concentration, these studies further illustrate the importance of controlling bioactive factor presentation in order to direct cell behavior.

Such techniques for immobilizing proteins to surfaces have only recently been available. Traditionally, researchers have studied the effects of soluble protein gradients using methods such as the Boyden chamber and under-agarose assays (Boyden, 1962; Nelson *et al.,* 1975). In the Boyden chamber assay, cells are initially seeded on one side of a chamber that is separated by a porous filter membrane into two compartments. A chemotactic factor is added to the other compartment and then allowed to diffuse through pores in the filter membrane. Cells can respond to the chemotactic factor by actively migrating through the pores, and thus, provide an indication of a protein's chemotactic activity. The under-agarose assay is a similar system that relies on the diffusion of a chemotactic factor (Nelson *et al.,* 1975). In this system, a tissue culture dish is filled with agarose. Chemoattractant diffuses from wells in the agarose to form a gradient. Cells initially seeded within wells are then monitored as they migrate towards the chemoattractant source. These assays, generally, demonstrate the chemotactic activity of a protein on a population of cells. These assays are also limited to studying two-dimensional chemotaxis.

Alternative methods exist that enable the study of three-dimensional chemotaxis *in vitro* combined with continuous monitoring and recording of cell tracks. Moghe *et al.* assayed neutrophil migration in a fibrin gel where the cells were uniformly dispersed (1995). A gradient of interleukin-8 (IL-8) was presented via "free-diffusion" from a conjoined fibrin gel that caused neutrophils to migrate up the concentration gradient rather than randomly. This system also allowed direct cell tracking using time-lapse video microscopy and automated cell tracking methods. Thus, this system combines direct cell tracking with a relevant three-dimensional model of the extracellular matrix to assay neutrophil chemotaxis. Unfortunately, the IL-8 gradient fades quickly (within a few hours) as it diffuses away. As a result, this system is unsuitable for studying the chemotactic response of slower-moving cells like fibroblasts and smooth muscle cells.

Knapp *et al.* modified the assay of Moghe *et al.* in order to study the chemotactic response of slower-migrating cells like fibroblasts, smooth muscle cells, and endothelial cells (1999). To accomplish this, a barrier was used to divide the three-dimensional fibrin gel into two regions. A small gap in the barrier allowed for the diffusion of a peptide, GRGDSP that is reported to be chemotactic for fibroblasts. This modification extended the time course available for presenting a stable gradient of GRDGSP and resulted in opportunities to observe fibroblast alignment along with migration relative to the gradient axis. Unfortunately, a stable concentration gradient can only be maintained for 24 hours. Gradient effects on tissue formation will require longer exposure times not possible with this system. Additionally, this system cannot be used in combination with mechanical forces or *in vivo* as the gradient can be easily disrupted by agitation. Finally, there are also biochemical cues intrinsic to the fibrin gel that can influence cell behavior

and migration making it difficult to control the presentation of bioactive factors. Sequences in fibrin, for example, can interact with cells and extracellular matrix proteins, which can increase fibroblast and endothelial cell proliferation and promote angiogenesis (Mosesson *et al.,* 2001; Van Hinsbergh *et al.,* 2001).

Thus, several technologies exist that aid in controlling the pattern of bioactive factor presentation. These strategies, however, fall short in enabling the sustained presentation of protein patterns in three-dimensional biomaterials. In contrast, PEG-based hydrogel scaffolds provide the opportunity to control the identity and concentration of adhesive peptide presentation. For example, fibroblasts, osteoblasts, and vascular smooth muscle cells (SMCs) have all been shown to adhere to and grow on PEG-based hydrogel scaffolds when these scaffolds were modified with adhesion peptides (Hern and Hubbell, 1997; Burdick and Anseth, 2002; Mann *et al.,* 2001; Gobin and West, 2003). Notably, the incorporation of adhesion peptides was required for cells to interact at any significant level with the hydrogel scaffolds. Cell attachment and spreading were also shown to vary depending on the bulk peptide concentration. These cell-interactive effects are due to PEG's hydrophilicity and the ability to covalently incorporate bioactive factors. In summary, PEG-hydrogel scaffolds provide a blank slate to which cell adhesion peptides can be added in a controlled fashion to enable cell interaction with PEG-based hydrogel scaffolds.

Although these cell adhesion studies focused on two-dimensional cell interaction with nondegradable PEG hydrogels, these scaffolds can be further modified to promote three-dimensional remodeling of hydrogel constructs. For example, protease-sensitive peptide sequences can be inserted into the backbone of PEG-polymer chains. These

sequences can then be cleaved to make room for cell proliferation, extracellular matrix protein production, and migration. Thus, PEG-hydrogels may provide a solution for controlling the pattern of bioactive factor presentation in a three-dimensional tissue engineering scaffold.

This study extends the capability for directing cell behavior using PEG-based hydrogels to include control over the spatial distribution of cell adhesion peptides. Gradient hydrogels are formed by adapting a gradient maker normally used to make polyacrylamide gels for electrophoresis. A continuous linear gradient is formed using the gradient maker to control how polymer solutions containing varying concentrations of the fibronectin-derived adhesive peptide, RGDS, are combined and then locking the gradient in place via photopolymerization as it is poured into a mold. The ability to make gradient hydrogels with varying slopes was assessed and the effect of RGD-gradients on fibroblast alignment and cell migration was studied. A concentration gradient may mimic the presentation of bioactive factors found *in vivo* and may be useful for eliciting enhanced and directional cell migration, which may be useful for optimizing tissue formation.

MATERIALS AND METHODS

Cell maintenance

Human dermal fibroblasts (HDFs) were obtained from Clonetics (San Diego, CA). They were maintained at 37°C/5% CO_2 on Dulbecco's modified Eagle medium (DMEM) supplemented with 10% fetal bovine serum (FBS, BioWhittaker, Walkersville, MD), 2 mM L-glutamine (Sigma, St. Louis, MO), 1000 units/l penicillin (Sigma, St. Louis, MO) and 100 mg/l streptomycin (Sigma, St. Louis, MO). All experiments were conducted using cells at passages 8-12.

PEG diacrylate synthesis

As depicted in Figure 1, PEG diacrylate was synthesized by dissolving 12 g dry PEG (6000 Da; Fluka, Milwaukee, WI) in 36 ml anhydrous dichloromethane. 0.25 g
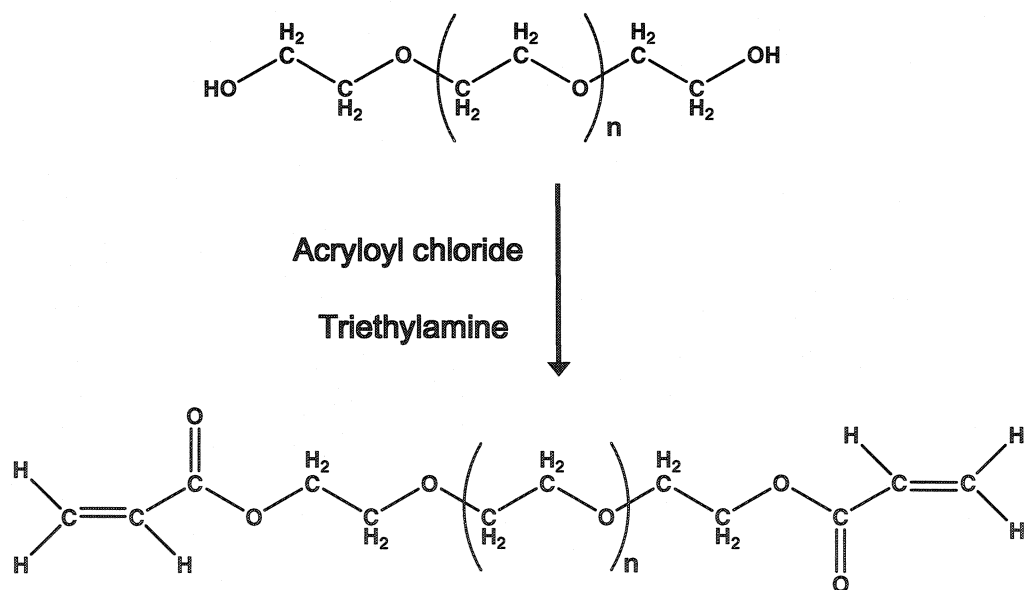
Figure 1. Reaction scheme for the synthesis of PEG diacrylate.

triethylamine and then 0.43 g acryloyl chloride (Lancaster Synthesis, Windham, NH) were added dropwise, and the mixture was stirred under argon for 48 hr. The resulting solution was then washed with 2 M K_2CO_3 and separated into aqueous and dichloromethane phases to remove HCl. The dichloromethane phase was subsequently dried with anhydrous $MgSO_4$ (Fisher Scientific, Pittsburg, PA), and the PEG diacrylate was then precipitated in diethyl ether, filtered, and dried under vacuum at room temperature overnight. The resultant polymer was dissolved in N,N-dimethylformamide-d_7 (Sigma, St.Louis, MO) and characterized via proton NMR (Avance 400 MHz; Bruker, Billerica, MA) to determine the degree of acrylation.

A cell adhesive component was prepared by reacting acryloyl-PEG-NHS with the adhesion peptide, RGDS (American Peptide, Sunnyvale, CA), in 50 mM sodium bicarbonate (pH 8.5) at a 1:1 molar ratio for 2 hr. The solution was then lyophilized and stored at -20°C. PEG-peptide conjugates and PEG standards were analyzed using gel permeation chromatography equipped with UV/vis (260 nm) and evaporative light-scattering detectors (Polymer Laboratories, Amherst, MA).

Detection of entrapped gradients of BSA

As depicted in Figure 2, hydrogels containing gradients of entrapped BSA were formed using a gradient maker (CBS Scientific Co., Del Mar, CA) to pour the hydrogel precursor solutions prior to photopolymerization. Gradient flow was controlled by a Teflon valve centered between two chambers containing polymer solution with or without BSA. Coomassie Brilliant Blue Staining Solution (BioRad, Hercules, CA) was then used to detect the entrapped BSA gradient. Briefly, hydrogels containing a gradient

of 0 to 2 mg/ml and 0 to 1 mg/ml of BSA were rinsed in PBS (Sigma) for 1 hr and

subsequently stained with 1.5 ml Coomassie blue staining solution in 50 ml PBS. After 2

hr, the gels were scanned, converted to grayscale, and then assessed for mean staining
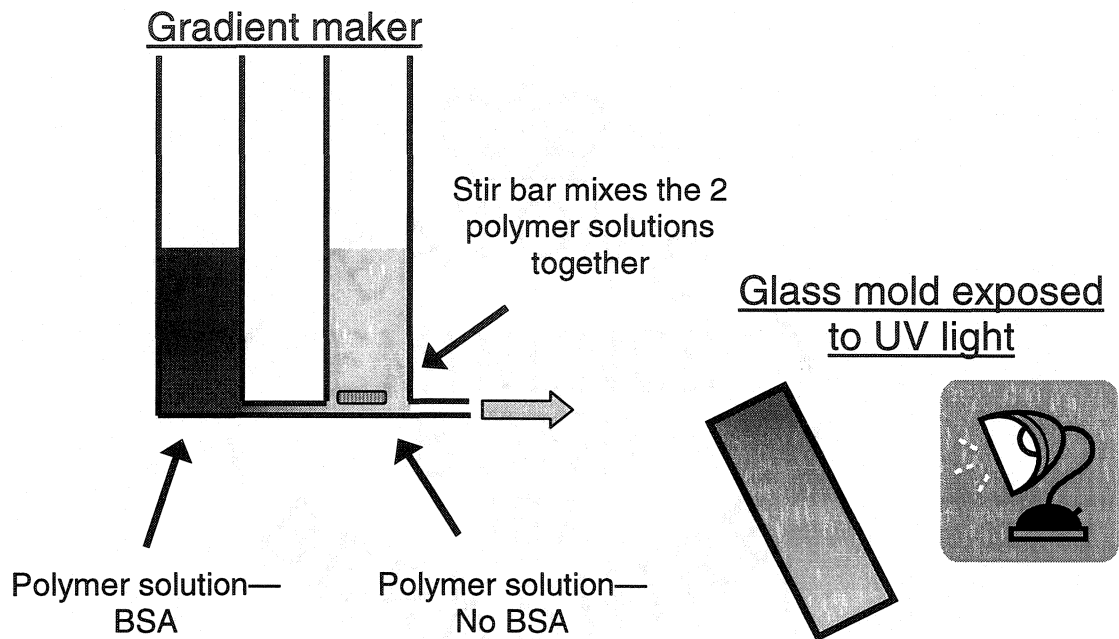
intensity at 0.5 cm increments using Image J (NIH, http://rsb.info.nih.gov/ij/).

Figure 2. Gradient hydrogels were formed using a gradient maker as depicted above in combination with a peristaltic pump to control the combination of polymer solutions with and without BSA. The resulting polymer solution is then poured into a mold where it is exposed to UV light to lock in the concentration gradient.

Cell alignment on hydrogel surfaces with a gradient of tethered RGDS

A hydrogel with a gradient of tethered RGDS was formed using a gradient maker

as described above (CBS Scientific Co., Del Mar, CA). In this study, the gradient maker

chambers contained polymer solution with and without the PEG-RGDS conjugate. Both

polymer solutions contained 0.1 g/ml PEG diacrylate and 10 µl/ml of 2,2-dimethyl-2-

phenyl-acetophenone in N-vinylpyrrolidone (300 mg/ml). The polymer solutions were

slowly combined in a rectangular glass mold (2 mm thickness) and exposed to long

wavelength UV light (365 nm, 10 mW/cm^2) to form a hydrogel with tethered RGDS

ranging from 0 to 1 µmol/ml. Control hydrogels were also formed from polymer

solutions containing a constant concentration of the PEG-RGDS conjugate (0.75

µmol/ml). These hydrogels contained the same concentrations of PEG diacrylate and

2,2-dimethyl-2-phenyl-acetophenone in N-vinylpyrrolidinone as the hydrogel with a

gradient of tethered RGDS. Cells were then seeded on the gels at a density of 10,000

cells/cm^2 and allowed to attach overnight. After 1, 2, and 4 days, hydrogel surfaces were

photographed in several areas and assessed for cell alignment under phase contrast

microscopy using Image J. Cell alignment was determined for each cell by measuring

the cell's angle relative to the direction of the RGDS gradient. Cell angles were

determined for at least 100 cells on each hydrogel surface, and then these angles were

categorized into nine different groups based on their relative angle to the RGDS gradient.

These groups included cells positioned relative to the RGDS gradient within ± 0 to 10, 10

to 30, 30 to 50, 50 to 70, or 70 to 90 degrees.

Cell migration on hydrogel surfaces with a gradient of tethered RGDS

As depicted in Figure 3, cell migration was also assessed on hydrogel surfaces

with a gradient of tethered RGDS (0 to 6 umol/ml or 0 to 12 umol/ml). Cells were

seeded within a square stainless steel mold (7.7 mm × 7.7 mm × 10.1 mm), which was

positioned 1.5 cm above the gradient hydrogels bottom edge and compared to cells

seeded on hydrogels with a constant concentration (2 or 6 µmole/ml) of tethered RGDS.

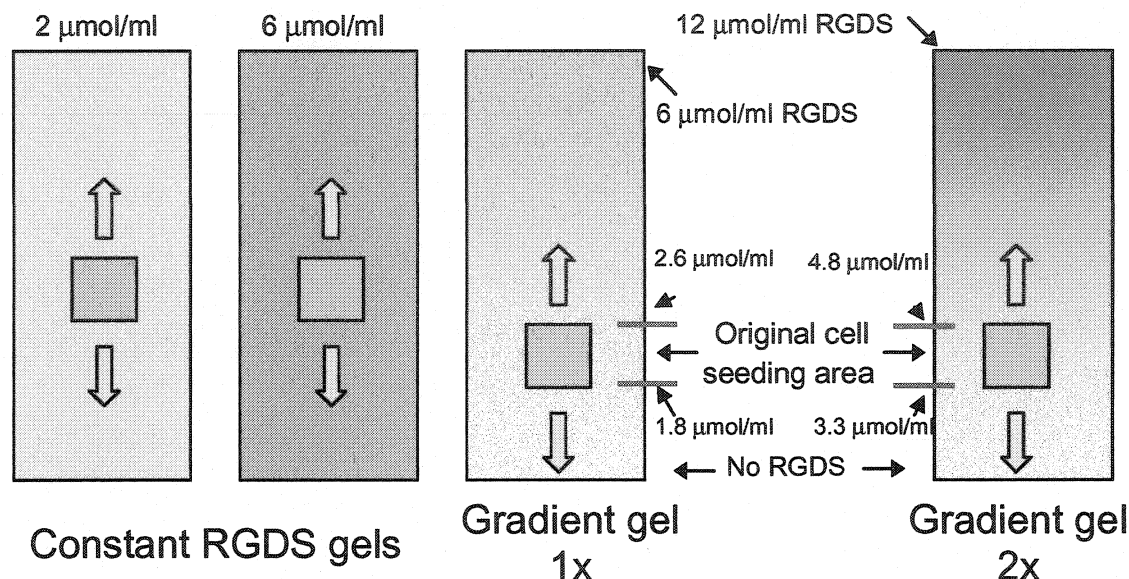For the 1x gradient hydrogel, the starting edge concentrations were 2.6 and 1.8 µmol/ml,

Figure 3. This schematic depicts the setup for the gradient migration study. Fibroblast migration was monitored in the directions of increasing and decreasing RGD concentrations on each of the RGD-gradient hydrogels containing either 1 to 6 μmol/ml RGD (1x gradient) or 1 to 12 μmol/ml RGD (2x gradient). This migration was compared to migration on each of the control hydrogel surfaces (2 μmol/ml and 6 μmol/ml RGD).

respectively, for the top and bottom edges. For the 2x gradient hydrogel, the starting edge concentrations were 4.8 and 3.3 μmol/ml, respectively, for the top and bottom edges. In addition to the various concentrations of tethered RGDS, the hydrogels contained 0.1g 6k PEG diacrylate and 10 μl/ml 2,2-dimethoxy-2-acetophenone in N-vinylpyrrolidinone. Cells were given a chance to attach and adhere to the hydrogels. After 27 hr, the stainless steel ring creating the initial boundary was then removed, and the cells were photographed under phase contrast microscopy. Two days later, the cells were photographed again.

Statistical analysis

Data sets were compared using Minitab 14 (downloaded from www.minitab.com) to perform a one-way analysis of variance (ANOVA) followed by post hoc comparisons using Tukey to determine which means were significantly different. In addition, two factors (time and cell angle) were analyzed using the General Linear Model to perform univariate analysis of variance on an unbalanced design. This two-factor analysis was followed by multiple comparisons using Tukey. P-values less than 0.05 were considered statistically significant. All values are reported as the mean and standard deviation of the mean.

RESULTS

Detection of entrapped gradients of BSA

The gradient maker was used to form hydrogel scaffolds containing a gradient of entrapped BSA. Coomassie blue staining made the BSA gradient visible so that it could be analyzed using digital image processing. As depicted in Figure 4, the staining density increased linearly in the direction of increasing BSA concentration. This trend was
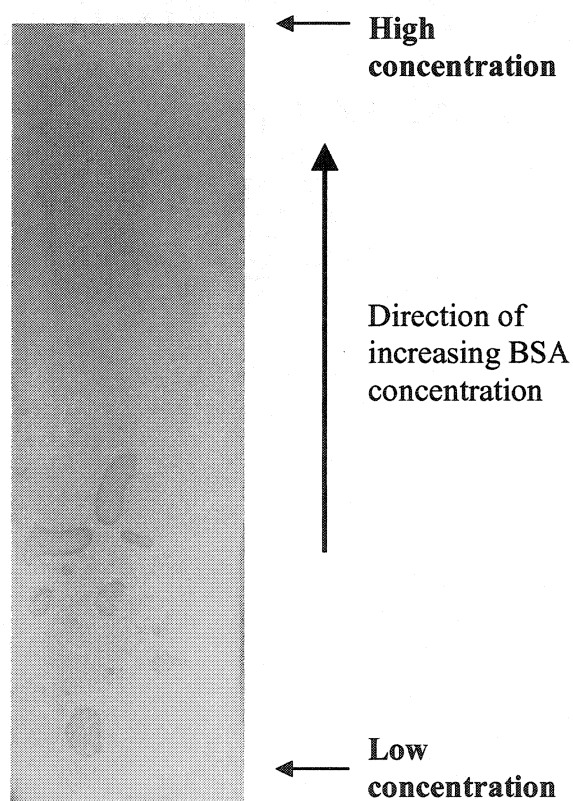

Figure 4. Representative image of a BSA-gradient hydrogel stained with Coomassie brilliant blue. Staining intensity increased with increasing concentrations of BSA.

evident for both hydrogel scaffolds examined regardless of BSA concentration range. However, the steepness of the gradient slope depended on the concentration range of incorporated BSA. As shown in Figure 5, the gradient slope for the hydrogel scaffold

containing BSA concentrations ranging from 0 to 2 mg/ml, was approximately two times

steeper than the gradient slope for the other hydrogel scaffold where the BSA
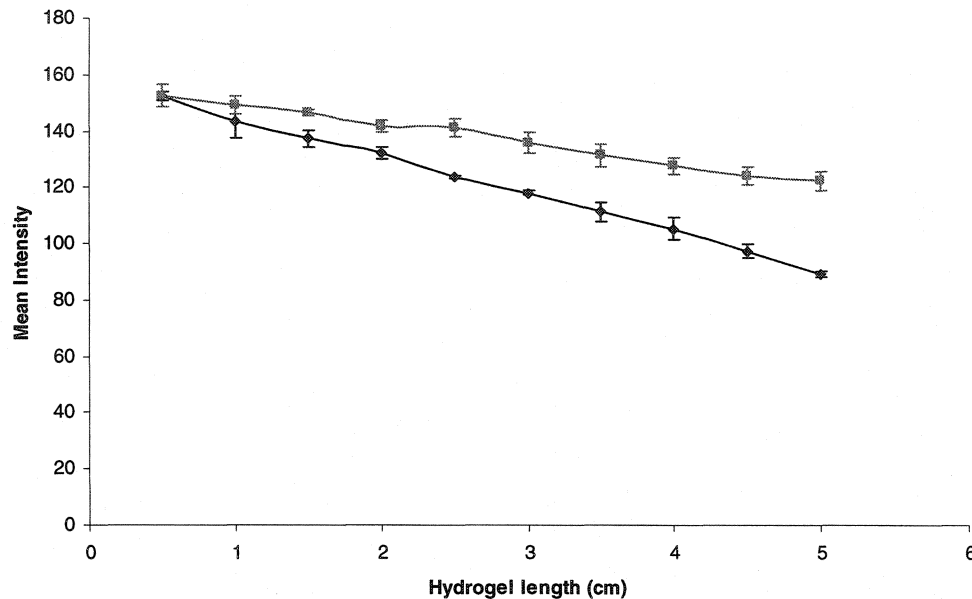
concentration ranged from 0 to 1 mg/ml.

**Figure 5. Hydrogels with varying gradient slopes (0 to 2 mg/ml and 0 to 1 mg/ml)
were stained with Coomassie brilliant blue and then scanned and analyzed for mean
stain intensity. The gradient slopes depended on BSA concentration: hydrogels with
BSA ranging from 0 to 2 mg/ml had a slope that was 2 times the slope of the
hydrogel with BSA ranging from 0 to 1 mg/ml.**

Cell alignment on hydrogel surfaces with a gradient of tethered RGDS

Alignment of human dermal fibroblasts in response to immobilized gradients of

the adhesion peptide, RGD, was examined and compared to cell alignment on hydrogels

containing a constant concentration of RGD. As shown in Figures 6 and 7, fibroblasts

aligned on gradient hydrogel scaffolds in the direction of increasing RGD concentration.

This alignment was evident on all regions of the RGD-gradient hydrogel within 1 day

after seeding, but did not occur on control hydrogels with a constant concentration of
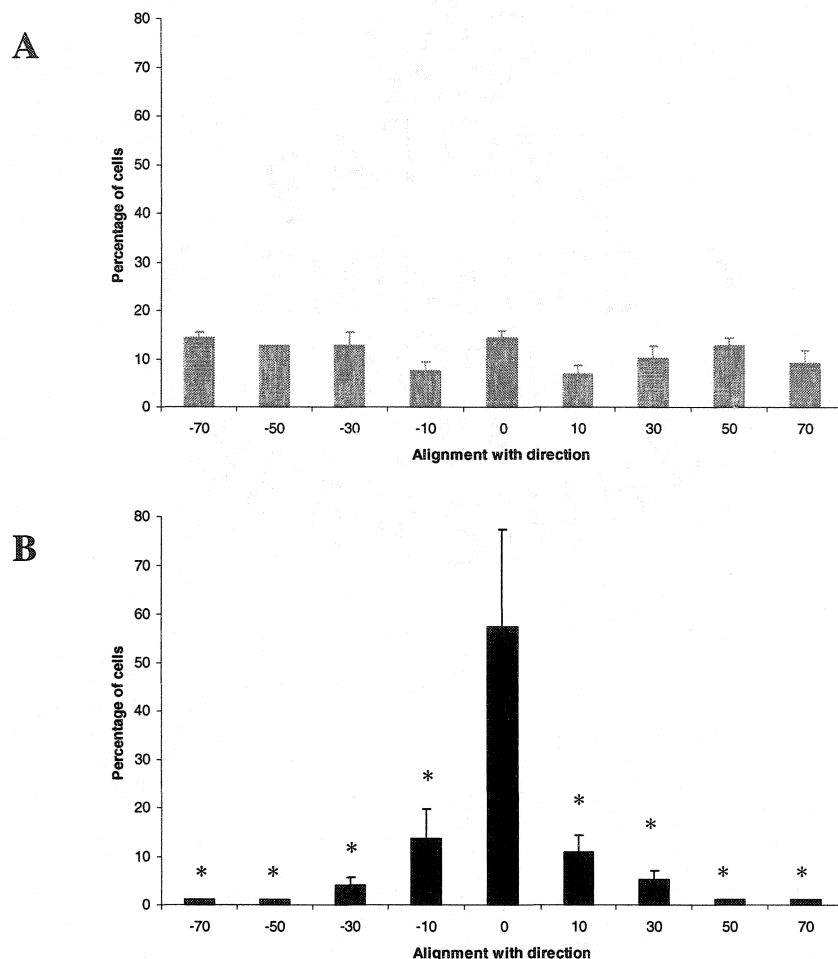
Figure 6. A gradient of tethered RGD influenced cell alignment (B). More fibroblasts were aligned in the direction of increasing RGD concentration than on the control hydrogel surface, which lacked an RGD gradient (0.75 μmol/ml RGD, A). (*) p < 0.05 compared to cells aligned with the gradient axis (within ±10°).

RGD (0.75 μmol/ml). Further, cell alignment increased with time. Maximum cell alignment, as shown in Figure 8, was observed after 4 days where ~58% of cells aligned with the RGD-gradient axis (±10°) compared to ~46% of cells aligned with the gradient axis (±10°) on day 1 (p < 0.05). In comparison, fibroblasts on control hydrogels were randomly distributed with cells showing no significant preference for alignment in any particular direction on these control surfaces (p < 0.52).
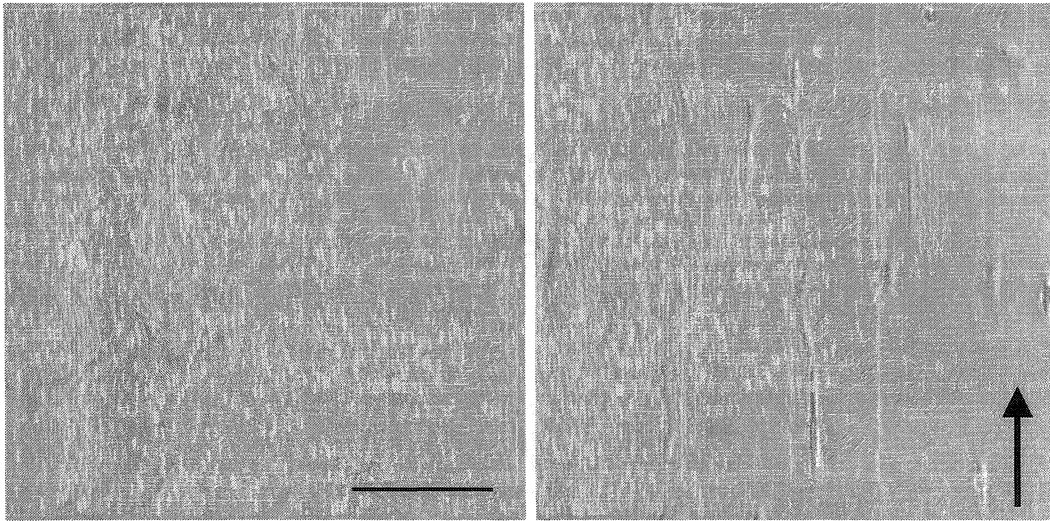
Figure 7. More fibroblasts were aligned on hydrogel surfaces with a gradient of tethered RGD (indicated by arrow) than on hydrogel surfaces containing RGD at a constant concentration (0.75 umol/ml; bar = 100 μm).

Cell migration on hydrogel surfaces with a gradient of tethered RGDS

Fibroblast migration depended on the presentation of covalently incorporated RGD on hydrogel surfaces. As shown in Figure 9, fibroblasts migrated ~52% further on hydrogel surfaces containing 6 μmol/ml PEG-RGD than on hydrogel surfaces containing 2 μmol/ml PEG-RGD. Fibroblasts also migrated further up the concentration gradient than down the concentration gradient. This RGD-gradient effect was evident on both gradient hydrogel surfaces where fibroblasts on the 1x gradient surface (0 to 6 μmol/ml RGD) migrated ~48% further going up the concentration gradient than going down and fibroblasts on the 2x gradient surface (0 to 12 μmol/ml RGD) migrated ~218% further going up the concentration gradient than going down the concentration gradient. Fibroblasts migrated furthest up the 2x gradient hydrogel surface, although this migration distance was not significantly different from the control hydrogel surface with
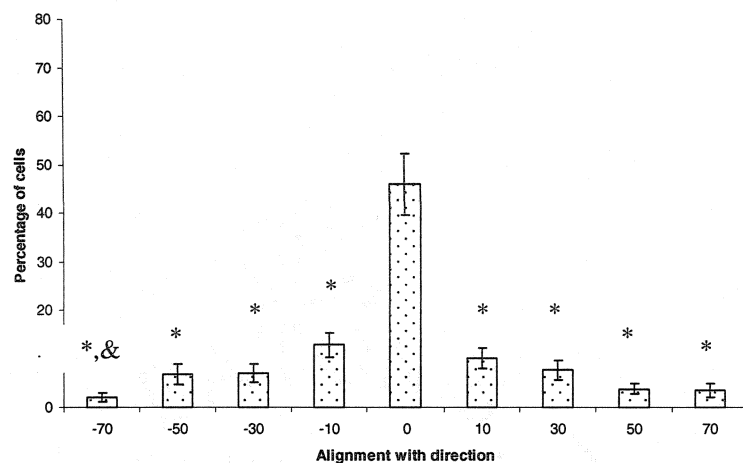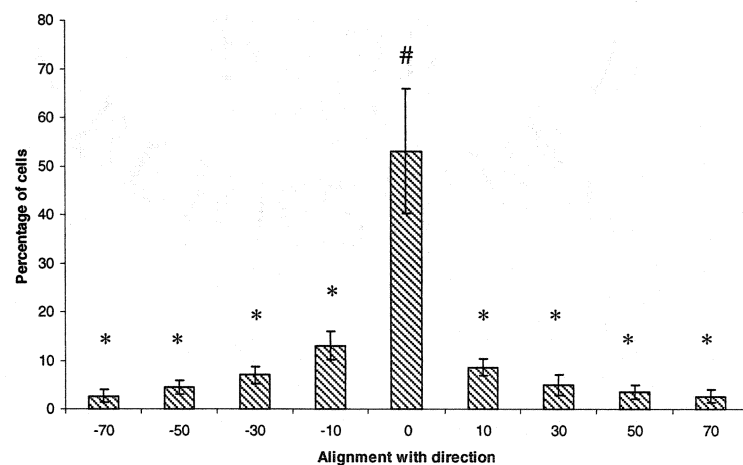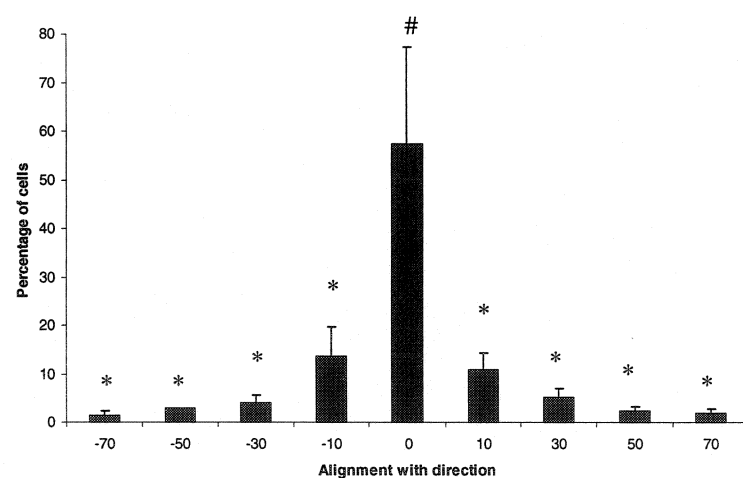
Figure 8. Cell alignment was evident within 24 hours (~46% of cells aligned relative to the gradient axis) and became slightly more apparent with time on the RGD-gradient hydrogel surfaces. Maximum cell alignment was observed after 4 days where ~58% of cells were aligned with the RGD-gradient axis. (*) $p < 0.05$ compared to cells aligned with the gradient axis. (#) $p < 0.05$ compared to cells aligned with the gradient axis at 24 hours.(&) $p < 0.05$ compared to cells with angles ranging from -10 to 0 degrees.
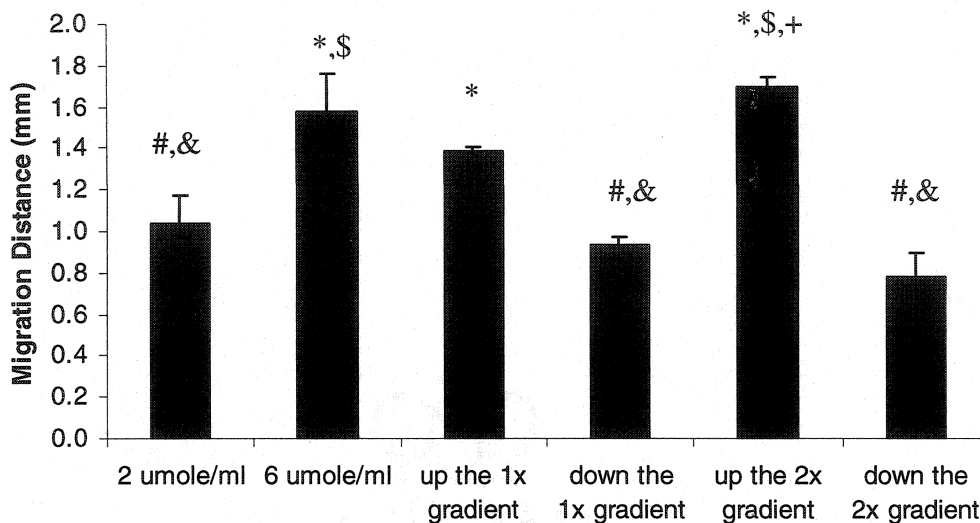
Figure 9. Fibroblast migration depended on the presentation of RGDS. Fibroblast migration was increased on RGD-gradient hydrogels compared to control hydrogels with a constant concentration of RGD (2 μmol/ml). This migration response was further enhanced by increasing the gradient slope. In contrast, migration down the concentration gradient was decreased. (*) $p < 0.05$ compared to fibroblast migration on the control hydrogel surface containing 2 μmol/ml tethered RGD. (#) $p < 0.05$ compared to fibroblast migration on the control hydrogel surface containing 6 μmol/ml tethered RGD. (&) $p < 0.05$ compared to fibroblast migration up the 1x RGD-gradient hydrogel.($) $p < 0.05$ compared to fibroblast migration down the 1x RGD-gradient hydrogel. (+) $p < 0.05$ compared to fibroblast migration down the 2x RGD-gradient hydrogel.

6 μmol/ml RGD. Fibroblast migration was reduced going down the 2x gradient hydrogel surface and was significantly different from fibroblast migration on all surfaces with the exceptions of migration down the 1x gradient hydrogel surface and the control hydrogel surface containing 2 μmol/ml RGD.

DISCUSSION

PEG-based hydrogels are promising materials for use as tissue engineering scaffolds. These hydrogels provide the opportunity to more closely control bioactive factor presentation due to PEG's hydrophilicity and the ability to incorporate covalently

immobilized adhesion peptides (Merrill and Salzman, 1983; Gombotz *et al.,* 1991; Hern and Hubbell, 1998; Mann *et al.,* 2001). Previous studies demonstrated that RGD-peptide incorporation enables fibroblasts, osteoblasts, and smooth muscle cells to attach and spread on PEG hydrogels (Hern and Hubbell, 1998; Mann *et al.,* 2001; Burdick and Anseth, 2002). Cell attachment and spreading on hydrogel surfaces depended on the bulk concentration of incorporated RGD where increasing RGD concentrations enhanced cell adhesion. Alternative peptide sequences have also been investigated including fibronectin-derived, REDV, and elastin-derived, VAPG, which support cell adhesion on protein resistant substrates (Massia and Hubbell, 1992; Gobin and West, 2003). Thus, hydrogel scaffolds are useful for controlling both the identity *and* concentration of adhesion peptide presentation. This study extends the capability for directing cell behavior on hydrogel scaffolds to include the spatial distribution of the RGD-adhesion peptide.

Hydrogels with gradients of entrapped BSA were successfully formed by coordinating the use of a gradient maker to combine polymer solutions containing varying concentrations of BSA with photopolymerization of the resulting polymer solution. This system produced entrapped gradients of BSA that could be visualized by staining with Coomassie brilliant blue. Simply changing the relative BSA concentrations present in each of the gradient maker's chambers made it possible to control the range of BSA concentrations presented and the steepness of the gradient slope. This flexibility should be useful for optimizing the production of hydrogel scaffolds for particular applications where the incorporated peptide is presented at the appropriate concentration range and steepness. Since BSA was simply entrapped rather than covalently

immobilized, it may also be possible to apply this system to three-dimensional applications where the hydrogel contains sequences susceptible to proteolytic degradation. That is, soluble proteins could be released from the hydrogel scaffold as cells secrete proteases that break down the hydrogel. Lutolf *et al.*, for example, used a similar system to promote bone formation in critical-sized defects of rat crania (2003). PEG-based scaffolds containing MMP-sensitive linker substrates and entrapped bone morphogenetic protein-2 (BMP-2) recruited cells to infiltrate the scaffold and replace it with bony tissue. Perhaps, bone formation can be further improved in this system by controlling the three-dimensional presentation of the soluble growth factor. Three-dimensional gradients of BMP-2 can make this possible by enhancing cell infiltration into the hydrogel scaffold such that cells migrate up a concentration gradient of BMP-2.

Since staining with Coomassie brilliant blue confirmed the production of entrapped gradients of BSA in PEG-based hydrogel scaffolds, gradient hydrogels with covalently immobilized RGD were also formed and examined for their effect on cell morphology. Cells responded dramatically to the presentation of an RGD-gradient by aligning with the gradient axis. This alignment was detected as early as 1 day after seeding where ~46% of cells aligned with the gradient axis (within $\pm 10°$). Cells also remained aligned for at least 4 days indicating that the RGD-gradient had a sustained effect on cell behavior. In contrast, soluble gradient systems have demonstrated short-term morphological effects—24 hours or less, which is too short to impact engineered tissue formation since significant cell migration into a scaffold requires several days (Moghe *et al.*, 1995; Knapp *et al.*, 1999). An additional disadvantage of these soluble gradient systems is that they cannot be combined with the application of mechanical

forces (i.e. shear stress and strain), which may be crucial for the formation of a variety of engineered tissues including cartilage, bone, and blood vessels.

In addition to altering cell morphology, RGD-gradient hydrogels influenced cell migration. Cells migrated ~48% further up the concentration gradient (0 to 6 μmol/ml PEG-RGDS) than down the concentration gradient. Migration up the concentration gradient was also ~33% greater than migration on control surfaces with a constant concentration of PEG-RGDS (2 μmol/ml), while migration down the gradient was reduced ~12% relative to the control hydrogel surface (2 μmol/ml PEG-RGDS). Thus, immobilized gradients of RGD can increase cell migration on PEG-based hydrogel scaffolds. The application of this technology may be useful for directing endothelial cell migration on to vascular graft surfaces, which can result in enhanced endothelialization. Moreover, the incorporation of cell-specific adhesion peptides including REDV, which binds to the integrin $\alpha_4\beta_1$ on the endothelial cell, but not platelets and VAPG, which binds to smooth muscle cells, but not fibroblasts, may help further organize the regrowth of tissues by directing cell migration to specific areas (Massia and Hubbell, 1992; Gobin and West, 2003).

Directed migration on PEG-based hydrogels was further enhanced in this study by increasing the RGD-gradient's slope. Migration up the 2x gradient hydrogel (0 to 12 μmol/ml) was ~23% greater than migration up the 1x gradient hydrogel (0 to 6 μmol/ml). Migration up the 2x gradient hydrogel was also significantly greater than migration on all other hydrogel surfaces with the exceptions of the constant hydrogel containing 6 μmol/ml PEG-RGDS and the 1x gradient hydrogel in the direction of increasing RGD concentration. However, migration on this control hydrogel surface (6 μmol/ml PEG-

RGDS) was reduced by ~7% relative to migration up the 2x gradient hydrogel and migration up the 1x gradient hydrogel was reduced by ~19%.. Thus, the steepness of the gradient slope can enhance directional migration on PEG hydrogel scaffolds. Further studies using covalently immobilized gradients of RGD can indicate a minimum gradient slope required for directed cell migration. Additional improvements in directed migration may also be possible by further increasing the gradient slope's steepness.

FUTURE DIRECTIONS

These tissue-engineering scaffolds can also be used to investigate cell response in more detail. For example, other cell types can be grown on these RGD-gradient hydrogels including vascular endothelial cells and vascular smooth muscle cells. These investigations should indicate that the spatial distribution of the adhesive peptide sequence, RGD, impacts both vascular cell morphology and vascular cell migration. In addition, RGD-gradient hydrogels may be useful for directing cell migration to particular regions of a scaffold. For example, RGD-gradients can potentially direct endothelial cell migration onto tissue-engineering scaffolds, leading to enhanced endothelialization. Alternatively, RGD-gradients can be used to direct smooth muscle cell migration away from the intima, which can potentially prevent neointimal formation. Finally, directed cell migration can be further investigated using time-lapse video microscopy and automated cell tracking methods. These methods provide the opportunity to monitor individual cells rather than a population of cells and reduce the potential inhibitory effects of cell-cell interactions and of extracellular matrix protein production.

CHAPTER 3: COVALENTLY IMMOBILIZED bFGF FOR OPTIMIZED TISSUE FORMATION

INTRODUCTION

Growth factors play an important role in modulating cell behavior in both physiological and pathological processes. Basic fibroblast growth factor (bFGF), for example, can impact angiogenesis, wound healing, and restenosis following balloon angioplasty. The application of bFGF stimulates therapeutic angiogenesis in various animal models (Yanagisawa-Miwa *et al.*, 1992; Baffour *et al.*, 1992; Chlebourn *et al.*, 1992) and in restenosis, bFGF stimulates vascular smooth muscle cell (SMC) migration and proliferation, which results in neointimal formation (Lindner *et al.*, 1992; Lindner and Reidy, 1993; Jackson and Reidy, 1993; reviewed in Bikfalvi *et al.*, 1997). In general, bFGF is a potent mitogen and chemotactic agent for many cell types including vascular endothelial cells and vascular SMCs. bFGF can also affect plasminogen activator and interstitial and type IV collagenase expression. Thus, bFGF can dramatically affect cell response, which can lead to changes in a tissue's structure. Similarly, bFGF application may also be useful for modulating cell behavior in tissue-engineering scaffolds.

Growth factors can have profound effects on engineered tissue formation. Neidert *et al.* showed that the addition of transforming growth factor-$\beta 1$ (TGF-$\beta 1$) to cell culture medium can increase collagen production by fibroblasts seeded within fibrin constructs by approximately ten-fold (2002). Enhanced collagen production also combined with increased crosslinking of extracellular matrix proteins to result in improved tissue

stiffness and strength. Similarly, Pei *et al.* used growth factors sequentially to promote cell proliferation in cartilage constructs followed by extracellular matrix production (2002). TGF-β1 and basic fibroblast growth factor (bFGF) were combined to stimulate chondrocyte proliferation in polyglycolic acid (PGA) scaffolds. This application resulted in a two-fold increase in cell density compared to untreated controls after 2 weeks. Sequential supplementation with insulin-like growth factor-1 (IGF-1) stimulated glycosaminoglycan and collagen production. This sequential approach produced constructs that better mimicked native cartilage tissues than constructs exposed to either TGF-β1/bFGF or IGF-1 alone. These improved constructs contained only collagen type II as found in mature cartilage and high wet weight fractions of glycosaminoglycans and collagen. Thus, growth factor supplementation can improve engineered tissue formation by promoting cell proliferation and extracellular matrix production.

Alternatively, growth factors can be covalently immobilized to biomaterials to control their localized concentration. Kuhl and Griffith-Cima tethered epidermal growth factor (EGF) to glass slides via a PEG-based polymer chain and showed that immobilized EGF stimulated DNA synthesis and morphological changes in rat hepatocytes (1996). These alterations were comparable to those observed in the presence of soluble EGF, while physically adsorbed EGF had lost its activity. Similarly, TGF-β2 can retain its effect on collagen tissue deposition when conjugated to collagen via a PEG-based chain (Bentz *et al.*, 1998). Moreover, covalent immobilization of TGF-β2 to fibrillar collagen increased its stability and significantly improved the *in vivo* response to TGF-β2 in a subcutaneous rat model. Thus, conjugation to a polymer chain does not impede the interaction between cell receptor binding sites and the growth factors, EGF and TGF-β2,

making it possible to control the growth factor's localized concentration. This application can be used to improve the formation of engineered tissues and is especially advantageous for wound healing applications where engineered scaffolds are remodeled *in vivo*. Soluble growth factors would simply diffuse away—diminishing the localized growth factor concentration.

This technology for covalently immobilizing growth factors can be readily applied to PEG hydrogel scaffolds to influence cell behavior. For example, EGF and TGF-β have been tethered to PEG-chains by reaction with an N-hydroxysuccinimidyl ester of PEG monoacrylate (Gobin and West, 2003; Mann *et al.,* 2001). These PEG-modified growth factors can then be immobilized to PEG hydrogel scaffolds during photopolymerization. As depicted in Figure 1, tethered bioactive factors are incorporated three-dimensionally throughout the bulk of the hydrogel scaffold. The immobilized
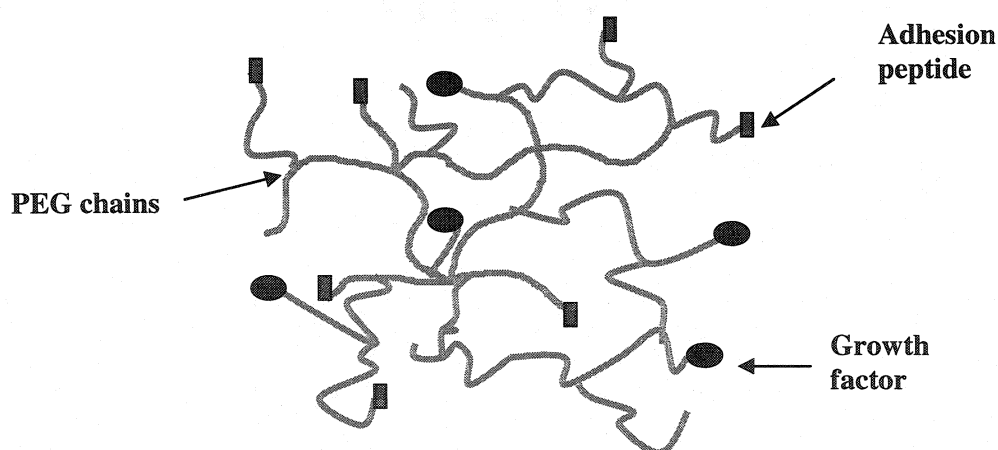

Figure 1. This schematic depicts the covalent immobilization of bioactive factors within hydrogel scaffolds. The bioactive factors can include adhesion peptides and growth factors, which enable cells to interact with the scaffold. Meanwhile, the PEG chains form a crosslinked network that is resistant to protein adsorption.

EGF retains its mitogenic activity and also promotes cell migration on hydrogel surfaces containing both the EGF and the RGD adhesion peptide (Gobin and West, 2003). The TGF-β-modified scaffolds promote collagen production by vascular SMCs seeded within the hydrogel scaffolds, and the resultant engineered tissues have improved mechanical properties compared to those formed with scaffolds modified with only RGD (Mann *et al.*, 2001). From these two examples, it is clear that growth factor immobilization in the PEG diacrylate hydrogel system is feasible and can help to influence cell behavior within the scaffold to optimize tissue formation.

In this study, hydrogel scaffolds were modified with bFGF to stimulate two important aspects of tissue formation—proliferation and migration. bFGF was selected because it is a potent mitogen and chemotactic agent for vascular SMCs (Jackson and Reidy, 1993; Bikfalvi *et al.*, 1997). bFGF is also normally found in the vascular environment as it is associated with the extracellular matrix (Jackson and Reidy, 1993; Bikfalvi *et al.*, 1997). Further, cells can respond to bFGF even after it has been sequestered in the ECM. Thus, this growth factor may play an important role in developing engineered tissues that more closely mimic the structural and functional properties of native blood vessels. Furthermore, we have developed methods that allow immobilization of the growth factor in a concentration gradient. This should mimic the presentation of bioactive factors found *in vivo* to elicit enhanced and directional cell migration, which may be useful for optimizing tissue formation. The ability to create a stable, immobilized gradient with a known concentration profile of a growth factor should improve our understanding of cellular responses to gradients. Such materials should also allow guidance of cell migration in many tissue engineering applications.

MATERIALS AND METHODS

Cell maintenance

Human aortic smooth muscle cells (HASMCs) were obtained from Cell Applications (San Diego, CA). They were maintained at 37°C/5% CO_2 on Dulbecco's modified Eagle's medium (DMEM) (Sigma, St. Louis, MO) supplemented with 10% fetal bovine serum (FBS; BioWhittaker, Walkersville, MD), 2mM L-glutamine (Sigma, St. Louis, MO), 1000 units/l penicillin (Sigma, St. Louis, MO) and 100 mg/l streptomycin (Sigma, St. Louis, MO). For the gradient bFGF studies, SMCs were maintained on Smooth Muscle Cell Growth Medium (Cell Applications) without the bFGF supplement. All experiments were conducted using cells at passages 6-8.

Synthesis and Characterization of the PEG-bFGF conjugate

As shown in Figure 2, recombinant human bFGF (Promega, Madison, WI) was conjugated to PEG by reacting it with acryloyl-PEG-N-hydroxysuccinimide (acryloyl-PEG-NHS, 3400 Da; Shearwater Polymers, Huntsville, AL) in a 1:15 (peptide:PEG) molar ratio in 50 mM sodium bicarbonate (pH 8.5) for 2 hr. The polymer solution was then lyophilized and stored at -80°C.
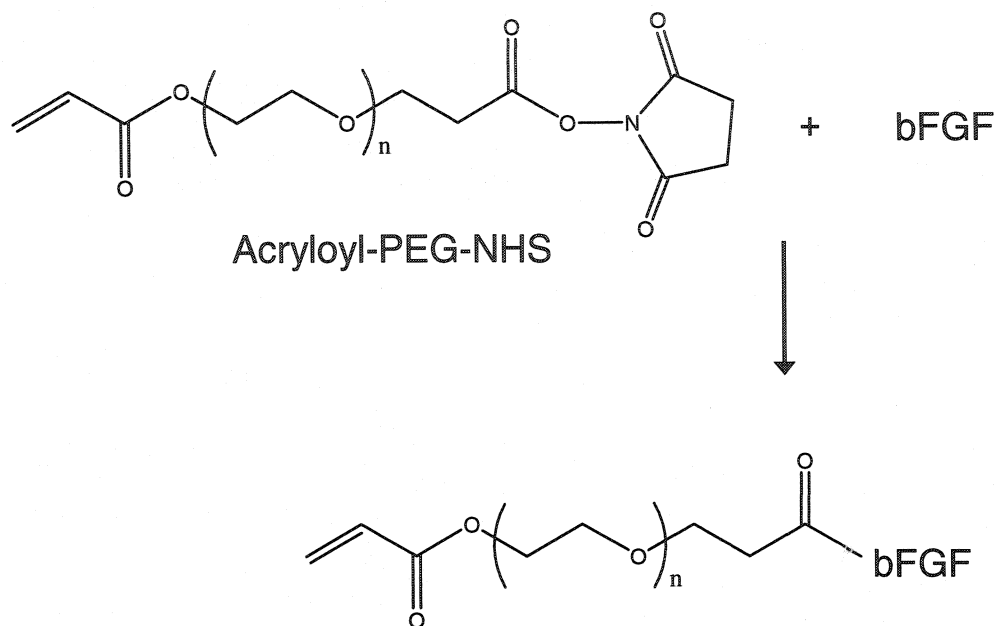
Figure 2. Reaction scheme for the conjugation of bFGF to an acrylated PEG chain.

A Western blot was used to analyze the resulting acryloyl-PEG-bFGF. 480 ng of

unmodified and PEG-conjugated bFGF were separated on a 4-15% SDS-PAGE gel

(BioRad, Hercules, CA) and transferred to a Trans-blot Transfer Medium nitrocellulose

membrane (BioRad). The membrane was incubated overnight at 4°C with 5% milk in

buffer containing 0.1% (vol/vol) Tween 20 in TBS (TBST). The membrane was

incubated with rabbit anti-bFGF (Sigma) at a 1:2000 dilution for 1 hr at room

temperature. After 2 washes (5 min each) with TBST, peroxidase-labeled goat anti-rabbit

IgG (Sigma) was added at 1:3000 dilution and incubated for 1 hr at room temperature.

The membrane was washed again in TBST and then treated with Opti-4CN

chemiluminescence reagent (BioRad) for detection.

Bioactivity of the PEG-bFGF conjugate

The bioactivity of the PEG-bFGF conjugate was assessed by monitoring cell proliferation in response to medium supplemented with no bFGF, unmodified bFGF, or PEG conjugated bFGF. HASMCs were seeded in 24-well plates at a density of 7900 cells/cm^2 and incubated overnight in a 37°C/5% CO_2 environment. The media was then exchanged for media supplemented with 0, 2.86 nmol/L unmodified bFGF, or 2.86 nmol/L PEG conjugated bFGF. After 2 days, cells were rinsed with phosphate buffered saline, trypsinized, and then counted using a Coulter counter (Multisizer #0646; Coulter Electronics, Hialeah, FL) to determine cell numbers.

Hydrogel Preparation

PEG diacrylate was synthesized by dissolving 12 g dry PEG (6000 Da; Fluka, Milwaukee, WI) in 36 ml anhydrous dichloromethane. 0.25 g triethylamine and then 0.43 g acryloyl chloride (Lancaster Synthesis, Windham, NH) were added dropwise, and the mixture was stirred under argon for 48 hr. The resulting solution was then washed with 2 M K_2CO_3 and separated into aqueous and dichloromethane phases to remove HCl. The dichloromethane phase was subsequently dried with anhydrous $MgSO_4$ (Fisher Scientific, Pittsburg, PA), and the PEG diacrylate was then precipitated in diethyl ether, filtered, and dried under vacuum at room temperature overnight. The resultant polymer was dissolved in N,N-dimethylformamide-d$_7$ (Sigma, St.Louis, MO) and characterized via proton NMR (Avance 400 MHz; Bruker, Billerica, MA) to determine the degree of acrylation.

A cell adhesive component was prepared by reacting acryloyl-PEG-NHS with the adhesion peptide, RGDS (American Peptide, Sunnyvale, CA) in 50 mM sodium bicarbonate (pH 8.5) at a 1:1 molar ratio for 2 hr. The solution was then lyophilized and stored at -20°C.

Hydrogels were formed by combining 0.1 g/ml PEG diacrylate and 2.8 µmol/ml acryloyl-PEG-RGDS in 10 mM HEPES buffered saline (pH 7.4). This solution was then sterilized by filtration (0.8 µm prefilter and 0.2 µm filter; Gelman Sciences, Ann Arbor, MI). For hydrogels containing bFGF, 2.86 nmol/L unmodified bFGF or 2.86 nmol/L PEG conjugated bFGF was added to the polymer solution. 10 µl/ml of 2,2-dimethyl-2-phenyl-acetophenone in N-vinylpyrrolidone (300 mg/ml) was added as the photoinitiator. This solution was then placed in a rectangular glass mold (0.2 mm thickness) and exposed to long wavelength UV light (365 nm, 10 mW/cm^2) for 60 sec.

bFGF Incorporation in Hydrogels

Hydrogels (50 µL volume) were formed in a round mold (32 mm^2) as described above except for the addition of a set of hydrogels containing 0, 2.86, 14.3, 28.6, or 57.2 nmol/L immobilized bFGF. None of these hydrogels contained immobilized RGDS. Hydrogels were allowed to swell for 24 hrs at 4°C in 0.250 ml phosphate buffered saline (Sigma). The supernatant was then collected and stored at −80°C. The release of bFGF was also examined for the 4 days following this initial 24 hr period by collecting the resultant supernatant and storing it at −80°C. The supernatants from both time periods were then tested using an ELISA kit for bFGF (R&D Systems Inc., Minneapolis, MN) and compared to bFGF standards.

Cell Proliferation on Hydrogels

A cork borer (10 mm diameter) was used to cut disk-shaped gels, which were individually placed in the wells of a 48-well tissue culture plate. Cells were then seeded on the surfaces of these RGDS-modified PEG hydrogels at a density of 7840 cells/cm^2. DNA content was determined after 5 days in culture. The cell-seeded hydrogels were hydrolyzed in 0.1 N NaOH overnight at 37°C, neutralized with 0.1 N HCl, and stored at −20°C prior to being assayed. To determine DNA content, a fluorescent DNA binding dye, PicoGreen (Molecular Probes, Eugene, OR) was used, and its fluorescence measured using a fluorometer (excitation filter at 480 nm and emission filter at 590 nm).

Cell migration on bFGF-modified surfaces

Hydrogels were formed as described above except for the addition of a set of hydrogels containing 14.2 nmol/L immobilized bFGF. The hydrogel scaffolds were used in a fence-style migration assay. Cells were seeded on these gels within the confines of a Teflon mold (17 mm outer diameter, 6 mm inner diameter) at a density of 45,000 cells/cm^2. After 22 hr, the molds were removed and cell culture medium exchanged for medium containing 0.5 µg/ml mitomycin C (Calbiochem, SanDiego, CA) to block proliferation. Photographs were taken of the area covered by the cells 3 days after removing the ring, which formed the initial boundary for determining the extent of migration.

Preparation and detection of covalently immobilized gradients of bFGF

A hydrogel with a gradient of tethered bFGF was formed using a gradient maker (CBS Scientific Co., Del Mar, CA) to pour the hydrogel precursor solutions prior to photopolymerization (see Figure 2 in Chapter 2). Gradient flow was controlled by a Teflon valve centered between two chambers containing polymer solution with or without the PEG-bFGF conjugate. Both polymer solutions contained 0.1 g/ml PEG diacrylate, 3.5 μmole/ml acryloyl-PEG-RGDS, and 10 μl/ml of 2,2-dimethyl-2-phenyl-acetophenone in N-vinylpyrrolidone (300 mg/ml). The polymer solutions were slowly combined in a rectangular glass mold (2 mm thickness) and exposed to long wavelength UV light to form a hydrogel with tethered bFGF ranging from 0 to 51 nmol/L. A silver stain kit (BioRad, Hercules, CA) was used to detect the tethered bFGF gradient. Briefly, a hydrogel containing a gradient of 0 to 51 nmol/L tethered bFGF was rinsed in deionized water for 20 min, placed in a staining and development solution (5ml silver complex solution, 5ml reduction moderator solution, 5ml image development reagent, 35ml deionized water, and 50ml development accelerator solution as provided in the silver stain kit) for 20 minutes, and then placed in a stopping solution (5% acetic acid) for 15 min followed by rinsing in deionized water. The mean staining density at each position was analyzed under light microscopy using Scion Image.

Cell alignment and migration on hydrogel surfaces with a gradient of tethered bFGF

Hydrogels were also formed from polymer solutions containing 0 or 26 nmol/L of the PEG-bFGF conjugate. These hydrogels contained the same concentrations of PEG

diacrylate, acryloyl-PEG-RGDS, and 2,2-dimethyl-2-phenyl-acetophenone in N-vinylpyrrolidinone as the hydrogel with a gradient of tethered bFGF. Cells were then seeded on the gels at a density of 12,500 cells/cm^2 and allowed to attach overnight. After 24 hr, hydrogel surfaces were photographed in several areas and assessed for cell alignment under phase contrast microscopy using Scion Image. Cell alignment was determined for each cell by finding the cell's angle relative to the direction of the bFGF gradient. Cell angles were determined for 150 cells on each hydrogel surface, and then these angles were categorized into nine different groups based on their relative angle to the bFGF gradient. These groups included cells positioned relative to the bFGF gradient within ± 0 to 10, 10 to 30, 30 to 50, 50 to 70, or 70 to 90 degrees.

As depicted in Figure 3, cell migration was assessed on hydrogel surfaces with a gradient of tethered bFGF. Cells were seeded within a square stainless steel mold (7.7 mm × 7.7 mm × 10.1 mm), which was positioned at the gradient hydrogel's midsection and compared to cells seeded on hydrogels without bFGF and a constant concentration (26 nmol/L) of tethered bFGF. In addition to the various concentrations of tethered bFGF, the hydrogels contained 0.1g 6k PEG diacrylate, 5.0 umole/ml acryloyl-PEG-RGDS, 10 μl/ml 2,2-dimethoxy-2-acetophenone in N-vinylpyrrolidinone. After 16 hr, the stainless steel ring creating the initial boundary was removed, and the cells were photographed under phase contrast microscopy. Two days later, the cells were photographed again.
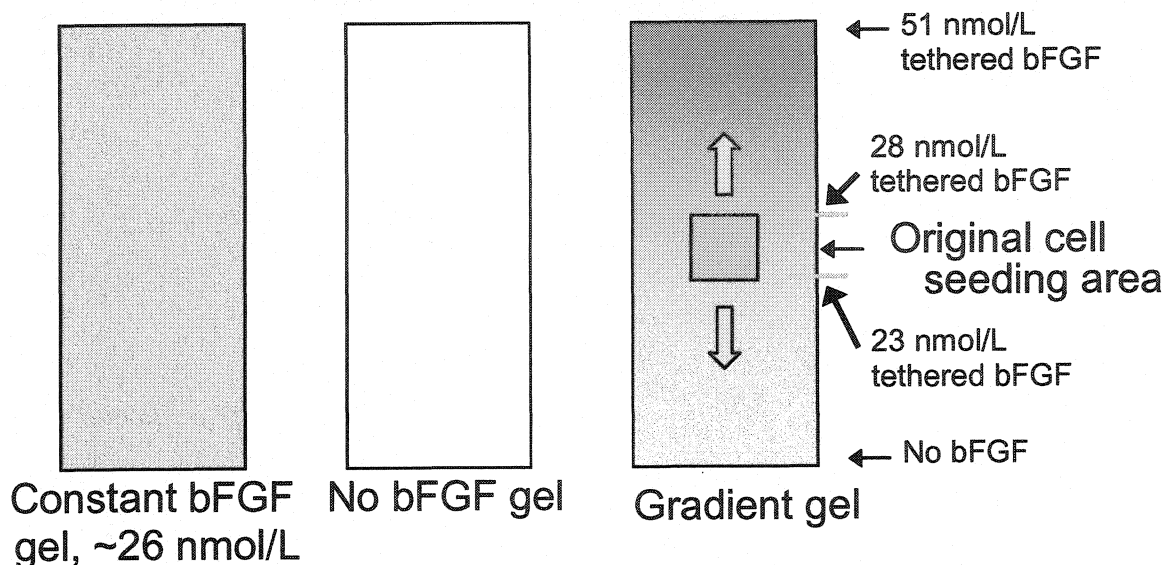
Figure 3. This schematic depicts the setup for the gradient migration study. SMC migration was monitored in the directions of increasing and decreasing bFGF concentrations on the bFGF-gradient hydrogel (0 to 51 nmol/ml bFGF). This migration was compared to migration on each of the control hydrogel surfaces containing either 0 or 26 nmol/L covalently immobilized bFGF.

Statistical analysis

Data sets were compared using Minitab 14 (downloaded from www.minitab.com) to perform a one-way analysis of variance (ANOVA) followed by post hoc comparisons using Tukey to determine which means were significantly different. In addition, two factors (time and cell angle) were analyzed using the General Linear Model to perform univariate analysis of variance on an unbalanced design. This two-factor analysis was followed by multiple comparisons using Tukey. P-values less than 0.05 were considered statistically significant. All values are reported as the mean and standard deviation of the mean.

RESULTS

Characterization of PEG conjugated bFGF

Western blot analysis demonstrated that bFGF was successfully conjugated to

PEG. Visual inspection of the gel (Figure 4) showed that only a small percentage, if any,

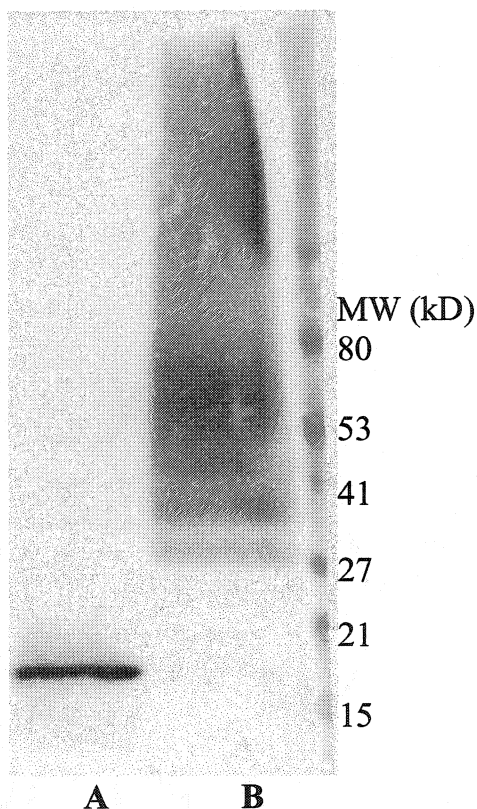of the growth factor remained unmodified, while the majority of the growth factor

Figure 4. Western analysis of unmodified bFGF (A, MW = 17.5kD) and PEG conjugated bFGF (B) demonstrated that bFGF was successfully conjugated to PEG (MW 3400). This conjugation was indicated by the increase in MW corresponding to the attachment of PEG chains.

showed an increase in molecular weight corresponding to the attachment of PEG chains.

Multiple PEG chains attached to bFGF resulting in a product with a range of molecular

weights (MW of unmodified bFGF = 17.5 kDa; MW of PEG = 3.4 kDa). Thus, bFGF

was conjugated to PEG via the reaction between acryloyl-PEG-NHS and primary amines within the growth factor.

PEG-conjugated bFGF retained the ability to stimulate SMC proliferation (Figure 5). After 48 hr, SMCs grown on standard tissue culture polystyrene and treated with unmodified bFGF or PEG-conjugated bFGF (soluble, not photopolymerized into a hydrogel) at a concentration of 2.86 nmol/L showed significant increases in cell number
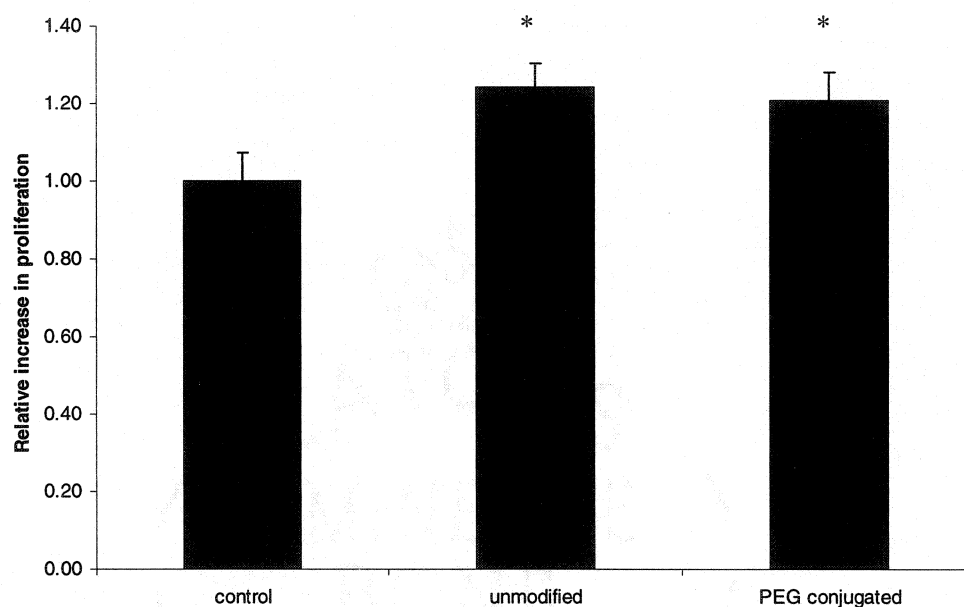

Figure 5. PEG-conjugated bFGF significantly stimulated SMC proliferation over 48 hours (p < 0.05). Wells treated with PEG-conjugated bFGF contained ~21% more cells than wells not treated with bFGF. A similar increase was observed in the presence of unmodified bFGF where SMC number increased by ~24% compared to the untreated control. However, the difference in cell number between samples treated with unmodified bFGF and PEG-conjugated bFGF was not significantly different (p > 0.05).

compared to the untreated control cells. SMC number increased by ~24% when treated with unmodified bFGF and by ~21% when treated with PEG-conjugated bFGF (p <

0.00006 versus control for both cases). The difference in cell number was not statistically significant between the samples treated with unmodified bFGF and those treated with PEG-conjugated bFGF. Thus, bFGF was successfully conjugated to a polymer tether with retention of its stimulatory effect on SMC proliferation.

PEG-conjugated bFGF was also successfully incorporated within hydrogel scaffolds. The release of bFGF from hydrogel scaffolds containing PEG-bFGF concentrations ranging from 2.86 to 57.2 nmol/L was examined using ELISA. After 24 h, less than 0.5% of the bFGF was released into the supernatant. This level of incorporation was evident at all concentrations of immobilized bFGF tested. Further, bFGF release decreased significantly after the initial 24 hr period. In the 4 days following this initial release period, no more than 0.01% bFGF could be detected in the supernatant.

Cell proliferation and migration in response to covalently immobilized PEG-bFGF

PEG-conjugated bFGF was covalently incorporated into PEG diacrylate hydrogel scaffolds to assess its effects on both SMC proliferation and migration. As shown in Figure 6, cell proliferation on hydrogel surfaces containing unmodified bFGF (2.86 nmol/L) and immobilized bFGF (2.86 nmol/L) were compared. After 5 days, the increase in cell number on immobilized bFGF surfaces was ~41% over the amount seen on gels without bFGF. Meanwhile, the relative proportion of SMCs was ~21% greater on hydrogel surfaces with unmodified bFGF compared to hydrogels without bFGF (p > 0.05). However, this increase was less than that seen with covalently immobilized bFGF and not significantly different from SMC number on control hydrogel
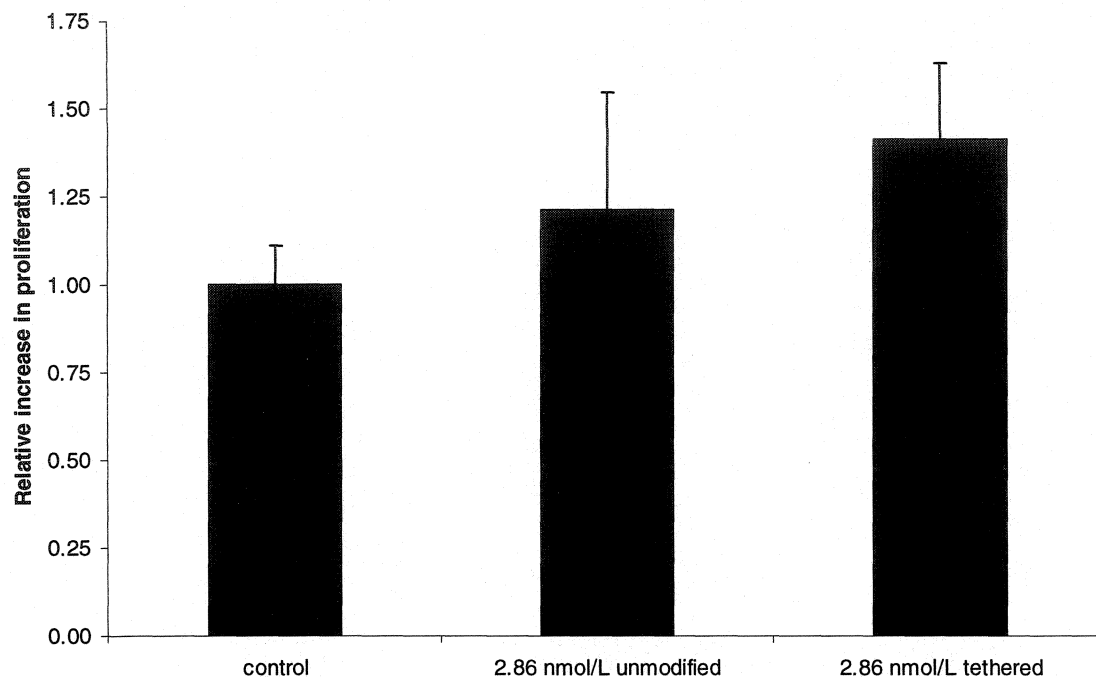
Figure 6. Covalently incorporated bFGF stimulated cell proliferation on hydrogel surfaces modified with RGDS compared to cell proliferation on hydrogels without bFGF. This was determined using a fluorescent DNA binding dye, PicoGreen (Molecular Probes) to detect DNA content on the gels. After 5 days, it was ~1.41 times the amount seen on gels without bFGF.

surfaces.

Cell migration was also improved on hydrogel surfaces modified with tethered

bFGF. This was determined using a fence-style migration assay. Migration depended on

the bulk concentration of tethered bFGF. On hydrogel surfaces containing 2.86 nmol/L

immobilized bFGF, migration was increased ~8% after 72 hours in the presence of

mitomycin c, which blocks cell proliferation (Figure 7). Migration was greater when the

hydrogel surfaces contained 14.2 nmol/L immobilized bFGF such that migration
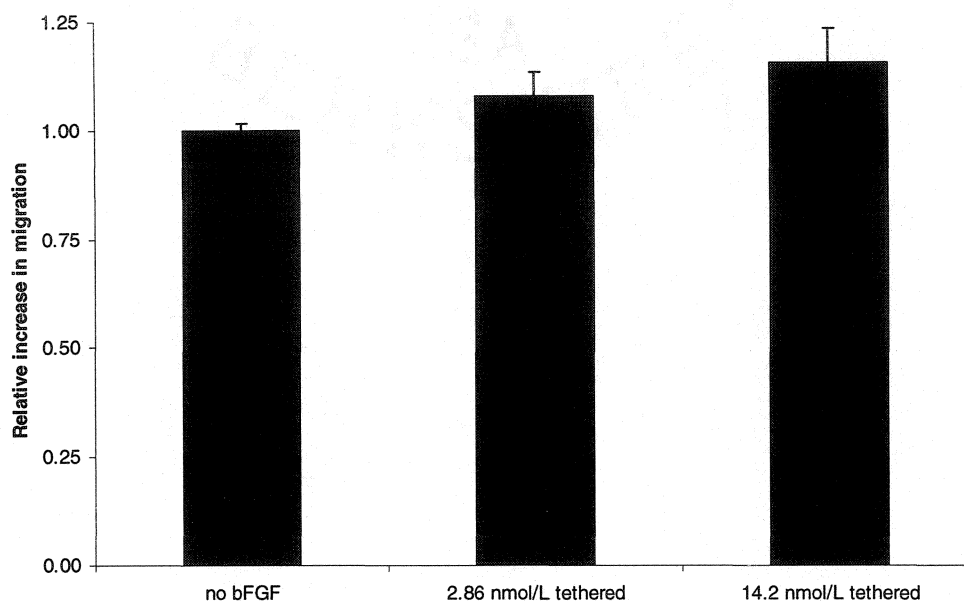
increased ~15% after 72 hours.

Figure 7. Cell migration was improved on hydrogel surfaces modified with tethered bFGF (2.86 nmol/L. This was determined by measuring the diameter of the cellularized areas after the boundary was removed. The relative diameter was increased ~8% after 72 hours. Higher concentrations of acryloyl-PEG-bFGF corresponded with increased migration such that the relative diameter was increased ~15% after 72 hours. Cells were treated with mitomycin C to prevent proliferation. Thus, the response observed is due to the stimulatory effect of bFGF on migration alone and not influenced by an increase in the number of cells.

bFGF-gradient scaffolds affect vascular SMC behavior

A gradient maker was used to fabricate hydrogel scaffolds with a covalently immobilized bFGF gradient. The gradient maker was used with polymer solutions with and without PEG-conjugated bFGF to generate a continuous linear gradient of the PEG-conjugated bFGF. As the hydrogel precursor was poured into the mold, it was photopolymerized to lock the bFGF gradient in place. The resulting hydrogel was then silver stained to detect the presence of the bFGF gradient, which ranged in concentration from 0 to 51 nmol/L. Silver staining made the bFGF gradient visible under light

microscopy making it possible to analyze the gradient using digital image processing. As depicted in Figure 8, the staining density increased linearly in the direction of increasing bFGF concentration (R^2=0.85).
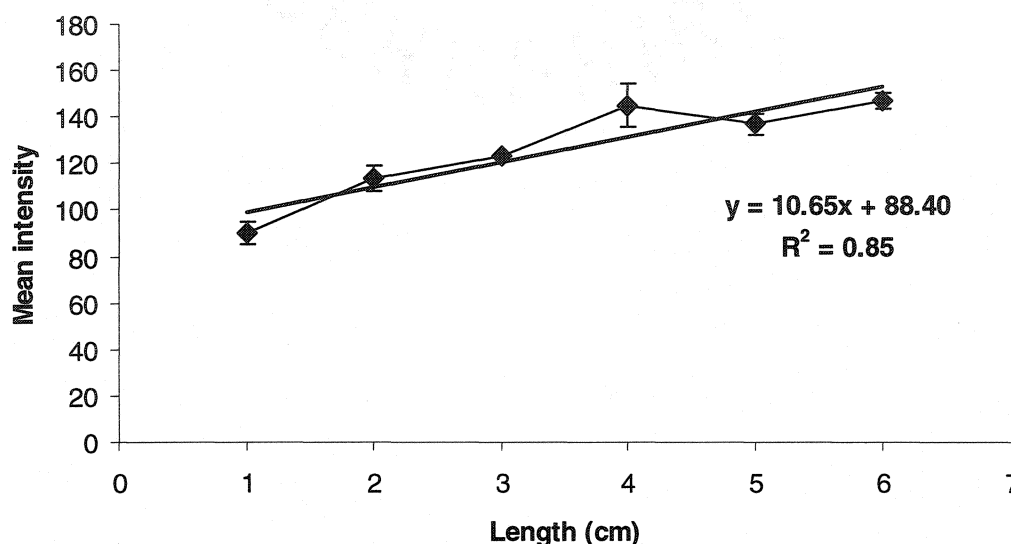

Figure 8. The bFGF gradient was visualized by silver staining, analyzed under light microscopy using digital image processing, and found to be linear.

The effects of the immobilized bFGF gradient on cell alignment were assessed. SMCs were seeded on hydrogel scaffolds with a gradient of immobilized bFGF (ranging from 0 to 51 nmol/L) or a constant concentration of bFGF (26 nmol/L) and also without bFGF. As shown in Figures 9 and 10, SMC alignment was observed on gradient-bFGF scaffolds in the direction of increasing tethered bFGF concentration. This alignment was not evident on the other hydrogel surfaces, which either lacked tethered bFGF or contained a constant concentration of tethered bFGF (26 nmol/L). In addition, SMC alignment on bFGF-gradient scaffolds was more pronounced after 48 hr than at 24 hr as shown in Figure 11. SMC alignment also depended on the concentration of tethered
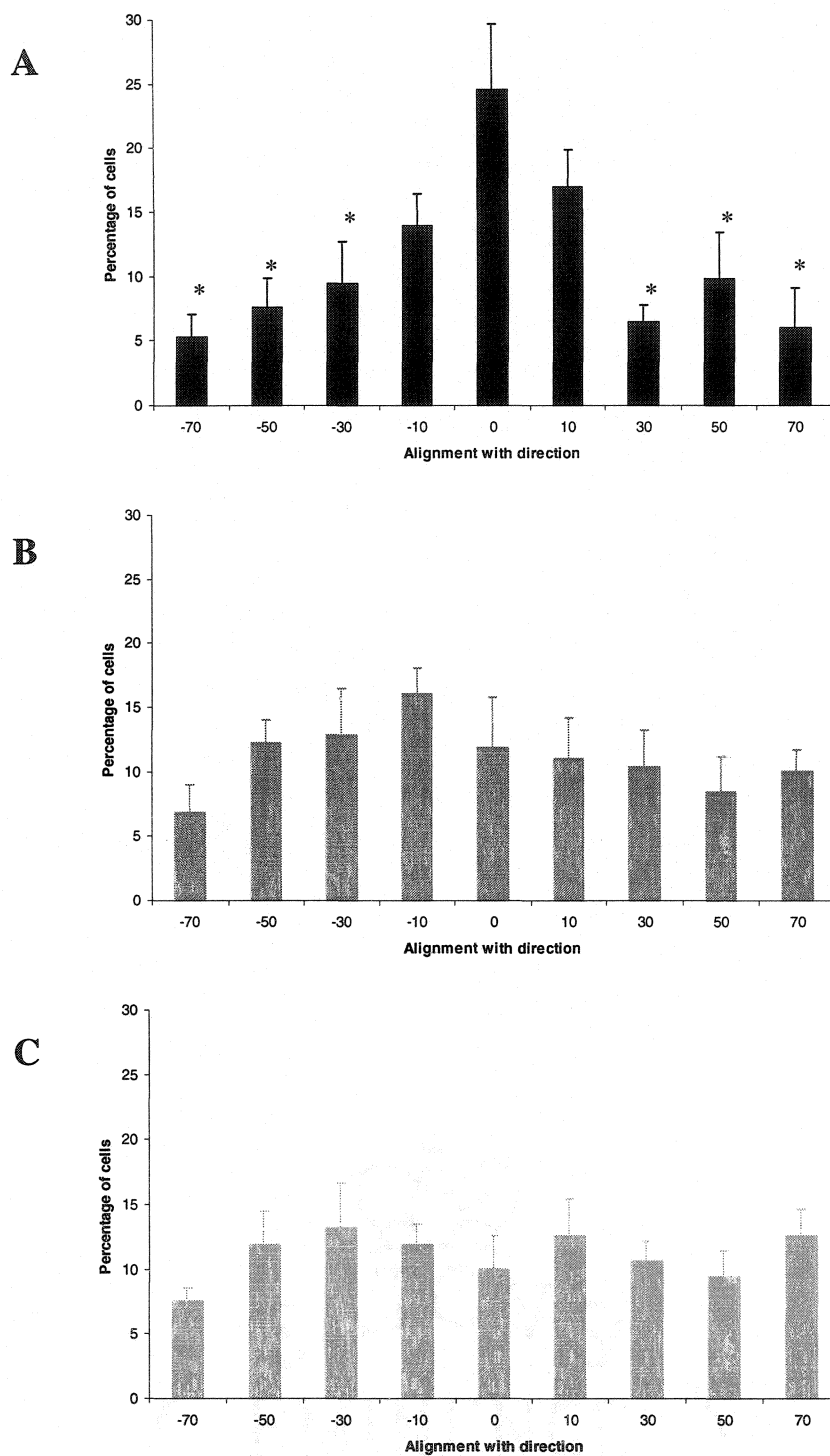
Figure 9. A gradient of tethered bFGF influenced cell alignment (A). More cells were aligned in the direction of increasing bFGF concentration than on the other hydrogel surfaces (constant bFGF, B; no bFGF, C), which lacked a gradient of tethered bFGF. (*) $p < 0.05$ compared to cells aligned with the gradient axis (within $\pm 10°$).

bFGF as it was not as evident in regions of the hydrogel scaffold with lower bFGF

concentrations (below ~17 nmol/L).
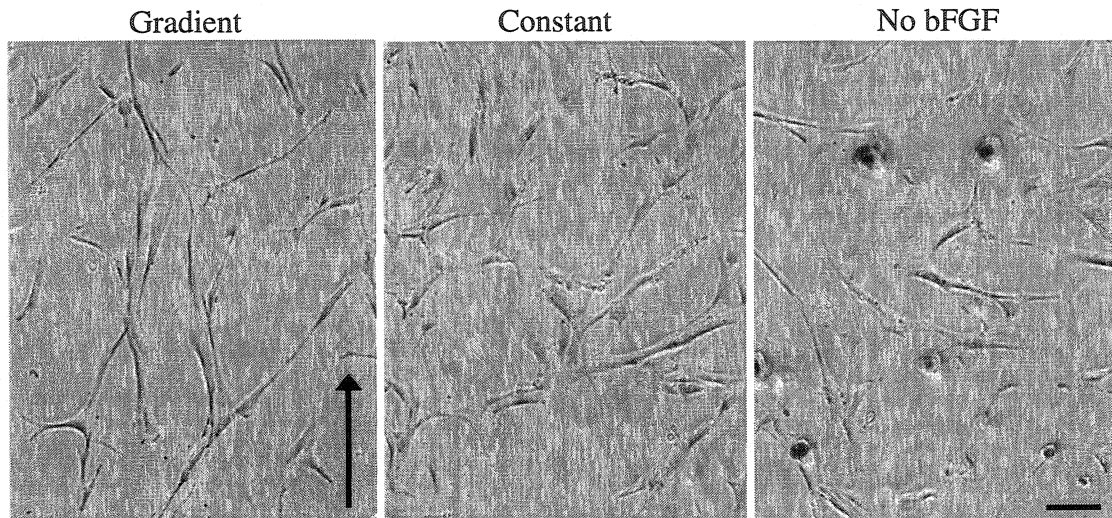
| Gradient | Constant | No bFGF |

Figure 10. More cells were aligned on hydrogel surfaces with a bFGF gradient (indicated by arrow) than on the other hydrogel surfaces, which lacked a gradient of tethered bFGF (bar = 10 μm).

SMC migration on bFGF-gradient hydrogel scaffolds was also examined using a

fence-style migration assay. As shown in Figure 12, cells migrated further when seeded

on hydrogel surfaces with a gradient of tethered bFGF (where the cells were initially

exposed to immobilized bFGF concentrations ranging from ~23 to ~28 nmol/L)

compared to control surfaces lacking tethered bFGF. Migration on gradient hydrogels

also varied depending on cell movement up and down the concentration gradient. Cells

migrated ~47% further when they moved in the direction of increasing bFGF

concentration compared to control surfaces without tethered bFGF. Migration was lower

(just 25% greater than cells on control surfaces), when the cells migrated down the

concentration gradient. The migration distance was also improved (~13% greater) in the

direction of increasing bFGF concentration compared to surfaces containing a constant
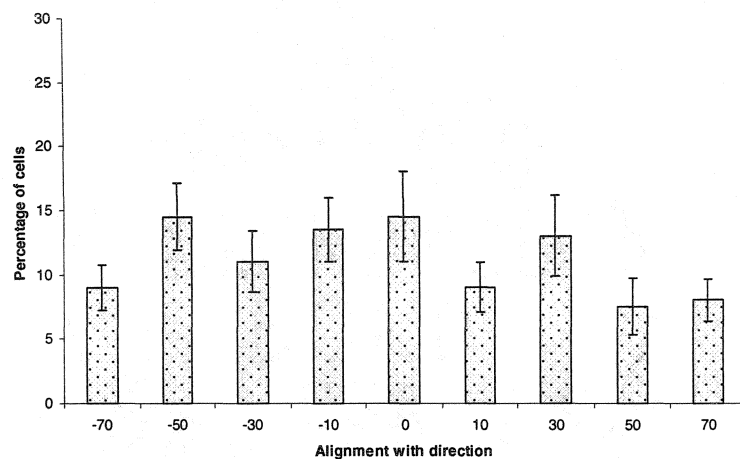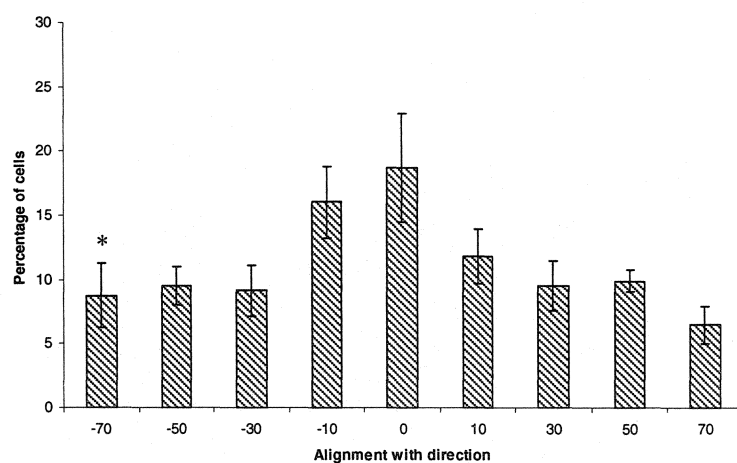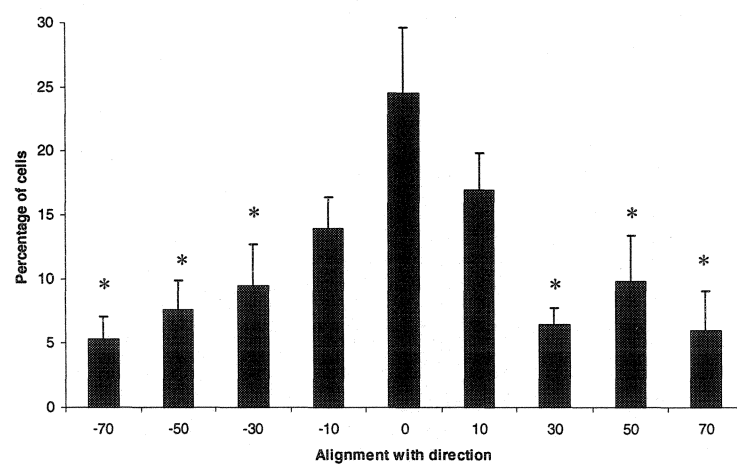
Figure 11. Cell alignment became more apparent with time on the bFGF-gradient hydrogel surface. (*) $p < 0.05$ compared to cells aligned with the gradient axis (within $\pm 10^{\circ}$).
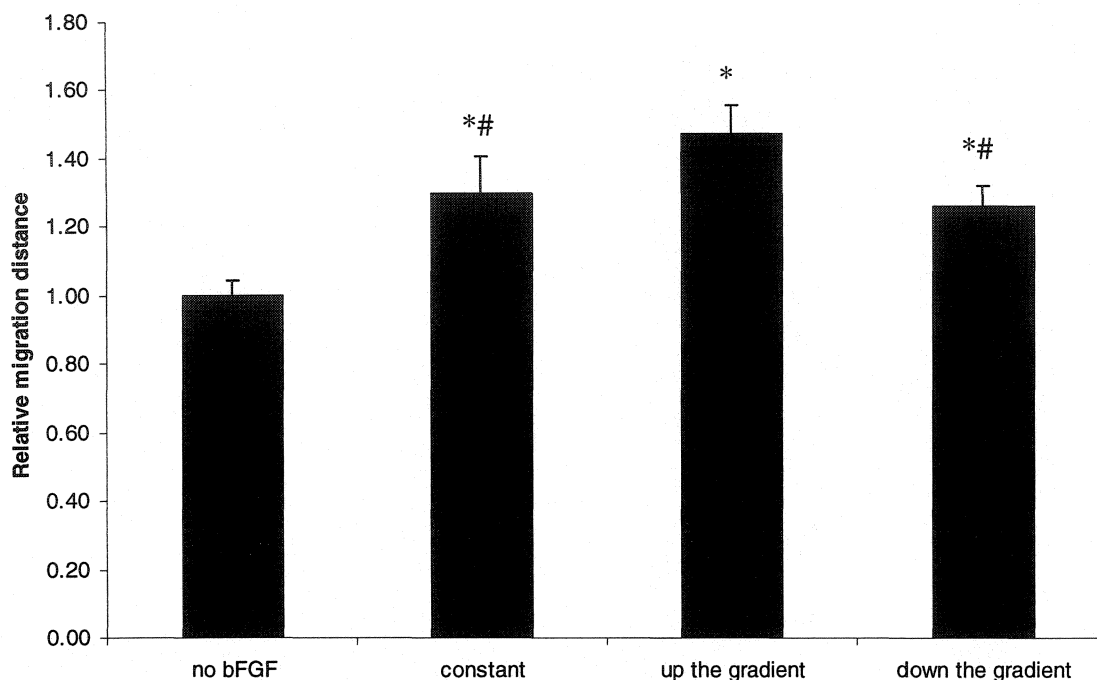
Figure 12. Cells migrated further on gradient-modified surfaces compared to surfaces with a constant concentration of bFGF when the cells were positioned to move away from areas of high cell density while moving in the direction of increasing bFGF concentration. (*) $p < 0.05$ compared to hydrogel surfaces without bFGF. (#) $p < 0.05$ compared to hydrogel surfaces with cells migrating up the concentration gradient.

concentration of tethered bFGF. Since this study was not performed in the presence of mitomycin C, this enhanced effect on migration down the concentration gradient compared to control surfaces without bFGF may have been influenced by cell proliferation.

DISCUSSION

PEG-conjugated bFGF was investigated for its effect on vascular SMC behavior when covalently incorporated within PEG-based hydrogel scaffolds. bFGF is a potent mitogenic and chemotactic agent present throughout the vascular environment and as a

result may be useful for developing an engineered blood vessel. In PEG-based hydrogels, covalently immobilized bFGF has the potential to elicit cell behavior that is conducive to the formation of engineered tissues, while providing the opportunity to control bioactive signal presentation. Previous studies have investigated the protein-resistant character of these PEG-based scaffolds and the ability to control cell interaction with these hydrogel scaffolds by varying the bulk concentration of incorporated RGD (Merrill and Salzman, 1983; Gombotz et al., 1991; Hern and Hubbell, 1998; Mann et al., 2001; Gobin and West, 2003; Burdick and Anseth, 2003). In addition, TGF-β1 and EGF have been covalently immobilized within PEG-based hydrogels and were shown to retain their respective effects on extracellular matrix production and migration (Gobin and West, 2003; Mann et al., 2001). This study has focused on the effects of covalently immobilizing bFGF into PEG-based hydrogels in combination with RGD on vascular SMC proliferation and migration and the potential to control bioactive signal presentation by using a bFGF gradient to influence vascular SMC alignment and migration.

RGD and bFGF were modified with an acrylated PEG-chain in order to provide a mechanism for their covalent incorporation within PEG-based hydrogels. Hern and Hubbell showed previously that 85% of an RGD-containing peptide was successfully conjugated to an acrylated PEG-chain when reacted in a 1:2 (peptide:acryloyl-PEG-NHS) molar ratio for 2 hours, and at least 97% of this product was covalently immobilized to the hydrogel material following photopolymerization (Hern and Hubbell, 1998). Similarly, Belcheva et al. conjugated NGF to PEG-fluorescein using a 1:10 (NGF: PEG-fluorescein) molar ratio for 24 hours and found that PEG chains were successfully attached to NGF (1999). In this study, bFGF was shown to react successfully with

acryloyl-PEG-NHS such that the majority of the growth factor was modified with at least one PEG chain, and at least 99.5% of the bFGF was covalently bound to the hydrogel material following photopolymerization.

While PEG-conjugation has the potential to reduce bFGF bioactivity by interfering with the binding of bFGF to cell surface receptors, this was not observed in the current study (Springer *et al.,* 1994; Gray *et al.,* 1995; Arakawa *et al.,* 1995). PEG-conjugated bFGF (soluble, not photopolymerized into a hydrogel) increased vascular SMC proliferation by ~21% and unmodified bFGF at the same concentration increased vascular SMC proliferation by ~24%. Thus, the effect of unmodified bFGF on vascular SMC proliferation was greater than that observed with PEG-conjugated bFGF, but the difference was small and not significant ($p<0.32$). The minimal impact of PEG-conjugation may depend on the lack of a primary amine in bFGF's higher affinity receptor binding surface, which is comprised of Tyrosine-103, Leucine-140, and Tyrosine-24 (Springer *et al.,* 1994). Since acryloyl-PEG-NHS targets primary amines, the PEG chain would not attach to this region where it might interfere with bFGF-receptor binding.

Once hydrogels were formed via photopolymerization, covalently incorporated bFGF retained its stimulatory effect on vascular SMC proliferation and migration. Vascular SMC number increased by ~41% after 5 days when exposed to covalently incorporated bFGF compared to a ~21% increase when exposed to unmodified bFGF. The higher SMC density in response to covalently incorporated bFGF may be due to the diffusion of unmodified bFGF from the hydrogels. Covalently incorporated bFGF had a similar enhancement on SMC migration. SMC migration increased by ~15% when

seeded on hydrogel surfaces containing 14.2 nmol/L immobilized bFGF compared to SMC migration on hydrogel surfaces lacking immobilized bFGF.

Since bFGF can be covalently bound to photopolymerized hydrogels with good retention of activity, this offers the opportunity to prepare biomaterials with covalently immobilized gradients of the growth factor. These were prepared using a gradient maker to pour the hydrogel precursors into a mold, then immediately photopolymerizing the hydrogel. The resultant bFGF gradient was visualized after silver staining and found to be linear. The bFGF gradient stimulated vascular SMC alignment and migration. This alignment appeared to increase over the first 48 h indicating that the bFGF gradient had a sustained effect on SMC behavior. SMCs also migrated differentially on gradient-bFGF hydrogel surfaces compared to control surfaces without bFGF or surfaces containing a constant concentration of bFGF. SMCs migrated furthest up the concentration gradient. Thus, covalent incorporation of bFGF provided the opportunity to present a bFGF-gradient to vascular SMCs that was long-lasting, making it possible to observe changes in SMC alignment and SMC migration over at least 48 hours. In comparison, other assay methods provide a transient soluble gradient, which makes it difficult to study behavior by cells that migrate much slower than immune cells. In addition, it may be possible to observe gradient effects on cell migration in three dimensions using this hydrogel system. This application would involve modifying the hydrogel so that proteolytically degradable peptide sequences were incorporated into the backbone of the polymer chain allowing cells to migrate through the hydrogel (Mann *et al.*, 2001; West and Hubbell, 1999). This system should allow guidance of engineered tissue formation and provide the opportunity to study detailed mechanisms of chemotaxis *in vitro*.

FUTURE DIRECTIONS

These tissue-engineering scaffolds can be further modified to affect cell response to growth factor presentation. For example, heparan sulfate proteoglycans can be covalently incorporated within hydrogel scaffolds to bind bFGF. Since bFGF reversibly binds to heparan sulfate proteoglycans, cells can potentially release the growth factor from its interaction with the ECM, leading to changes in cell proliferation and cell mgiration. This presentation method also better mimics the presentation of bFGF *in vivo* and can be potentially applied to other growth factors that bind these ECM molecules. In addition, by targeting heparan sulfate proteoglycans rather than the growth factor itself, this application provides the opportunity to present growth factors that can potentially lose their activity when targeted directly by amine-reactive polymers. Finally, combinations of growth factors and adhesive peptide sequences may have synergistic effects on cell response due to shared signaling cascades. This combined presentation may lead to improvements in the ability to use these tissue engineering scaffolds to modulate cell proliferation and to direct cell migration.

CHAPTER 4: PROTEASE-SENSITIVE HYDROGELS FOR ENGINEERED TISSUE FORMATION

INTRODUCTION

Matrix metalloproteinases (MMPs) play an important role in tissue development and remodeling. For example, MMPs are implicated in such physiological processes as wound healing, embryonic development, angiogenesis and in such pathological processes as cancer and restenosis following balloon angioplasty. More than 20 different MMPs have been identified (Seiki, 2002). These enzymes are secreted by cells and activated at the cell surface in order to degrade a wide variety of ECM components. Further, the availability of proteolytic enzymes and their ability to degrade several different types of ECM molecules provides cells with the potential to degrade nearly every component in the ECM. This MMP activity plays an important role in developing and remodeling the cellular environment in combination with ECM protein deposition.

Similarly, MMP activity has the potential to impact engineered tissue formation. MMPs, for example, can affect collagen scaffold remodeling. Seliktar *et al.* stimulated MMP-2 expression and activation by exposing vascular smooth muscle cells seeded within collagen constructs to cyclic strain (2001). Cyclic strain exposure increased the collagen construct's mechanical properties in terms of yield stress, ultimate stress, and modulus. More specifically, mechanical conditioning increased yield stress by 290%, ultimate stress by 390%, and modulus by 192% compared to static controls. However, this benefit depended on MMP activity such that these cyclic strain-dependent effects

were reduced in the presence of two inhibitors of MMPs. Treatment with high ribose medium (HRM) reduced the beneficial effects of mechanical conditioning such that yield stress was increased by only 91%, ultimate stress was increased by only 102%, and there was no significant difference in modulus compared to HRM treated static controls. In the presence of N-acetylcysteine, the benefits of mechanical conditioning were completely eliminated. There were no significant differences in yield stress, ultimate stress, or modulus compared to static controls. Thus, MMP activity plays an important role in collagen scaffold remodeling because it enables changes to occur in the scaffold composition that results in improved mechanical properties.

Synthetic polymer scaffolds, on the other hand, do not take advantage of this interplay between cells and the extracellular matrix. Pores must be pre-formed in these biodegradable scaffolds using a variety of techniques that rely on one or more of the following: solvents, heat, pressure, and additives that form pores (reviewed in Agrawal and Ray). These pores allow cells to migrate through PGA or PLA-based scaffolds without the requirement of localized proteolytic activity because the pore dimensions are much larger than cell dimensions. Scaffold degradation also depends on hydrolysis, which can be difficult to coordinate with ECM protein deposition. Thus, the scaffold may degrade too quickly and not provide the support needed by cells and which was initially provided by the polymeric scaffold, itself. Alternatively, ECM protein deposition can be limited by the space available to deposit ECM proteins.

Several researchers have investigated the specific degradation sites in ECM components, which can be targeted by a variety of proteolytic enzymes. The Van Wart group performed a series of studies that investigated the hydrolysis rates of several

MMPs (MMP-1, MMP-2, MMP-3, MMP-7, MMP-8, MMP-9) on 60 different

oligopeptides (Netzel-Arnett *et al.,* 1991; Netzel-Arnett *et al.,* 1993; reviewed in Imper

and Van Wart, 1998). These oligopeptides were based on the collagenase cleavage site in

collagen's α1(I)-chain, Glycine-Proline-Glutamine-Glycine┼Isoleucine-Alanine-

Glycine-Glutamine (GPQG┼IAGQ). The hydrolysis rates varied depending on changes

made to the substrate sequence and the particular MMP involved. For example, MMP

activity is reduced by 32% when the peptide sequence is truncated by one amino acid

(GPQG┼IAG) and by 85% when the peptide sequence is truncated by two amino acids

(GPQG┼IA). Amino acid substitutions can either decrease or increase the hydrolysis

rates. Replacing the alanine subsite with tryptophan (GPQG┼IWGQ) increased MMP-1

activity by 7.3-fold and MMP-8 activity by 8.3-fold. Alternatively, the alanine subsite

can be replaced with glutamic acid (GPQG┼IEGQ), which decreases MMP-1 activity by

2.8 fold and MMP-8 activity by 1.7 fold. The incorporation of these degradation

sequences in hydrogel scaffolds may be useful for tissue-engineering applications as it

provides a mechanism for cells to control the scaffold's degradation properties.

PEG-based hydrogel scaffolds can be modified to degrade in response to

proteolytic enzymes. West and Hubbell were the first to describe polymeric biomaterials

based on BAB block copolymers of PEG (A) and oligopeptides (B) susceptible to

proteolytic enzyme cleavage (1999). The addition of acrylate endgroups allowed

polymerization of these block copolymers to form crosslinked networks where the

collagenase-sensitive sequence, LGPA, or the plasmin-sensitive sequence, NRV, were

inserted into the backbone of the main polymer chain. These hydrogel scaffolds

degraded in response to their targeted proteolytic enzyme, but did not degrade in response

to the other protease. Thus, these scaffolds mimic the protease-sensitive characteristic of the native cellular environment.

Gobin and West then showed that fibroblasts could migrate through scaffolds susceptible to collagenase, plasmin, and elastase degradation (2002). Cell migration required adhesive and degradable peptide sequences where the adhesive component was covalently immobilized to the hydrogel. Migration through these collagenase-sensitive hydrogels was not significantly different from migration through type I collagen scaffolds. Moreover, migration varied depending on the concentration of incorporated RGD and was optimal at an intermediate concentration. Thus, these protease-sensitive hydrogels provide substrates that cells can degrade in order to make room for cell migration. In a similar system, the Hubbell group prepared hydrogels containing the adhesive peptide, GRGDSP, and an MMP-sensitive substrate (CRD-GPQG↓IWGQ-DRC) using conjugate addition reactions (Lutolf *et al.,* 2003a and 2003b). This approach produces hydrogel networks to which cells can adhere and remodel by degrading the MMP crosslinking substrates. Cell invasion into these three-dimensional networks depended on the RGD concentration where migration peaked at an intermediate ligand concentration and on the network crosslinking density where migration was completely impaired in the most highly crosslinked networks.

This study extends the capability of PEG-based hydrogels for mimicking the ECM to include sensitivity to proteolytic degradation. The MMP-sensitive sequence, GPQGILGQ, has been inserted into the backbone of the main polymer chain in order to form crosslinked hydrogel networks with degradable substrates. This sequence is particularly sensitive to degradation by MMP-2 and MMP-9, but can also be degraded by

other MMPs including MMP-1, MMP-3, MMP-7, and MMP-8. Thus, these hydrogel scaffolds combine opportunities to present adhesion peptides and growth factors that can influence cell behavior with opportunities to match scaffold degradation with ECM protein deposition. These scaffolds have the potential to more closely mimic key characteristics of the ECM and as a result produce engineered tissues that better mimic native tissues.

MATERIALS AND METHODS

Cell maintenance

Human dermal fibroblasts (HDFs) were obtained from Clonetics (San Diego, CA). Human aortic smooth muscle cells (HASMCs) were obtained from Cell Applications (San Diego, CA). Both cell types were maintained at 37°C/5% CO_2 on Dulbecco's modified Eagle medium (DMEM) supplemented with 10% fetal bovine serum (FBS, BioWhittaker, Walkersville, MD), 2 mM L-glutamine (Sigma, St. Louis, MO), 1000 units/l penicillin (Sigma, St. Louis, MO) and 100 mg/l streptomycin (Sigma, St. Louis, MO). All experiments were conducted using cells at passages 6-14.

PEG diacrylate synthesis

PEG diacrylate was synthesized by dissolving 12 g dry PEG (6000 Da; Fluka, Milwaukee, WI) in 36 ml anhydrous dichloromethane. 0.25 g triethylamine and then 0.43 g acryloyl chloride (Lancaster Synthesis, Windham, NH) were added dropwise, and the mixture was stirred under argon for 48 hr. The resulting solution was then washed with 2 M K_2CO_3 and separated into aqueous and dichloromethane phases to remove HCl. The dichloromethane phase was subsequently dried with anhydrous $MgSO_4$ (Fisher Scientific, Pittsburg, PA), and the PEG diacrylate was then precipitated in diethyl ether, filtered, and dried under vacuum at room temperature overnight. The resultant polymer was dissolved in N,N-dimethylformamide-d_7 (Sigma, St.Louis, MO) and characterized via proton NMR (Avance 400 MHz; Bruker, Billerica, MA) to determine the degree of acrylation.

PEG-GGPQGILGQGGK-PEG synthesis

The proteolytically degradable peptide sequence, GGPQGILGQGGK, was synthesized using standard dicyclohexylcarbodiimide (DCC) activation and 9-fluorenylmethoxycarbonyl (Fmoc) protection chemistry on an Applied BioSystems peptide synthesizer (model 431A; Foster City, CA). This peptide was dialyzed for 6 hours (3 deionized water exchanges) using 500 MWCO tubing membranes (Spectra/Por biotech cellulose ester dialysis tubing; Fisher Scientific, Pittsburgh, PA) and then lyophilized. The peptide was then dissolved in deuterium oxide (Sigma, St.Louis, MO) and characterized via proton NMR (Avance 400 MHz; Bruker, Billerica, MA) to confirm the amino acid content.

ABA block copolymers of PEG (A) and the degradable peptide sequence, GGPQGILGQGGK (B), were synthesized by reacting the peptide sequence with acryloyl-PEG-NHS (3400 Da) in a 1:2 (peptide:PEG) molar ratio in 50 mM sodium bicarbonate (pH 8.5) for 1 hr. The polymer solution was then dialyzed for 6 hours (3 deionized water exchanges) using 5000 MWCO tubing membranes and then lyophilized and stored at −80°C. Gel permeation chromatography with UV (260 nm) and evaporative light scattering detectors (Polymer Laboratories; Amherst, MA) was used to analyze the peptide and PEG-peptide copolymer.

Hydrogel preparation for the degradation study

Hydrogels were formed by dissolving 0.1 g/ml PEG-GGQPGILGQGGK-PEG in 10 mM HEPES buffered saline (HBS; pH 7.4). This solution was then sterilized by filtration (0.8 μm prefilter and 0.2 μm filter; Gelman Sciences, Ann Arbor, MI). 10 μl/ml

of 2,2-dimethyl-2-phenyl-acetophenone in N-vinylpyrrolidone (300 mg/ml) was added as

the photoinitiator. This solution was then placed in a disk-shaped mold (0.64 cm-

diameter, 0.25 cm-thickness) and exposed to long wavelength UV light (365 nm, 10

mW/cm^2) for 60 sec. Hydrogels were placed in HBS containing 0.2 mg/ml sodium azide

(Sigma) without type IV or V collagenase for the first 24 hours. This solution was then

removed and hydrogels were weighed and subsequently placed in HBS containing 0.2

mg/ml sodium azide (Sigma) with 0, 0.2, or 2 mg/ml type IV/V collagenase (Sigma).

Following the addition of collagenase, hydrogels were weighed at several time points (30

min, 1, 2, 4, 8, 24, 48, 72 hr, etc.). Hydrogels were maintained at 37°C throughout this

study.

Cell morphology changes in PEG-based hydrogels

A cell adhesive component was prepared by reacting acryloyl-PEG-NHS with the

adhesion peptide, RGDS (American Peptide, Sunnyvale, CA) in 50 mM sodium

bicarbonate (pH 8.5) at a 1:1 molar ratio for 2 hr. The solution was then lyophilized and

stored at −20°C.

Nondegradable hydrogels were formed by combining 0.2 g/ml PEG diacrylate

and 10 μmole/ml PEG-RGDS conjugate in HBS containing 230 mM triethanolamine (pH

8). An equal volume of this polymer solution was added to either an HDF or HASMC

suspension to form a cell-polymer solution with a cell density of 5×10^6 cells/ml and

polymer concentration of 0.1g/ml. 10 ul/ml of 10 mM eosin Y in HBS (pH 7.4) and 3.95

μl/ml N-vinylpyrrolidone (37 mM) were added. The cell-polymer solution was placed in

a glass mold (0.5 mm thickness) and exposed to light. Disks (10 mm-diameter) were cut

out using a cork-borer. These disks were placed in a 24-well plate and photographs were

taken under phase contrast microscopy at 1, 3, 5, and 7 days. Degradable hydrogels were formed as described above for the nondegradable hydrogels except that the polymer solution contained 0.2 g/ml PEG-GGPQGILGQGGK-PEG with 0 or 10 μmol/ml PEG-RGDS. These polymer solutions were combined with HDF suspensions and resulted in polymer-cell solutions with polymer concentrations of 0.1 g/ml and 0 or 5 μmol/ml PEG-RGDS. Additionally, degradable hydrogels containing 0.2 g/ml PEG-GGPQGILGQGGK-PEG and 10 μmole/ml PEG-RGDS were combined with an equal volume of cell suspension to form hydrogels with a polymer concentration of 0.1 g/ml, 5 μmol/ml PEG-RGDS, and 250 ng/ml PEG-bFGF conjugate.

Three-dimensional observation of cell morphology changes in PEG-based hydrogels

Viral supernatant was provided by Dr. Wafa Elbjeirami. Briefly, this supernatant was prepared by cloning enhanced GFP cDNA into a retroviral expression vector (PLE-N1; Clontech; Palo Alto, CA). The retrovirus was produced by transient transfection of the amphotropic Phoenix packaging cell line (provided by Dr. Gary Nolan, Stanford University), and pseudotyped with vesicular stomatitis virus G-glycoprotein. Fibroblast cells were plated at 5300 cells/cm^2 and supplemented with the viral supernatant at 1 ml/9.5 cm^2 and 1μl/9.5 cm^2 of 1000x polyprene. The expression cassette harbored a neomycin-resistance gene that enabled selection with G418 (CalBiochem; San Diego, CA). At 48 hr after transfection, cells were passaged and then allowed to select with G418 at a final concentration of 0.5 mg/ml. The medium was changed every 2 days for a 7 day selection period. Resistant cells were then trypsinized and seeded within PEG-based hydrogel scaffolds.

GFP-transfected fibroblasts were seeded within hydrogel scaffolds as described above with a few exceptions. Polymer scaffolds were formed to have a final cell concentration of 10×10^6 cells/ml and a final PEG-RGDS concentration of 2 µmol/ml. The cell-polymer solution (30 µl) was also aliquot onto a Teflon plate and exposed to light for 2 minutes. Cells within these hydrogel constructs were then examined using confocal microscopy (Zeiss LSM 510; Germany) at 4 hr and 4 d after seeding. An argon laser was used to excite the fluorophore at 477 nm and a band pass filter allowed for the emitted light to be collected between 500 and 550 nm.

Cell migration out of hydrogel clusters

Hydrogels with a high concentration of cells (30,000 cells/µL) were formed by aliquoting 2 µL of cell-polymer solution onto a Teflon mold and exposed to light for 2 minutes. The cell-polymer solution contained a final concentration of 0.1 g/mL PEG-GGPQGILGQGGK-PEG in HBS containing 230 mM triethanolamine (pH 8), 10 ul/ml of 10 mM eosin Y in HBS (pH 7.4), 3.95 µl/ml N-vinylpyrrolidone (37 mM), and 2 µmol/ml PEG-RGDS. These cell clusters were then embedded in either nondegradable or degradable hydrogels modified with 2 µmol/ml PEG-RGDS. Cell migration out of the cell clusters and into three-dimensional hydrogel networks was then monitored at 4 hours and 4 days.

RESULTS

Peptide and polymer characterization

The degradable peptide sequence, GGPQGILGQGGK, was synthesized using standard dicyclohexylcarbodiimide (DCC) activation and 9-fluorenylmethoxycarbonyl (Fmoc) protection chemistry. The amino acid content was confirmed by analyzing the proton NMR spectrum of this degradable peptide sequence as depicted in Figure 1. This peptide was then conjugated to PEG chains using acryloyl-PEG-NHS. The success of this conjugation was confirmed using gel permeation chromatography with UV and evaporative light scattering detectors as shown in Figure 2. Multiple PEG chains attached to the peptide due to the reaction between acryloyl-PEG-NHS and primary
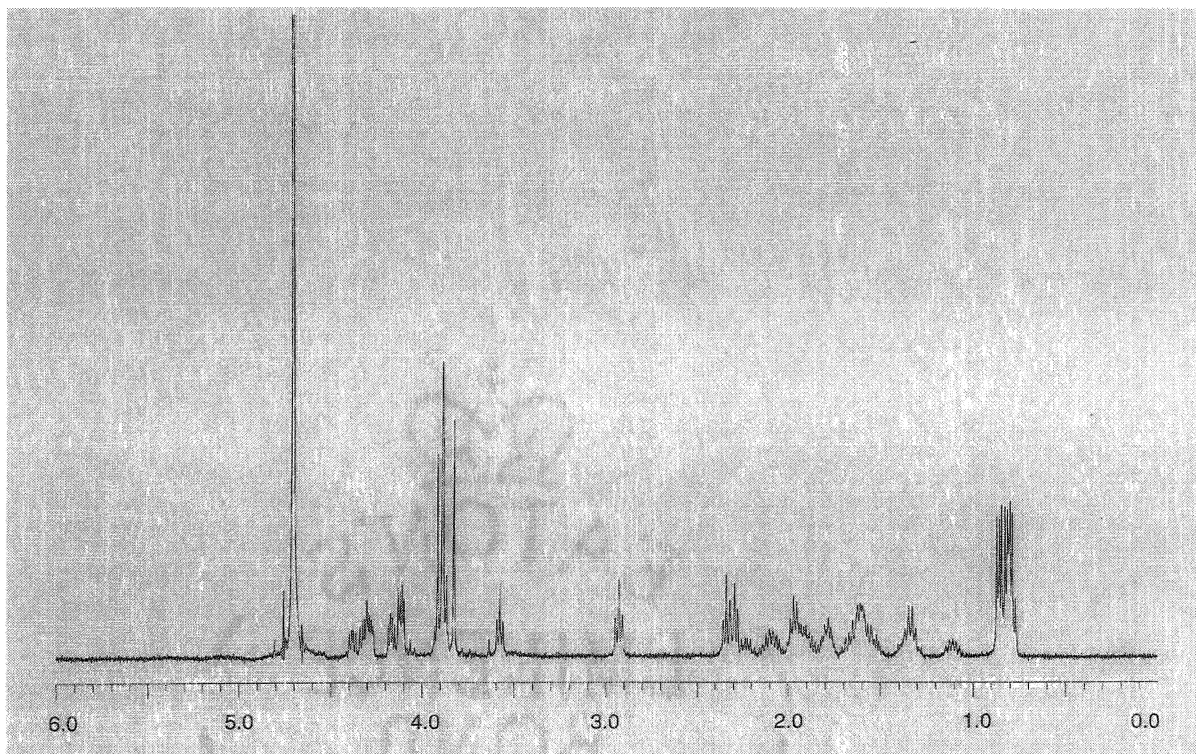

Figure 1. The degradable peptide sequence, GGPQGILGQGGK, was analyzed using proton NMR to confirm the amino acid content.
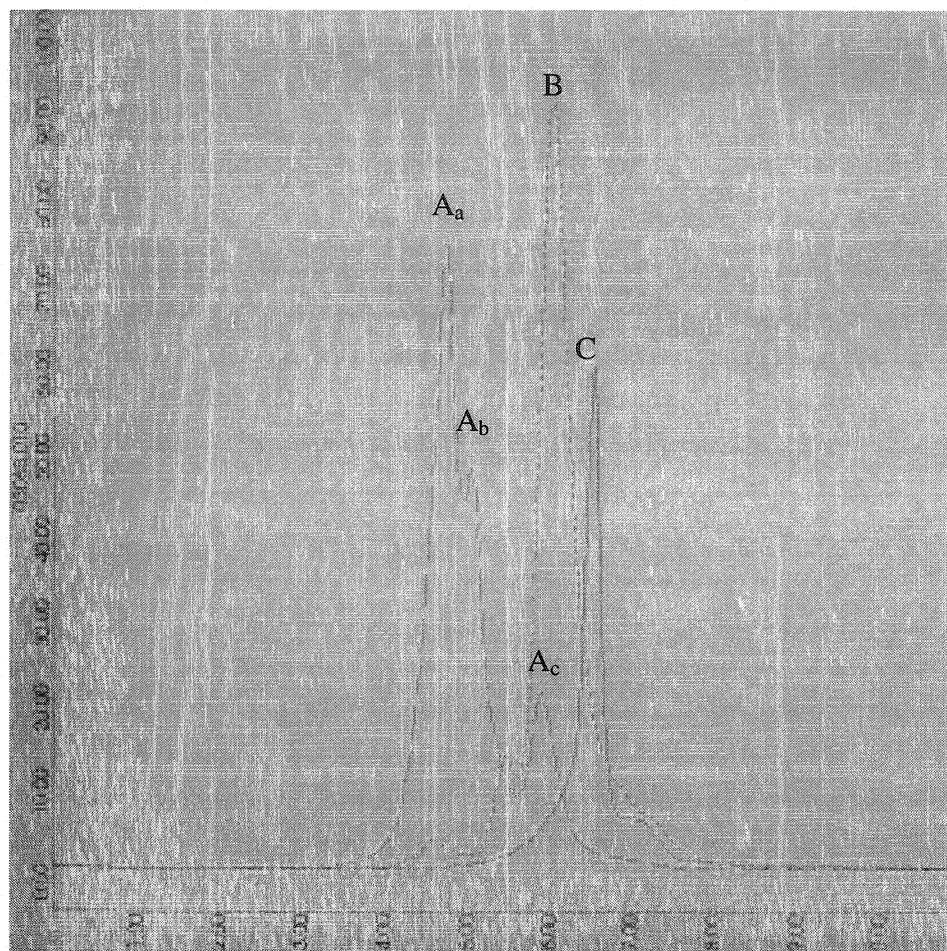
Figure 2. Gel permeation chromatography with UV (260 nm) and evaporative light scattering detectors was used to analyze the degradable polymer (A). Multiple PEG chains (B; acryloyl-PEG-NHS) attached to the degradable peptide sequence, GGPQGILGQGGK (C), resulting in a non-uniform product (A_a, A_b, A_c) where the shift in MW corresponded with the attachment of PEG chains.

amines. More specifically, acryloyl-PEG-NHS targeted the N-terminus and lysine and glutamine residues, which results in a non-uniform product.

Enzymatic degradation of PEG-based hydrogels

Hydrogels containing the MMP-sensitive sequence, GGPQGILGQGGK, were examined for their susceptibility to enzymatic degradation. Gels treated with 0.2 mg/ml type IV collagenase degraded within 12 hours, while gels treated with 2 mg/ml type IV

collagenase degraded more quickly, within 6 hours (Figure 3). Gels did not degrade in

the absence of collagenase. In fact, the control gels' weight remained relatively constant

Type IV Collagenase Degradation
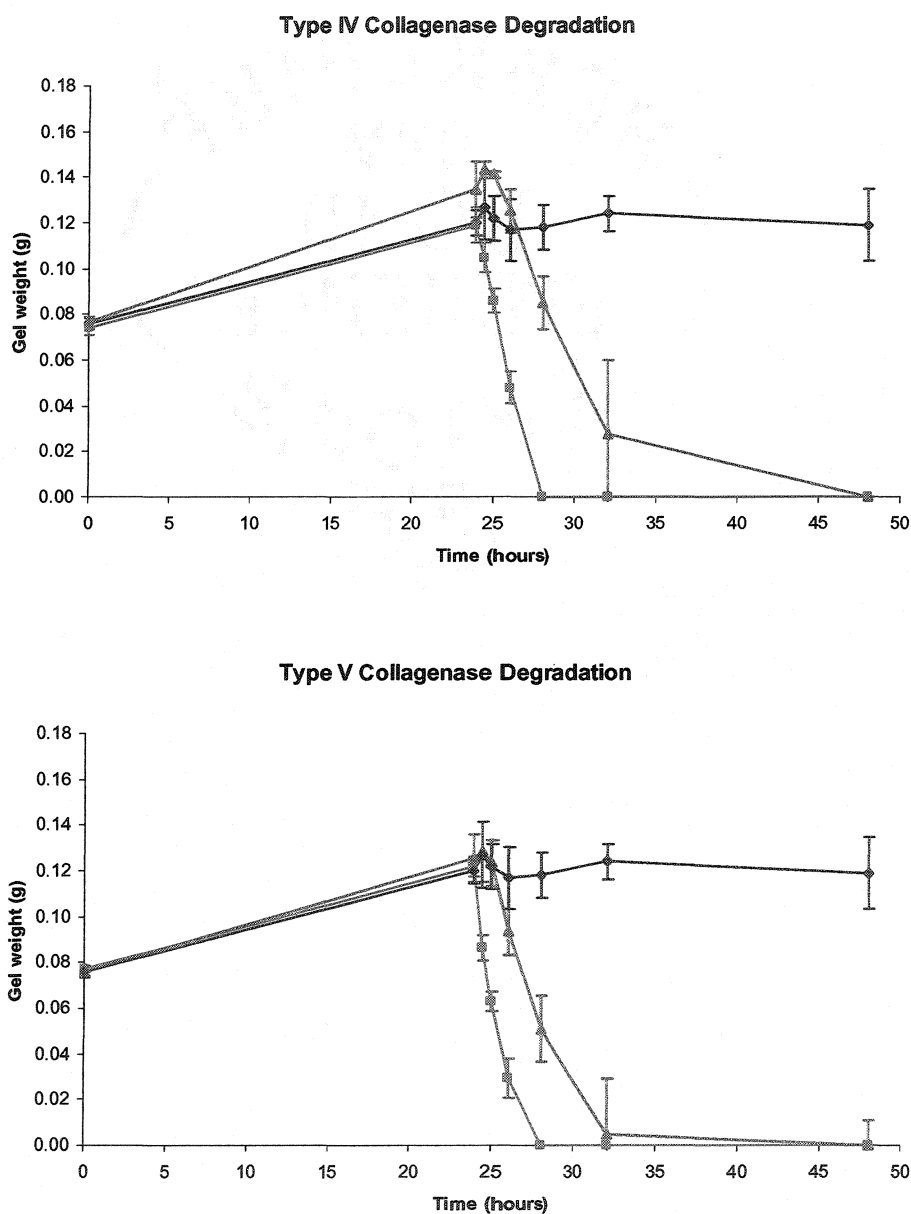

Type V Collagenase Degradation

Figure 3. Collagenase-sensitive hydrogels degraded in the presence of types IV and V collagenase. Gels treated with 0.2 mg/ml collagenase (shown in green) degraded within 12 hours, while gels treated with 2 mg/ml collagenase (shown in pink) degraded within 6 hours. Gels did not degrade in the absence of collagenase (0 mg/ml; shown in blue).

Type IV Collagenase Degradation
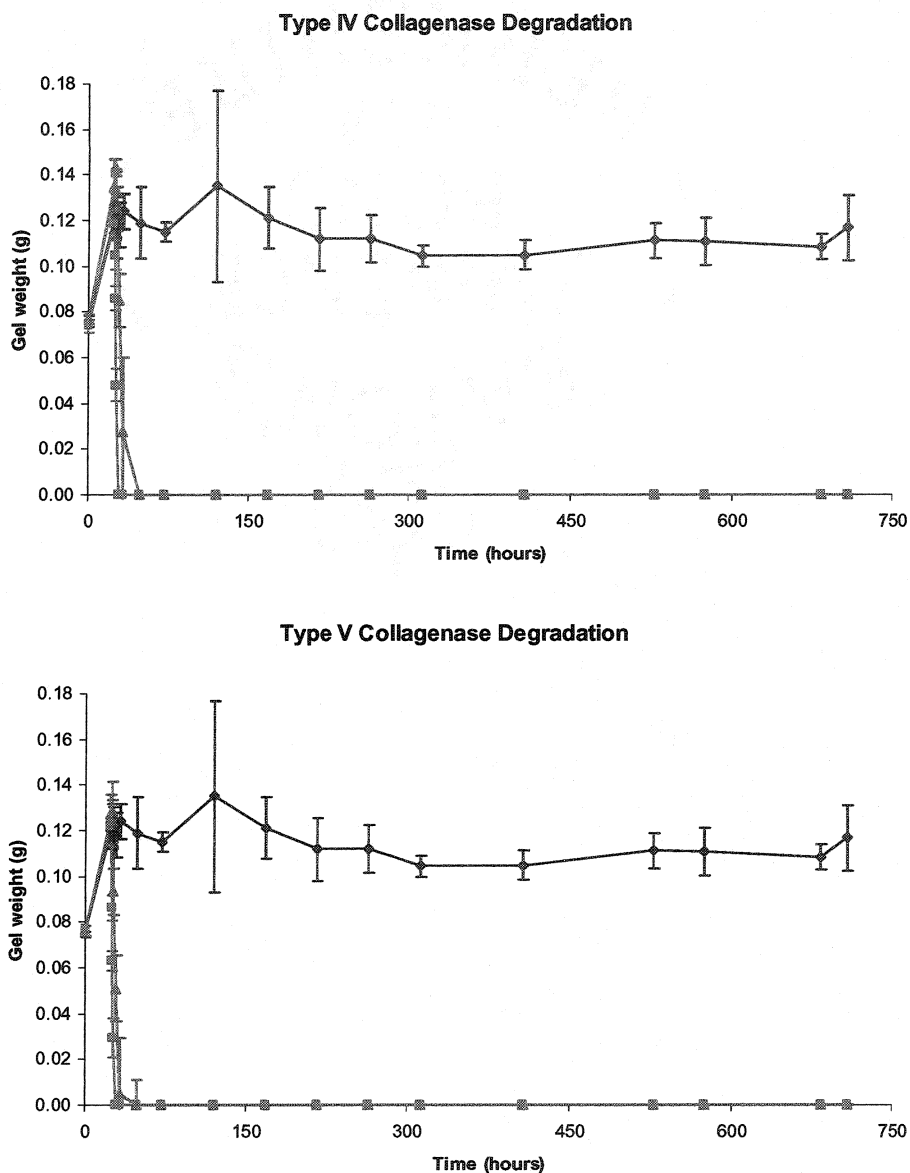

Type V Collagenase Degradation

Figure 4. Gels treated with 0 mg/ml types IV or V collagenase did not degrade. In fact, the control gels' weight (shown in blue) remained relatively constant throughout a 30 day period.

throughout a 30 day period (Figure 4). Similarly, gels treated with type V collagenase

degraded within 8 and 4 hours, respectively, when treated with 0.2 mg/ml and 2 mg/ml

enzyme (Figure 3). A slight increase in gel weight was also initially observed for

degradable hydrogels treated with 0.2 mg/ml type IV collagenase. This increase in gel

weight is due to an initial increase in swelling as some of the GPQGILGQ sequences are

cleaved allowing more water to enter the hydrogel network. This increase is then

followed by a decrease in mass as more degradable sequences are cleaved.

Cell morphology changes in PEG-based hydrogels

Fibroblasts and smooth muscle cells altered their morphology in degradable

hydrogels containing covalently immobilized RGD (Figure 5 and 6). These cells

remained rounded in nondegradable hydrogels with the RGD-cell adhesion peptide and in

degradable hydrogels lacking RGD. Alterations in cell morphology were evident as early

as 3 days after seeding. Further analysis using confocal microscopy provided three-
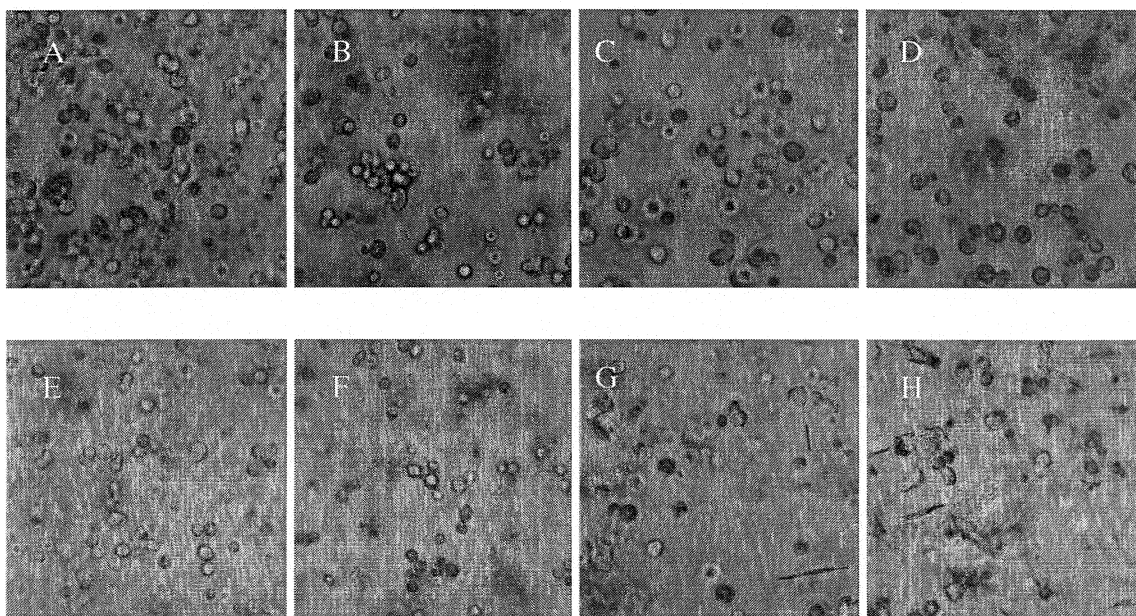

Figure 5. Fibroblast morphology remains rounded in all hydrogel scaffolds at day 1 (nondegradable with RGDS, A; degradable without RGDS, B; degradable with 5 μmole/ml PEG-RGDS, C; degradable with 5 μmol/ml PEG-RGDS and 250 ng/ml PEG-bFGF, D). Fibroblast morphology changes dramatically after 3 days in degradable hydrogels containing PEG-RGDS (G and H). In contrast, fibroblasts remain rounded in degradable hydrogels lacking PEG-RGDS (F) and in nondegradable hydrogels containing PEG-RGDS (E).
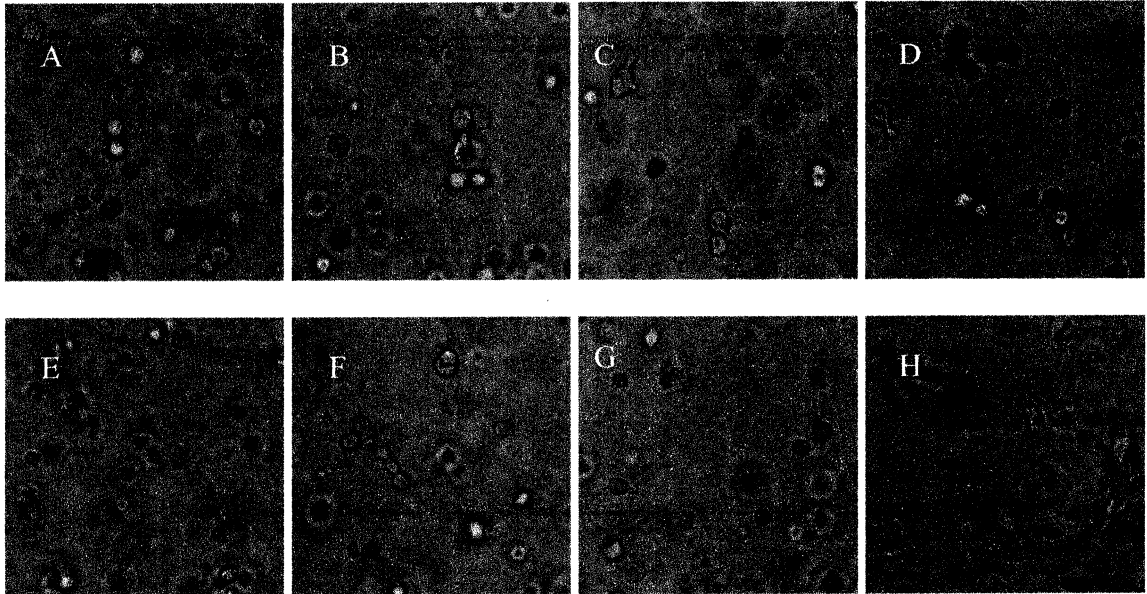
Figure 6. SMC morphology remains rounded in all hydrogel scaffolds at day 1 (nondegradable with RGDS, A; degradable without RGDS, B; degradable with 5 μmol/ml PEG-RGDS, C; degradable with 5 μmol/ml PEG-RGDS and 250 ng/ml PEG-bFGF, D). SMC morphology changes dramatically after 3 days in degradable hydrogels containing PEG-RGDS (G and H). In contrast, SMCs remain rounded in degradable hydrogels lacking PEG-RGDS (F) and in nondegradable hydrogels containing PEG-RGDS (E).
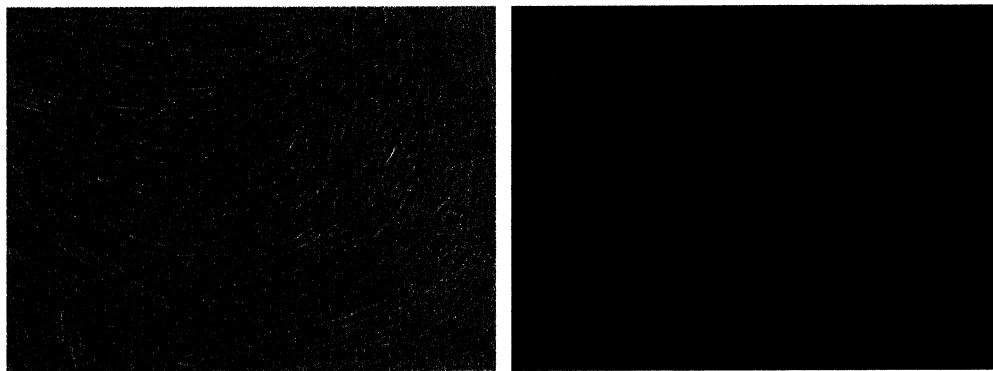

Figure 7. Fibroblasts were successfully transfected with green fluorescent protein (GFP).

Nondegradable gel, 4h   Degradable gel, 4h

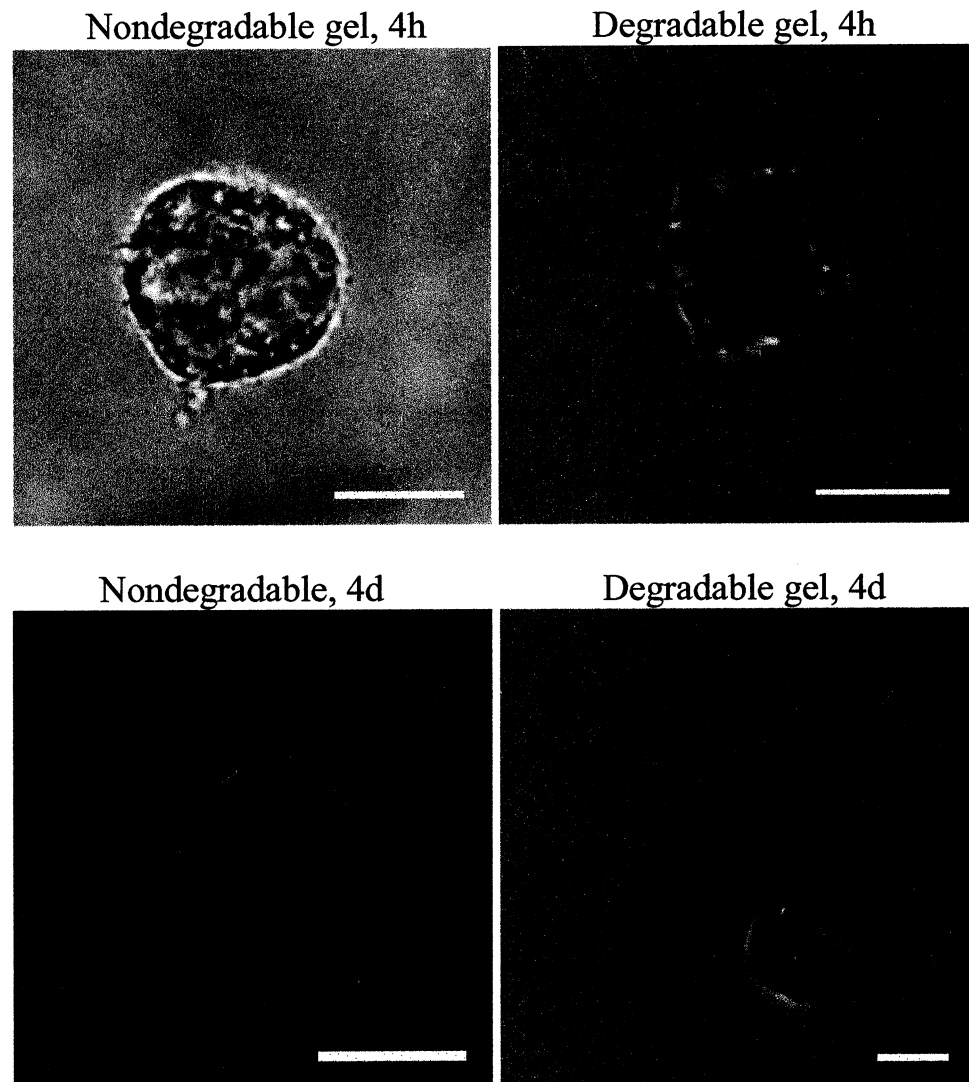Nondegradable, 4d   Degradable gel, 4d

Figure 8. Fibroblasts remained rounded in nondegradable hydrogels at both 4 hours and 4 days. In contrast, fibroblasts in degradable hydrogels altered their morphology by extending processes. These processes could be detected using confocal microscopy to observe cell morphology in three-dimensions (bar = 10μm).

dimensional images of GFP-transfected fibroblasts (Figure 7) changing their morphology in degradable hydrogels with the RGD-adhesion peptide (Figure 8). Fibroblasts were observed to extend processes in several directions on day 4. In contrast, fibroblasts in nondegradable hydrogels were more rounded and did not exhibit a similar ability to extend processes into the scaffold material.
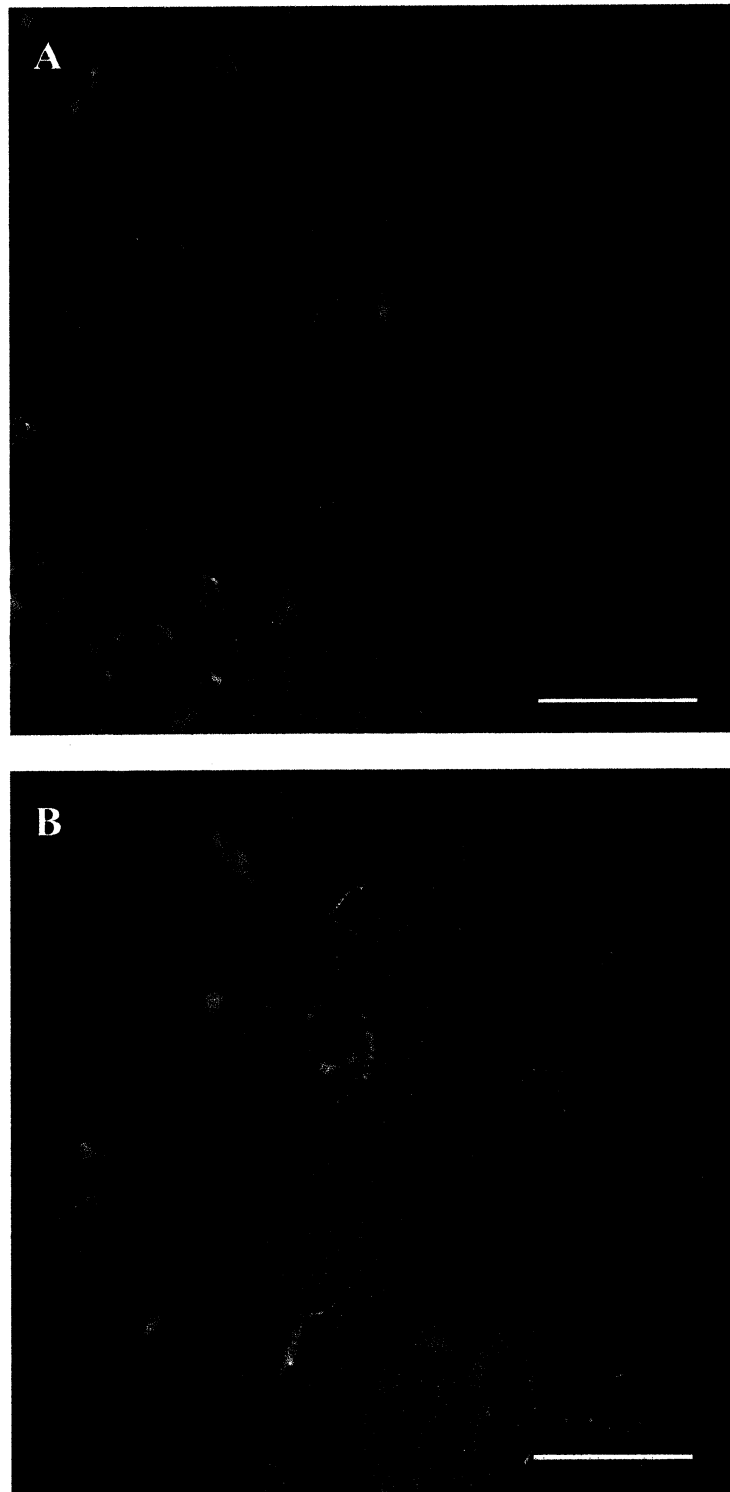
Figure 9. Fibroblasts altered their morphology in degradable hydrogels (B). In contrast, fibroblasts could not extend processes in nondegradable hydrogels (A; bar = 50μm).

Cell migration into a three-dimensional hydrogel network

Figure 10. Fibroblasts migrated into hydrogel networks containing both adhesive and degradable sequences (B). In contrast, fibroblast migration was impaired into nondegradable hydrogels (A) containing only the adhesive sequence.

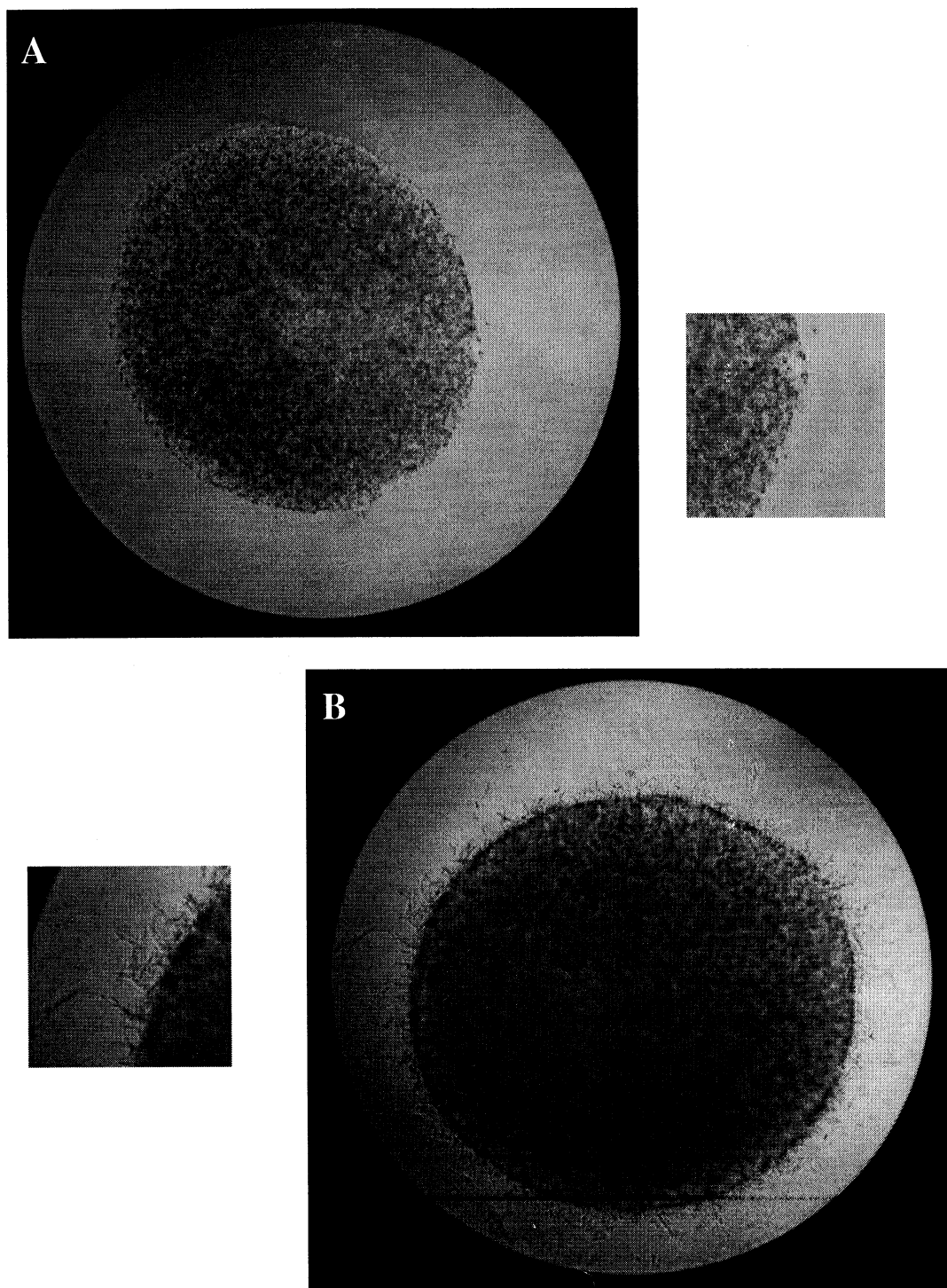As shown in Figure 10, fibroblasts migrated out of hydrogel clusters containing a high cell density and then into three-dimensional hydrogel networks containing both adhesive and degradable sequences. In contrast, fibroblast migration out of hydrogel clusters was impaired when the fibroblasts were presented with a surrounding networking lacking the degradable sequence, GPQGILGQ.

DISCUSSION

Since MMPs play an important role in tissue remodeling, the application of these proteolytic enzymes may also be useful for developing engineered tissues. In this study, PEG-based hydrogel scaffolds were designed to have the MMP-sensitive substrate, GPQGILGQ, inserted into the backbone of the main polymer chains. The resulting hydrogel scaffolds degraded in the presence of types IV and V collagenase in 12 hours or less when exposed to 2 mg/ml collagenase and in 6 hours or less when exposed to 0.2 mg/ml collagenase, but did not degrade in the absence of collagenase. Similar results were also obtained by Mann *et al.* who investigated the degradation of PEG hydrogels containing the collagenase sensitive sequence, GGLGPAGGK, and the elastase sensitive sequence, AAAAAAAAK (2001). However, these hydrogel scaffolds degraded at a much slower rate than the MMP-sensitive hydrogel scaffolds described in this study. The elastase-sensitive hydrogels degraded within 100 hours and 140 hours when exposed to the targeted enzyme at a concentration of 2 mg/ml and 0.2 mg/ml, respectively. The collagenase-sensitive hydrogels degraded within 125 hours when exposed to 2 mg/ml collagenase and within 350 hours when exposed to 0.2 mg/ml collagenase. Thus, the MMP-sensitive hydrogels described in this study are more sensitive to enzymatic

degradation than those studied previously. Since these peptide sequences do not adopt secondary or tertiary structures, the MMP-sensitive substrate is most likely better able to conform to the structure of the enzyme's surface when it binds an enzyme (Imper and Van Wart, 1998). A good match between enzyme and substrate structure can then lead to faster hydrolysis rates.

Cells remodeled PEG hydrogel scaffolds containing both degradable and adhesive peptide sequences. This remodeling activity was evident as fibroblasts and smooth muscle cells extended processes into degradable hydrogels containing the RGD-adhesive peptide. The degradable peptide sequences also enabled fibroblasts to migrate into three-dimensional hydrogel networks. In contrast, migration was impaired within hydrogels lacking the MMP-sensitive substrate, GPQGILGQ. Thus, these degradable hydrogel scaffolds provide a mechanism for cells to alter their scaffold environment in order to make room for cell migration, proliferation, and ECM production. The application of cyclic strain and bioactive factors may enable the cells to increase their expression and activation of proteolytic enzymes leading to improved remodeling of these three-dimensional hydrogel networks (Seliktar *et al.,* 2001). Additionally, reducing the network crosslinking density can also result in improved migration (Lutolf *et al.,* 2003b). This objective can be achieved by using higher molecular weight PEG chains (Cruise *et al.,* 1998). Since it is also possible to incorporate alternative peptide sequences, this would allow cells to remodel these tissue-engineering scaffolds by secreting a variety of proteolytic enzymes (Mann *et al.,* 2001; Gobin and West, 2002; Lutolf *et al.* 2003a and 2003b).

FUTURE DIRECTIONS

These tissue-engineering scaffolds can be further modified to expand their usefulness. In future studies, the effect of additional degradable peptide sequences on the hydrogel scaffold's susceptibility to proteolytic degradation can be investigated. That is, two, three, or more peptide sequences may lead to hydrogel scaffolds that degrade at a faster rate than hydrogel scaffolds containing just one peptide sequence inserted into the backbone of the main polymer chain. Alternative peptide sequences may also be more susceptible to proteolytic degradation including peptide sequences containing amino acid substitutions near the cleavage site. These substituted amino acids may result in peptide sequences that better fit the enzyme's surface structure and as a result lead to faster degradation rates. A combination of bioactive signals and/or mechanical stimulation may also lead to increased secretion and activation of MMPs. This enhanced MMP activity can then lead to increased remodeling within the tissue engineering scaffold and potentially improve the mechanical properties of the resulting engineered tissue. Finally, tissue-engineering scaffolds containing both degradable peptide sequences and a gradient of adhesive peptide sequences can be used to investigate cell response to the three-dimensional presentation of an adhesive peptide gradient. These hydrogel scaffolds are expected to be useful for studying cell response to three-dimensional gradients of bioactive factors.

REFERENCES

Agrawal CM, Ray RB. Biodegradable polymeric scaffolds for musculoskeletal tissue engineering. J Biomed Mater Res 2001;55:141-150.

Alberts B, Johnson A, Lewis J, Raff M, Roberts K, Walter P. Cell junctions, cell adhesion, and the extracellular matrix. In: Molecular biology of the cell, Garland Science, New York, 2002. p. 1065-1125.

Andrade JD, Hlady V. Protein adsorption and materials biocompatibility: a tutorial review and suggested hypotheses. Adv Polym Sci 1986;79:1-63.

Bank AJ, Wang H, Holte JE, Mullen K, Shammas R, Kubo SH. Contribution of collagen, elastin, and smooth muscle to in vivo human brachial artery wall stress and elastic modulus. Circ 1996;94:3263-3270.

Bentz H, Schroeder JA, Estridge TD. Improved local delivery of TGF-$\beta2$ by binding to injectable fibrillar collagen via difunctional polyethylene glycol. J Biomed Mater Res 1998;39:539-548.

Bikfalvi A, Klein S, Pintucci G, Rifkin DB. Biological roles of fibroblast growth factor-2. Endocr Rev 1997;18:26-45.

Blobel CP. Remarkable roles of proteolysis on and beyond the cell surface. Curr Opin in Cell Biol 2000;12:606-612.

Boyden S. The chemotactic effect of mixtures of antibody and antigen on polymorphonuclear leucocytes. J Exp Med 1962;115:453-466.

Burdick JA, Anseth KS. Photoencapsulation of osteoblasts in injectable RGD-modified PEG hydrogels for bone tissue engineering. Biomater 2002;23:4315-4323.

Butler GS, Butler MJ, Atkinson SJ, Will H, Tamura T, Vanwestrum SS, Crabbe T, Clements J, d'Ortho MP, Murphy G. The TIMP2 membrane type 1 metalloproteinase "receptor" regulates the concentration and efficient activation of progelatinase A. J Biol Chem 1998;273:871-880.

Carmeliet P, Collen D. Development and disease in proteinase deficient mice: role of the plasminogen, matrix metalloproteinase and coagulation system. Thromb Res 1998;91:255-285.

Clark, RAF. Wound repair: overview and general considerations. In: The molecular and cellular biology of wound repair, edited by Clark RAF, Plenum Press, New York, 1988. p. 3-35.

Chen G, Ito Y. Gradient micropattern immobilization of EGF to investigate the effect of artificial juxtacrine stimulation. Biomater 2001;22:2453-2457.

Cruise GM, Scharp DS, Hubbell JA. Characterization of permeability and network structure of interfacially photopolymerized poly(ethylene glycol) diacrylate hydrogels. Biomater 1998;19:1287-1294.

Csiszar K. Lysyl oxidases: a novel multifunctional amine oxidase family. Prog Nucleic Acid Res Mol Biol 2001;70:1-32.

Dinbergs ID, Brown L, Edelman ER. Cellular response to transforming growth factor-β1 and basic fibroblast growth factor depends on release kinetics and extracellular matrix interactions. J Biol Chem 1996;271:29822-29829.

Eling B, Gorgolewski S, Pennings AJ. Biodegradable materials of poly(L-lactic acid): 1. Melt-spun and solution spun fibres. Polymer 1982;23:1587-1593.

Farrell DH, Thiagarajan P, Chung DW, Davie EW. Role of fibrinogen α and γ chain sites in platelet aggregation. Proc Natl Acad Sci USA 1992;89:10729-10732.

Feinstein G, Kupfer A, Sokolovsky M. N-acetyl-(L-Ala)3-p-nitroanilide as a new chromogenic substrate for elastase. Biochim Biophys Res Commun 1973;50:1020-1026.

Feng X, Clark RA, Galanakis D, Tonnesen MG. Fibrin and collagen differentially regulate human dermal microvascular endothelial cell integrins: stabilization of alphav/beta3 mRNA by fibrin1. J Invest Dermatol 1999;113:913-919.

Fessler JH, Fessler LI. Biosynthesis of procollagen. Ann Rev Biochem 1978;47:129-162.

Giannelli G, Falk Marzillier J, Schiraldi O, Stetler Stevenson WG, Quaranta V. Induction of cell migration by matrix metalloprotease-2 cleavage of laminin-5. Science 1997;277:225-228.

Gilding DK, Reed AM. Biodegradable polymers for use in surgery—polyglycolic/poly(lactic acid) homo- and copolymers: 1. Polymer 1979;20:1459-1464.

Gobin AS, West JL. Cell migration through defined, synthetic ECM analogs. FASEB J 2002;16:751-753.

Gobin AS, West JL. Val-ala-pro-gly, an elastin-derived non-integrin ligand: smooth muscle cell adhesion and specificity. J Biomed Mater Res 2003;67A:255-259.

Gobin AS, West JL. Effects of epidermal growth factor on fibroblast migration through biomimetic hydrogels. Biotechnol Prog 2003;19:1781-1785.

Gombotz WR, Guanghui W, Horbett TA, Hoffman AS. Protein adsorption to poly(ethylene oxide) surfaces. J Biomed Mater Res 1991;25:1547-1562.

Gospodarowicz D, Cheng J. Heparin protects basic and acidic FGF from inactivation. J Cell Physiol 1986;128:475-484.

Grassl ED, Oegema TR, Tranquillo RT. Fibrin as an alternative biopolymer to type-I collagen for the fabrication of a media equivalent. J Biomed Mater Res 2002;60:607-612.

Griffith LG. Emerging design principles in biomaterials and scaffolds for tissue engineering. Ann NY Acad Sci 2002;961:83-95.

Guerra PI, Acklin C, Kosky AA, Davis JM, Treuheit MJ, Brems DN. PEGylation prevents the N-terminal degradation of megakaryocyte growth and development factor. Pharm Res 1998;15:1822-1827.

Hedin U, Thyberg J. Plasma fibronectin promotes modulation of arterial smooth muscle-cells from contractile to synthetic phenotype. Differentiation 1987;33:239-246.

Hedin U, Bottger BA, Forsberg E, Johansson S, Thyberg J. Diverse effects of fibronectin and laminin on phenotypic properties of cultured arterial smooth muscle cells. J Cell Biol 1988;107:307-319.

Hern DL, Hubbell JA. Incorporation of adhesion peptides into nonadhesive hydrogels useful for tissue resurfacing. J Biomed Mater Res 1998;39:266-276.

Hill-West JL, Chowdhury SM, Slepian JM, Hubbell JA. Inhibition of thrombosis and intimal thickening by in situ photopolymerization of thin hydrogel barriers. Proc Natil Acad Sci USA. 1994;91:5967-71.

Hirai J, Matsuda T. Self-organized, tubular hybrid vascular tissue composed of vascular cells and collagen for low-pressure-loaded venous sytem. Cell Transplant 1995;4:597-608.

Hiraoka N, Allen E, Apel IJ, Gyetko MR, Weiss SJ. Matrix metalloproteinases regulate neovascularization by acting as pericellular fibrinolysins. Cell 1998;95:365-77.

Holmbeck K, Bianoc P, Caterina J, Yamada S, Kromer M, Kuznetsov SA, Mankani M, Robey PG, Poole AR, Pidous I, Ward JM, Birkedal-Hansen H. MT1-MMP-deficient mice develop dwarfism, osteopenia, arthritis, and connective tissue disease due to inadequate collagen turnover. Cell 1999;99:81-92.

Hubbell J. Hydrogels in biological control during graft healing. In: Tissue Engineering of Vascular Prosthetic Grafts, edited by Zilla P and Greisler HP, RG Landes Company, Austin, 1999. p. 561-576.

Hubbell JA. Materials as morphogenetic guides in tissue engineering. Curr Opin in Biotech 2003;14:551-558.

Hynes RO. Integrins: bidirectional, allosteric signaling machines. Cell 2002;110:673-687.

Imai Y, Busby WH, Smith CE, Clarke JB, Garmong AJ, Horwitz GD, Rees C, Clemmons DR. Protease-resistant form of insulin-like growth factor-binding protein 5 is an inhibitor of insulin-like growth factor-1 actions on porcine smooth muscle cells in culture. J Clin Invest 1997;100:2596-2605.

Imper V, Van Wart HE. Substrate specificity and mechanisms of substrate recognition of the matrix metalloproteinases. In: Matrix Metalloproteinases, edited by Parks WC and Mecham RP, Academic Press, San Diego, 1998. p. 219-242.

Ito Y, Hayashi M, Imanish Y. Gradient micropattern immobilization of heparin and its interaction with cells. J Biomater Sci Polym Ed 2001;12:367-378.

Jackson CL, Reidy MA. Basic fibroblast growth factor: its role in the control of smooth muscle cell migration. Am J Path 1993; 143:1024-1031.

Johnsen M, Lund LR, Romer J, Almholt K, Dano K. Cancer invasion and tissue remodeling: common themes in proteolytic matrix degradation. Curr Opin Cell Biol 1998;10:667-671.

Kim BS, Mooney DJ. Engineering smooth muscle tissue with a predefined structure. J Biomed Mater Res 1998a;41:322-332.

Kim BS, Putnam AJ, Kulik TJ, Mooney DJ. Optimizing seeding and culture methods to engineer smooth muscle tissue on biodegradable polymer matrices. Biotechnol Bieng 1998b;57:46-54.

Kim BS, Nikolovski J, Bonadio J, Smiley E, Mooney DJ. Engineered smooth muscle tissues: regulating cell phenotype with the scaffold. Exp Cell Res 1999;251:318-328.

Kim TH, Lee H, TG Park. Pegylated recombinant human epidermal growth factor (rhEGF) for sustained release from biodegradable PLGA microspheres. Biomater 2002;23:2311-7.

Kinoshita T, Sato H, Okada A, Ohuchi E, Imai K, Okada Y, Seiki M. TIMP-2 promotes activation of progelatinase A by membrane-type1 matrix metalloproteinase immobilized on agarose beads. J Biol Chem 1998;273:16098-16103.

Kleinman HK, Philp D, Hoffman MP. Role of the extracellular matrix in morphogenesis. Curr Opin Biotechnol 2003;14:526-532.

Knapp DM, Helou EF, Tranquillo RT. A fibrin or collagen gel assay for tissue cell chemotaxis: assessment of fibroblast chemotaxis to RGDSP. Exp Cell Res 1999;247:543-553.

Koshikawa N, Giannelli G, Cirulli V, Miyazaki K, Quaranta V. Role of cell surface metalloprotease MT1-MMP in epithelial cell migration over laminin-5. J Cell Biol 2000;148:615-624.

Kuhl PR, Griffith-Cima LG, Tethered epidermal growth factor as a paradigm for growth factor-induced stimulation from the solid phase. Nat Med 1996; 2:1022-1027.

Lee H, Jang IH, Ryu SH, Park TG. N-terminal site-specific mono-PEGylation of epidermal growth factor. Pharm Res 2003;20:818-825.

Lewis DH. Controlled release of bioactive agents from lactide / glycolide polymers. In: Biodegradable polymers as drug delivery systems, edited by Chasin M, Langer R, Marcel Dekker, New York, 1990. p. 1-41.

L'Heureux N, Paquet S, Labbe R, Germain L, Auger FA. A completely biological tissue-engineered human blood vessel. FASEB J 1998;12:47-56.

Li DY, Faury G, Taylor DG, Davis EC, Boyle WA, Mecham RP, Stenzel P, Boak B, Keating MT. Novel arterial pathology in mice and humans hemizygous for elastin. 1998;102:1783-1787.

Long JL, Tranquillo RT. Elastic fiber production in cardiovascular tissue-equivalents. Matrix Biol 2003;22:339-350.

Lusckinskas FW, Lawler J. Integrins as dynamic regulators of vascular function. FASEB J 1994;8:929-938.

Lutolf MP, Weber FE, Schmoekel HG, Schense JC, Kohler T, Müller R, Hubbell JA. Repair of bone defects using synthetic mimetics of collagenous extracellular matrices. Nat Biotechnol 2003a; 21:513-518.

Lutolf MP, Lauer-Fields JL, Schmoekel HG, Metters AT, Weber FE, Fields GB, Hubbell JA. Synthetic matrix metalloproteinase-sensitive hydrogels for the conduction of tissue regeneration: engineering cell-invasion characteristics. Proc Natl Acad Sci USA 2003b;100:5413-5418.

Mäki JM, Räsänen, J, Tikkanen H, Sormunen R, Mäkikallio K, Kivirikko KI, Soininen R. Inactivation of the lysyl oxidase gene *lox* leads to aortic aneurysms, cardiovascular dysfunction, and perinatal death in mice. Circ 2002;106:2503-2509.

Mann BK, Tsai AT, Scott-Burden T, West JL. Modification of surfaces with cell adhesion peptides alters extracellular matrix deposition. Biomater 1999;20:2281-2286.

Mann BK, Schmedlen RH, West JL. Tethered-TGF-β increases extracellular matrix production of vascular smooth muscle cells. Biomater 2001a;22:439-444.

Mann BK, Gobin AS, Tsai AT, Schmedlen RH, West JL. Smooth muscle cell growth in photopolymerized hydrogels with cell adhesive and proteolytically degradable domains: synthetic ECM analogs for tissue engineering. Biomater 2001b;22:3045-3051.

Mann BK, West JL. Cell adhesion peptides alter smooth muscle cell adhesion, proliferation, migration, and matrix protein synthesis on modified surfaces and in polymer scaffolds. J Biomed Mater Res 2002;60:86-93.

Massia SP, Hubbell JA. An RGD spacing of 440 nm is sufficient for integrin $\alpha_v\beta_3$-mediated fibroblast spreading and 140 nm for focal contact and stress fiber formation. J Cell Biol 1991;114:1089-1100.

Massia SP, Hubbell JA. Vascular endothelial cell adhesion and spreading promoted by the peptide REDV of the IIICS region of plasma fibronectin is mediated by integrin $\alpha_4\beta_1$. J Biol Chem 1992;267:14019-14026.

Mazzierri R, Masiero L, Zanetta L, Monea S, Onisto M, Garbisa S, Mignatti P. Control of type IV collagenase activity by components of the urokinase-plasmin system: a regulatory mechanism with cell-bound reactants. EMBO J 1997; 16:2319-2332.

Merrill EA, Salzman EW. Polyethylene oxide as a biomaterial. ASAIO J 1983;6:60-64.

Miller RA, Brady JM, Cutright DE. Degradation rates of oral resorbable implants (polylactates and polyglycolates): rate modification with changes in PLA/PGA copolymer ratios. J Biomed Mater Res 1977;11:711-719.

Moghe PV, Nelson RD, Tranquillo RT. Cytokine-stimulated chemotaxis of human neutrophils in a 3-D conjoined fibrin gel assay. J Immunol Methods 1995;180:193-211.

Moiseeva E. Adhesion receptors of vascular smooth muscle cells and their functions. Cardiovas Res 2001;52:372:386.

Moscatelli D. Metabolism of receptor-bound and matrix-bound basic fibroblast growth factor by bovine capillary endothelial cells. J Cell Biol 1988;107:753-759.

Mosesson MW, Siebenlist KR, Meh DA. The structure and biological features of fibrinogen and fibrin. Ann NY Acad Sci 2001;936:11-30.

Murphy G, Gavrilovic J. Proteolysis and cell migration: creating a path? Curr Opin Cell Biol 1999;11:614-621.

Myllyharju J, Kivirikko KI. Collagens and collagen-related diseases. Ann Med 2001;33:7-21.

Nagase H, Woessner JF. Matrix metalloproteinases. J Biol Chem 1999;274:21491-21494.

Nelson RD, Quie PG, Simmons RL. Chemotaxis under agarose: a new and simple method for measuring chemotaxis and spontaneous migration of human polymorphonuclear leucocytes and monocytes. J Immunol 1975;115:1650-1656.

Netzel-Arnett S, Fields GB, Birkedal Hansen H, Van Wart HE, Fields G. Sequence specificities of human fibroblast and neutrophil collagenases. J Biol Chem 1991;266:6747-6755.

Netzel-Arnett S, Sang QX, Moore WG, Navre M, Birkedal-Hansen H, Van Wart HE. Comparative sequence specificities of human 72- and 92-kDa gelatinases (type IV collagenases) and PUMP (matrilysin). Biochemistry 1993;32:6427-6432.

Niklason LE, Gao J, Abbott WM, Hirschi KK, Houser S, Marini R, Langer R. Functional arteries grown in vitro. Science 1999;284:489-493.

Nikolovski J, Mooney DJ. Smooth muscle cell adhesion to tissue engineering scaffolds. Biomater 2000;21:2025-2032.

Parker A, Gockerman A, Busby WH, Clemmons DR. Properties of an insulin-like growth factor-binding protein-4 protease that is secreted by smooth-muscle cells. Endocrin 1995;136:2470-2476.

Pauly RR, Passaniti A, Crow M, Kinsella JL, Papdopoulous N, Monticone R, Lakatta EG, Martin GR. Experimental models that miic the differentiation and dedifferentiation of vascular cells. Circulation 1992;86 Suppl:11168-11173.

Richardson TP, Peters MC, Ennett AB, Mooney DJ. Polymeric system for dual growth factor delivery. Nat Biotech 2001;19:1029-1034.

Ross R, Bornstein P. The elastic fiber: separation and partial characterization of macromolecular components. J Cell Biol 1969;40-366-381.

Rosso, F, Giordano A, Barbarisi M, Barbarisi A. From Cell-ECM interactions to tissue engineering. J Cell Physiol 2004;199:174-180.

Saksela O, Moscatelli D, Sommer A, Rifkin DB. Endothelial cell-derived heparan sulfate binds basic fibroblast growth factor and protects it from prtoeolytic degradation. J Cell Biol 1998;107:743-751.

Sawhney AZ, Pathak CP, Hubbell JA. Bioerodible hydrogels based on photopolymerized poly(ethylene glycol)-co-poly(α-hydroxy acid) diacrylate macromers. Macromol 1993;26:581-587.

Schense JC, Bloch J, Aebischer P, Hubbell JA. Enzymatic incorporation of bioactive peptides into fibrin matrices enhances neurite extension. Nat Biotech 2000;18:415-419.

Schlaepfer DD, Hanks SK, Hunter T, van der Geer P. Integrin-mediated signal transduction linked to Ras pathway by GRB2 binding to focal adhesion kinase. Nature 372:786-791.

Schwartz MA, Ingber DE. Integrating with integrins. Mol biol cell 1994;5:389-393.

Scott-Burden, T. Extracellular Matrix: The Cellular Environment. NIPS 1994;9:110-115.

Seiki M. The cell surface: the stage for matrix metalloproteinase regulation of migration. Curr Opin Cell Biol 2002;14:624-632.

Seliktar D, Nerem RM, Galis ZS. The role of matrix metalloproteinase-2 in the remodeling of cell-seeded vascular constructs subjected to cyclic strain. Ann Biomed Eng 2001;29:923-934.

Singhvi R, Kumar A, Lopez GP, Stephanopoulous GN, Wang DI, Whitesides GM, Ingber DE. Engineering cell shape and function. Science 1994;264:696-698.

Sottile J, Hocking DC, Swiatek P. Fibronectin matrix assembly enhances adhesion-dependent cell growth. J Cell Sci 1998;111:2933-2943.

Springer BA, Pantoliano MW, Barbera FA, Gunyuzlu PL, Thompson LD, Herblin WF, Rosenfeld SA, Book GW. Identification and concerted function of two receptor binding surfaces on basic fibroblast growth factor required for mitogenesis. J Biol Chem 1994;269:26879-26884.

Streuli CH, Bissell MJ. Expression of extracellular matrix components is regulated by substratum. J Cell Biol 1990;110:1405-1415.

Streuli C. Extracellular matrix remodeling and cellular differentiation. Curr Opin Cell Biol 1999;11:634-640.

Strongin AY, Collier I, Bannikov G, Marmer BL, Grant GA, Goldberg GI. Mechanism of cell surface activation of 72-kDa type IV collagenase. J Biol Chem 1995;270:5331-5338.

Swartz MA. Signaling in morphogenesis: transport cues in morphogenesis. Curr Opin Biotechnol 2003;14:547-550.

Tranquillo RT, Girton TS, Bromberek BA, Triebes TG, Mooradian DL. Magnetically-oriented tissue-equivalent tubes: application to a circumferentially-oriented media-equivalent. Biomat 1996;17:349-357.

van der Flier A, Sonnenberg A. Function and interactions of integrins. Cell Tissue Res 2001;305:285-298.

van der Kraan PM, Buma P, van Kuppevelt T, van den Berg WB. Interaction of chondrocytes, extracellular matrix and growth factors: relevance for articular cartilage tissue engineering. Osteoarthritis and Cartilage 2002;10:631-637.

Van Hinsbergh VW, Collen A, Koolwijk P. Role of the fibrin matrix in angiogenesis. Ann NY Acad Sci 2001;936:426-437.

Vrhovski B, Weiss AS. Biochemistry of tropoelastin. Eur J Biochem 1998;258:1-18.

West JL, Hubbell JA. Polymeric biomaterials with degradation sites for proteases involved in cell migration. Macromol 1999;32:241-244.

Weinberg CB, Bell E. A blood vessel model constructed from collagen and cultured vascular cell. Science 1986;231:397-400.

Werb Z. ECM and cell surface proteolysis: regulating cellular ecology. Cell 1997;91:439-442.

Wong AH, Waugh JM, Amabile PG, Yuksel E, Dake MD. *In vivo* vascular engineering: directed migration of smooth muscle cells to limit neointima. Tissue Eng 2002;8:189-199.

Ziegler T, Nerem RM. Tissue engineering a blood vessel: regulation of vascular biology by mechanical stresses. J Cell Biochem 1994;56:204-9.